



Summer Program 2020 - ONLINE

Miriam Raffalovich

Jessica Hofflich

Robert Wong

Ya-Chen's iPad

Juyi's iPad

Haijiao Liu

Yiwei Fang

Jonathan Sokolov

Michael Cuffio

Yuchen Zhou

Yifan Yin

Aniket Raut

Likun Wang

Fan Yang

Kuan-Che Feng

Yu-Chung Lin

marcia

Feng Zhang

Michael Gouzman

Jacob Myers

Katerina Popova

Mori Oso

Emily Zhang

Sebastian Beurnier

Esther Chal

Jessica L Guo

Tyler Stern

Sophia Cai

Jeffrey Huang

Jake Feldman

Michelle Chang

Haris Rana

Serena Yang

Benjamin Sherman

Christine Kong

Lindsay Wright

Jolene Hury

Anthony Del Valle

Leor Oved

Sana Marresh

Jang Choe

pikacal

Clarise H

Emily Zhou

Alyssa Kim

Lillian Sun

Eyal Noy

sabrina

Jonathan Xavier

Pranati Patnam

Kimberly Lu

Ziqi Jiao

Varun Nimmagadda

Wade Boohar

Ori M. Baer

Hannah Zhang

Larry

Daniel Luo

Christian Apostol

Jeffrey Zhang

Susan Zhang

Stephanie Tarrab

Yoni Levy

Yizhe Chen (Anthony)

Nava Schein

Zoe Lu

Chloe Zhang

hannaheven

Kuo Liu

Sabreen Alam

Hugh Rosshirt

Eric Song

Joshua Kang

Amisha Agrawal

Jacky Xie

David Zhang

Jonathan Kozlars

Amy Sharin

Leah Hersh

Jaiden Reddy

Annie Wang

Trevor Cai

Christine Zhang

Udithe Kothapalli

Junsangyoon

Samuel Liu

Kevin Kwon

Shivek Narang

David Liang

Ethan Wachsman

Jeannie She

Hyunkyung Katherine Lee

Stephanie Zhao

Kyle Shi

Anya Chabria

Anya Raju

Danny Li

Aditya Narayanan

Aditya Ramabadrán

Jessica Liu

Aaksh Misra

Ethan Pereira

Eric Kim

Jalaj Mehta

Jiale Lu

Nikhil Murthy

James Kim

Lawrence Zhao

Irene Lee

Evan Cheng

Ayelet Kornblau

Benjamin Roitman

Sohan Shetty

Nishanth Chinnadurai

Hugo Onghai

Jiayang Wang

tj bai

Amy Feng

Samantha Wang

Message to our students;



We were extremely proud of our students this year. They were hampered by the COVID-19 pandemic from coming on campus or meeting each other in person. In the last few days of the program, tropical storm, Isaias, wreaked havoc on the East Coast leaving many without power, and severing the precious internet link that kept us together. Yet, the Garcia Research Scholars persevered, and presented an outstanding program, where they met the scientific and moral challenges of COVID-19 directly, as well as explored new directions in nanocomposites, nanomedicine, clean energy, bioethics, and assistive mobilities.

Their bravery, resilience, and innovation was best expressed by Samantha (Jing) Wang, who designed this year's logo: "The grey dots represent coronavirus, but they are shot through by white lines, which are the spears of human wisdom, especially scientists' hard work. These lines can also be viewed as internet connections, which linked Garcia program to us in this special summer"

Sincerely,



August 10, 2020

Miriam Rafailovich and



Jonathan Sokolov

About the Garcia Center:

The Garcia Center for Polymers at Engineered Interfaces was founded in 1996 and is named after the late Queens College professor Narciso Garcia, who was a pioneer in the integration of education and research. The Center focuses on the integration of materials research with tissue engineering, biomaterials, drug delivery systems, sustainable energy, nanocomposites, and recently, additive manufacturing. The Center also supports innovation through entrepreneurship and has multiple collaborations with industry and national laboratories: <https://www.stonybrook.edu/commcms/garcia/>. The research scholar program offers the opportunity for high school teachers, undergraduate, and high school students to join us. Students work as part of focus research teams and are taught to make original contributions of interest to the scientific community. In addition to entering national competitions, the students are encouraged to publish in refereed scientific journals, present their results at national conferences, and develop patents to protect their intellectual property. Our goal is to convey to the students the excitement we enjoy daily in research and provide for them a supportive network within the scientific community. Research is a lifelong experience and we hope to remain a resource to our students long after "graduation".

High School Students



Agrawal, Amisha



Alam, Sabreen



Apostol, Christian



Baer, Ori



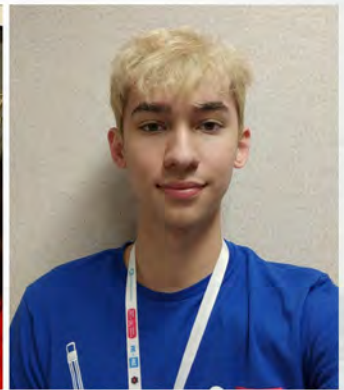
Bai, TJ



Beer, Jonathan



Beurnier, Sebastien



Boohar, Wade Richard



Cai, Sophia



Cai, Trevor



Centeno, Kevin



Chabria, Anya



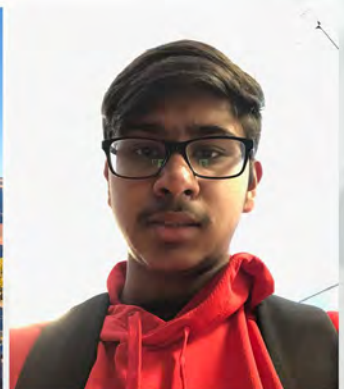
Chang, Michelle



Chen, Yizhe (Anthony)



Cheng, Evan



Chinnadurai, Nishanth

High School Students



Choe, Jang



Even, Hannah



Feldman, Jake



Feng, Amy



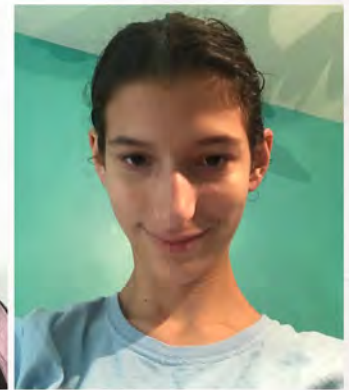
Gu, Kevin



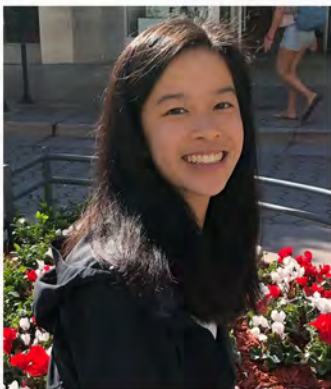
Guo, Jessica Liu



Han, Clarise



Hersh, Leah Q



Huey, Jolene



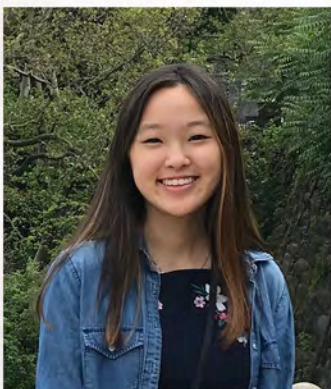
Jiao, Ziqi



Kang, Joshua



Kaushik, Samarjit



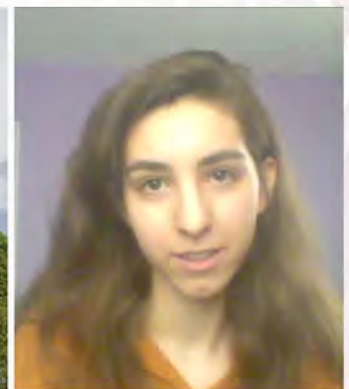
Kim, Alyssa



Kim, Eric



Kim, James



Kornblau, Ayelet

High School Students



Kothapalli, Udithi



Koziarz, Jonathan



Kwon, Kevin



Lee, Hyunkyung (Katherine)



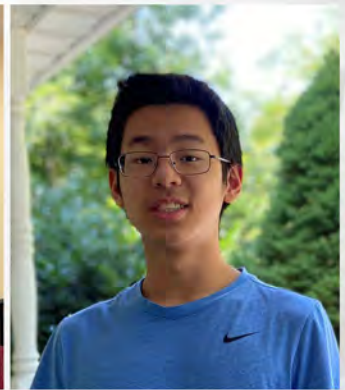
Lee, Irene



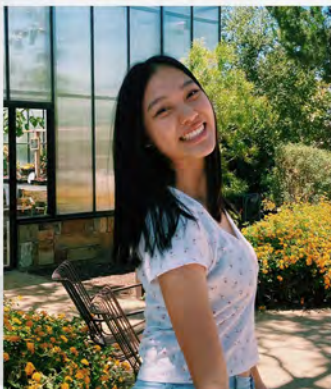
Levy, Yoni



Li, Danny



Liang, David



Liu, Jessica



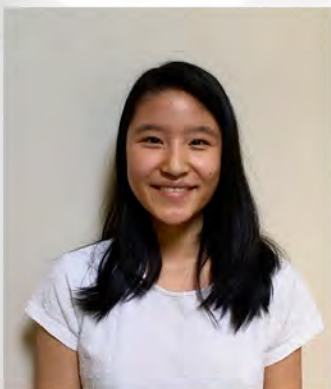
Liu, Kuo



Liu, Samuel



Lu, Jiale



Lu, Zoe



Luo, Daniel



Manesh, Sana



Mehta, Jalaj

High School Students



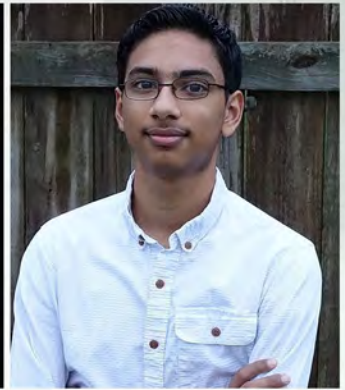
Misra, Aakrsh



Murthy, Nikhil



Narang, Shivek



Narayanan, Aditya



Nimmagadda, Varun



Noy, Eyal



Onghai, Hugo



Ono, Mori



Oved, Leor



Pan, Luisa



Patnam, Pranati



Pereira, Ethan



Popova, Katerina



Raju, Anya



Ramabadrán, Aditya



Rana, Haris

High School Students



Reddy, Jaiden



Roitman, Benjamin



Rosshirt, Hugh



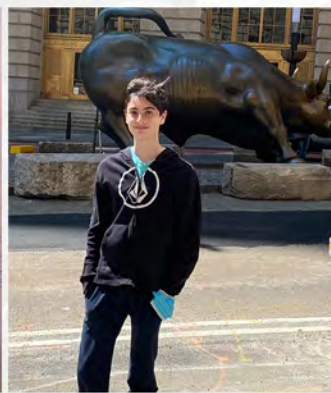
Schein, Nava



Sharin, Amy



She, Jeannie



Sherman, Benjamin



Shern, Tyler



Shetty, Sohan



Shi, Kyle



Song, Eric



Srinivasan, Anand



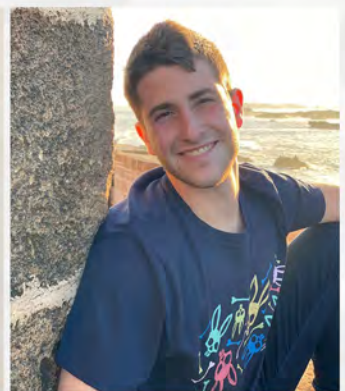
Su, Sabrina



Sun, Lillian



Tarrab, Stephanie



Wachsman, Ethan

High School Students



Wang, Annie



Wang, Daniel



Wang, Jiayang



Wang, Samantha



Wright, Lindsay



Xavier, Jonathan



Xie, Jacky



Yang, Serena



Yoon, Junsang



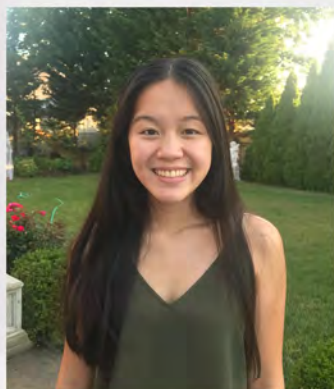
Zhang, Chloe



Zhang, Christine



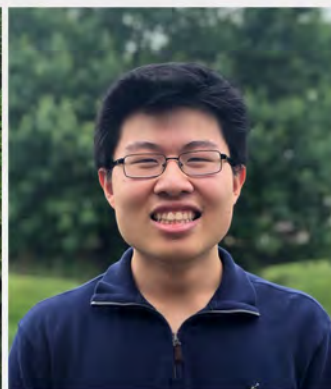
Zhang, David



Zhang, Emily



Zhang, Hannah



Zhang, Jeffrey



Zhang, Lingzi (Susan)

High School Students



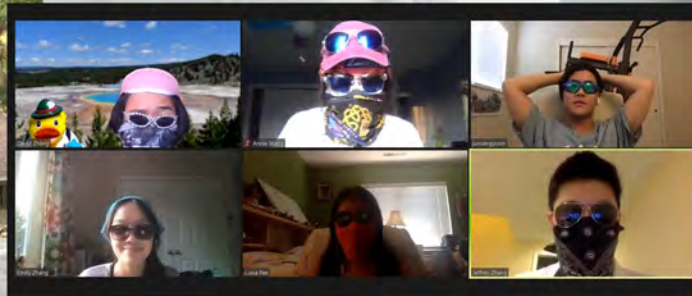
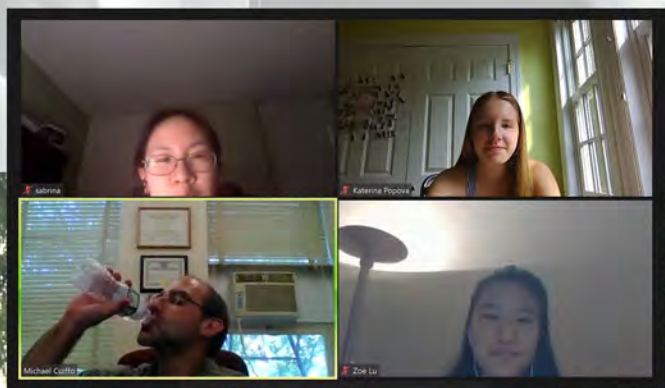
Zhao, Lawrence



Zhao, Qianyi (Stephanie)



Zhou, Emily



Research Experience for Undergraduates (REUs)



Cai, Senhuang (Pika)



Chai, Esther



Del Valle, Anthony



Huang, Jeffrey



Huang, Larry



Kong, Christine



Lu, Kimberly



Myers, Jacob F



Pandey, Ikshu



Winkler, Ethan

Research Experience for Teachers (RETs)



Isseroff, Rebecca



Sharma, Sarika

Graduate Students



Chuang, Ya-Chen



Fang, Yiwei



Hofflich, Jessica



Lee, Won-Il



Li, Kao



Lin, Yu-Chung



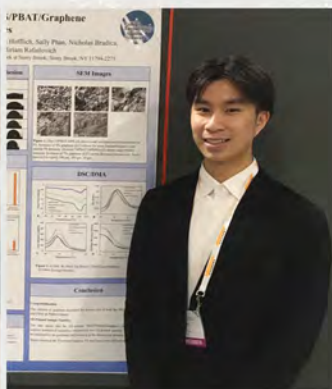
Liu, Haijiao



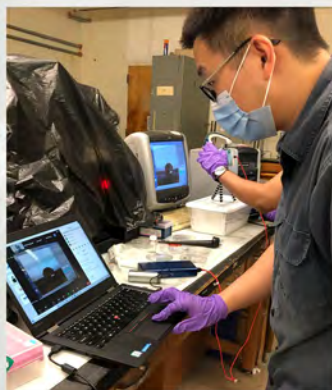
Raut, Aniket



Wang, Likun



Wong, Robert



Yang, Fan



Yin, Yifan



Zhou, Yuchen



F
A
C
U
L
T
Y
/
S
T
A
F
F



Stephen G. Walker



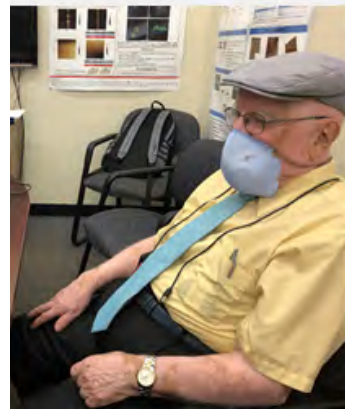
David Rafailovich Sokolov



Peng Zhang



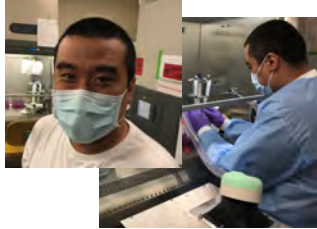
Michael Gouzman



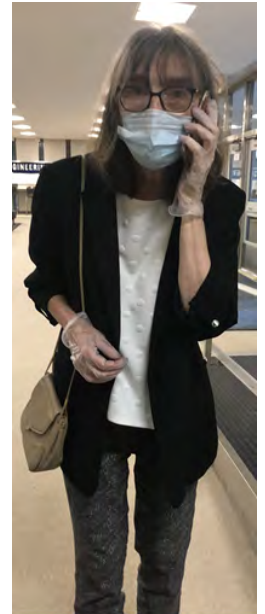
Dennis Galanakis



Xiaojun Bi



Kuan-Che Feng



Marcia Simon



Brooke Ellison



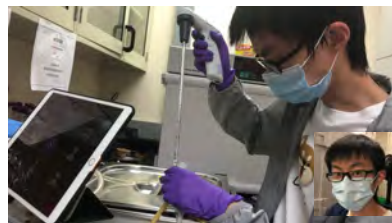
John Luckner Jerome



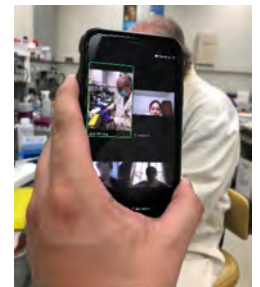
Michael Cuiffo



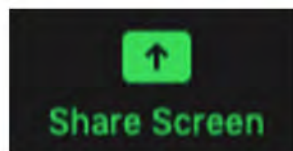
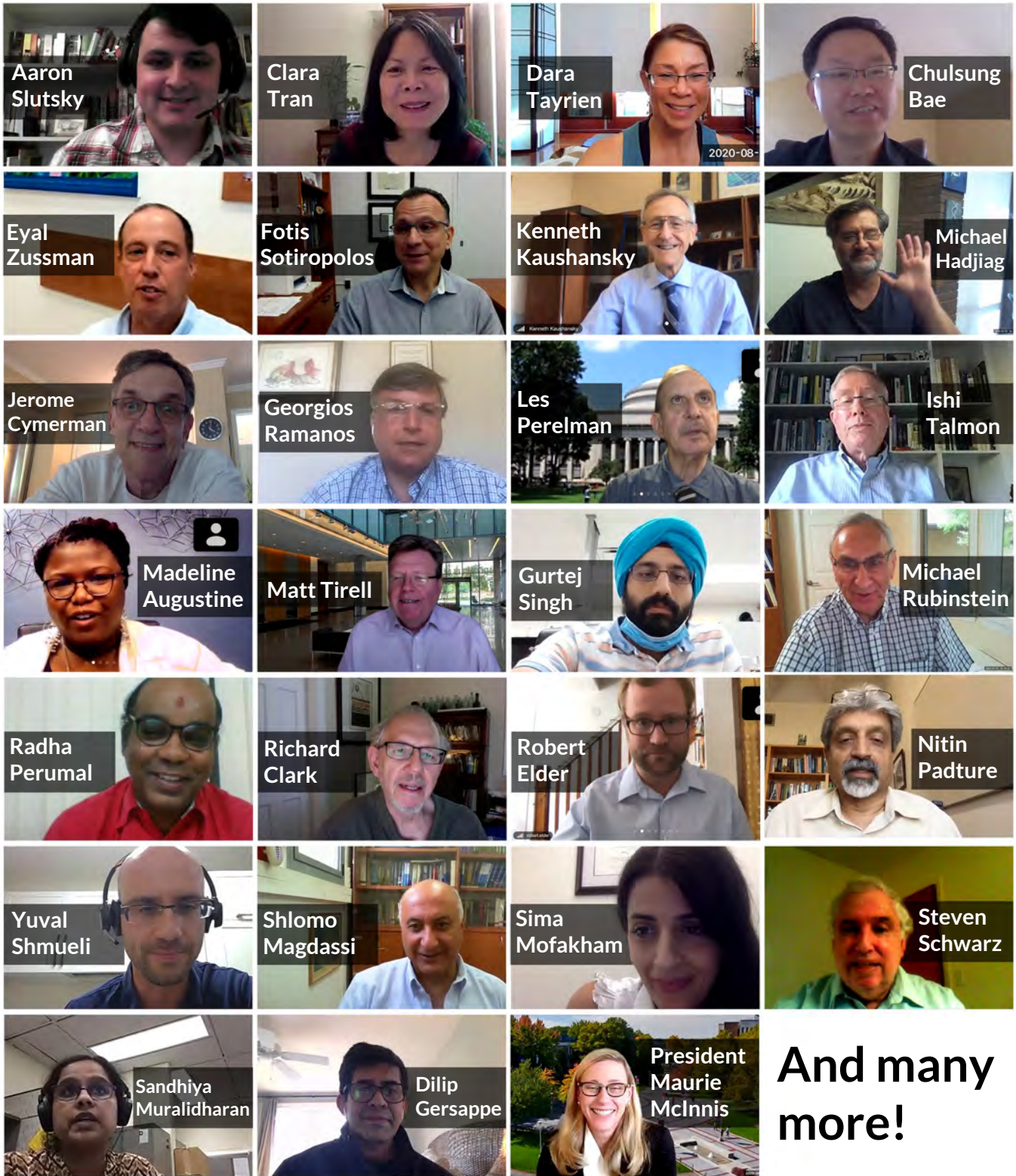
Chander Chandramouli Sadasivan

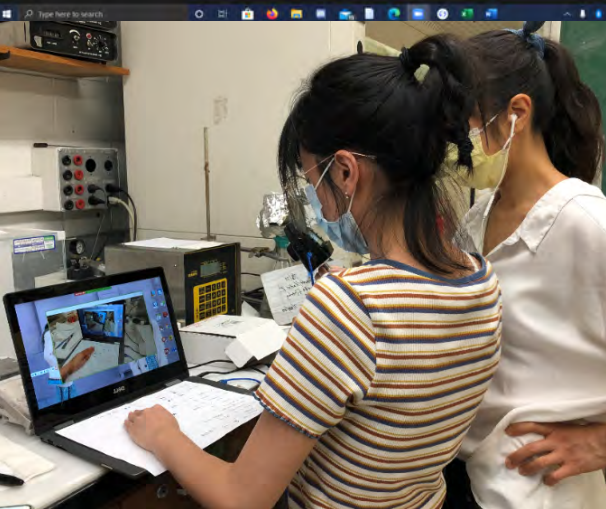
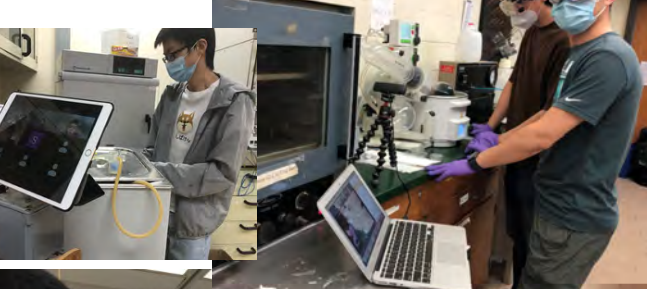
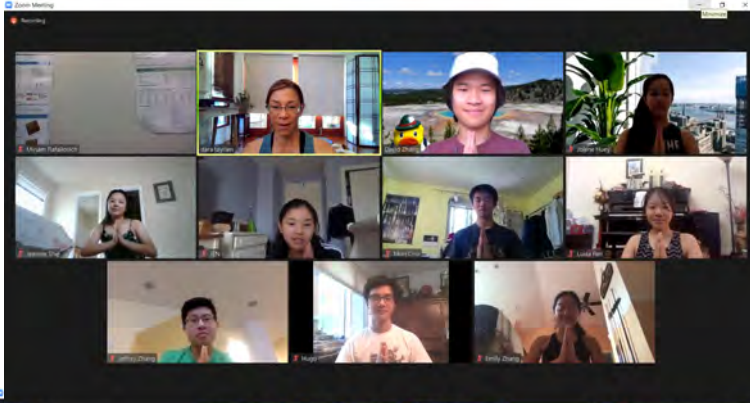


Juyi Li

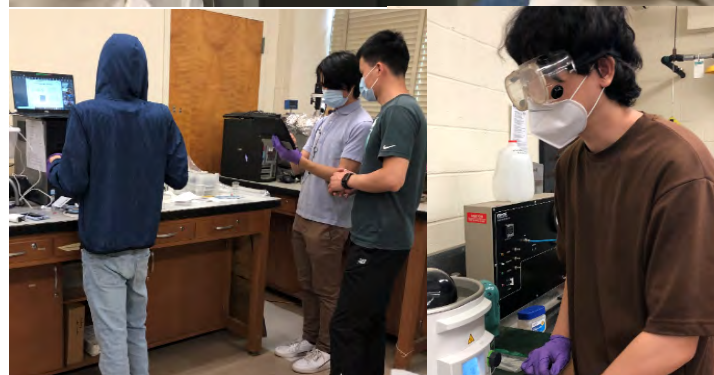
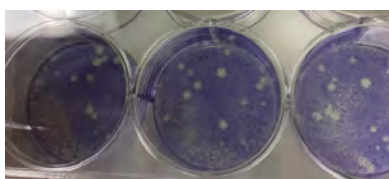


Guest Speakers!





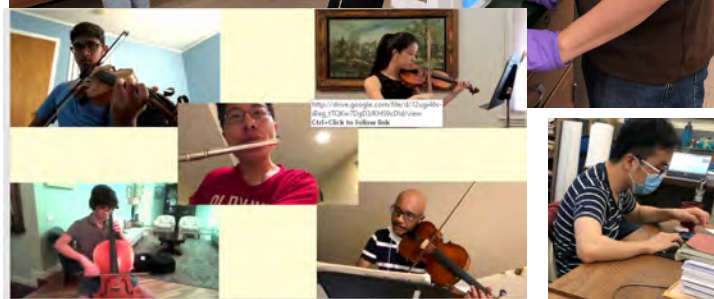
R
E
M
O
T
E
L
E
A
R
N
I
N
G



Yiwei Sensei

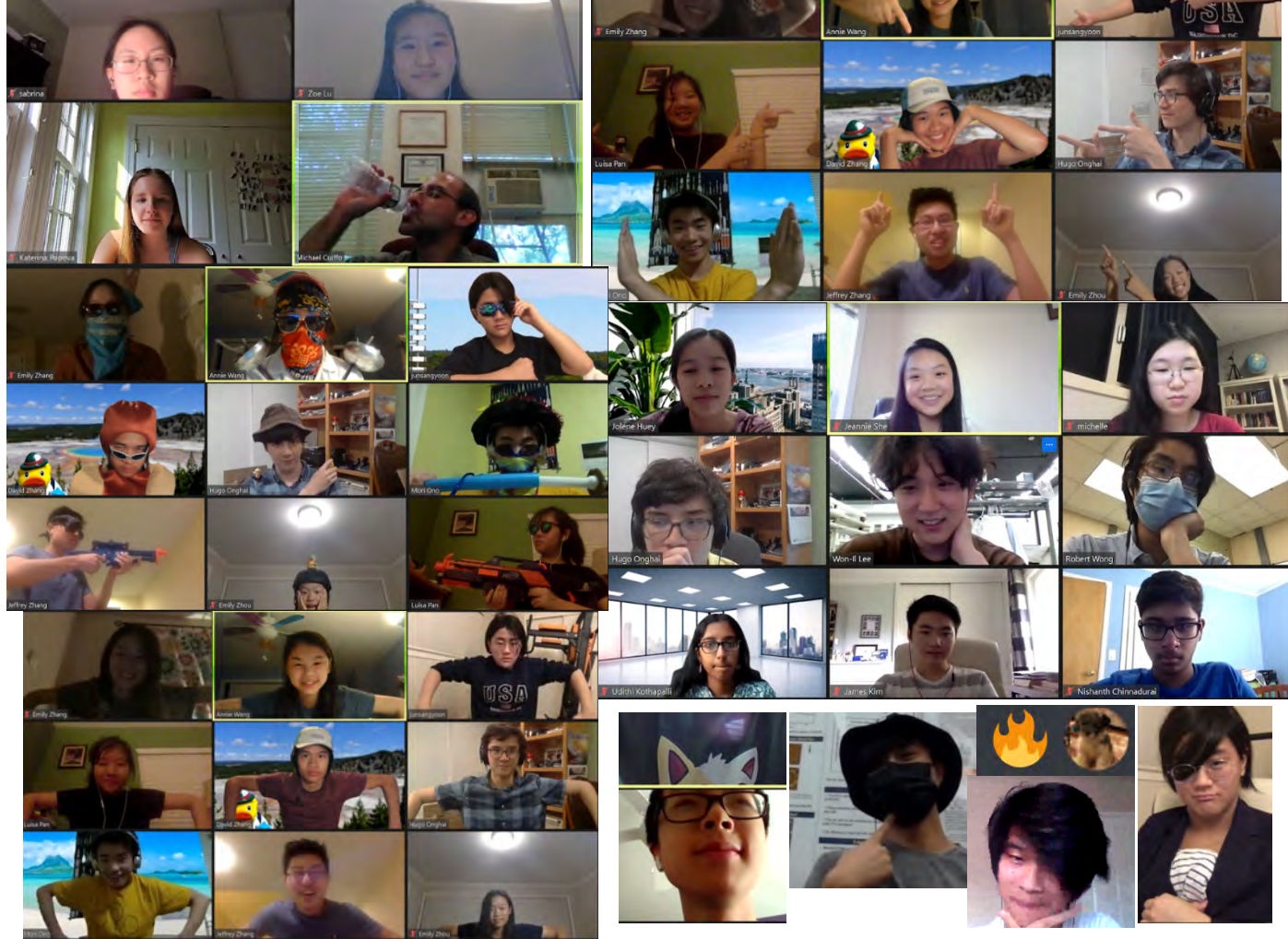


Chapman





REMOTE LEARNING



Summer Scholar Schedule of Weekly Activities

Each day starts with a mandatory group meeting at 10 AM!

Daily Schedule: Week of 6/29

MONDAY – 6/29	TUESDAY – 6/30	WEDNESDAY – 7/1	THURSDAY – 7/2	FRIDAY – 7/3
<p>10:00 am – 10:10 am AnnMarie Scheidt: Welcome to Garcia</p> <p>10:10 am – 10:30 am Introductions</p> <p>10:30 am – 11:30 am Madeline Augustin: Science & Engineering at Boeing</p> <p>11:30 am – 12:00 pm Kenneth Kaushansky: Welcome & Introduction to the Stony Brook School of Medicine</p> <p>12:00 pm – 1:00 pm LUNCH</p> <p>1:00 pm – 2:00 pm Prof. Les Perelman, MIT: Communicating Science</p> <p>2:00 pm – 3:00 pm Dr. Robert Elder: Life at the FDA</p> <p>3:00 pm – 4:00 pm Mrs. Rebecca Isseroff: Keeping a lab notebook and presenting at MRS</p>	<p>10:00 am – 12:00 pm ELS 003: Class on Laboratory Safety Biological Hazards</p> <p>12:00 pm – 1:00 pm LUNCH</p> <p>1:00 pm – 2:00 pm Dilip Gersappe: Theoretical Modeling</p> <p>2:00 pm – 3:00 pm Chang-Yong Nam: Research at Brookhaven National Labs</p> <p>3:00 pm – 4:00 pm Marcia Simon: Tissue engineering and stem cell biology</p>	<p>10:00 am – 10:10 am Fotis Sotiropoulos, Dean of Stony Brook's CEAS: Welcome</p> <p>10:10 am – 12:00 pm Dr. Ying Liu: Hazardous Chemicals & Writing the SOP</p> <p>12:00 pm – 1:00 pm LUNCH</p> <p>1:00 pm – 2:00 pm Aaron Sloutsky: Biomedical Polymers</p> <p>2:00 pm – 2:30 pm Ikshu Pandey: Research at 2019 Garcia</p> <p>2:30 pm – 3:30 pm Prof. Michael Rubinstein: Polymer Physics</p> <p>3:30 pm – 4:00 pm Prof. Michael Hadjiagrou: Advances in Bioengineering</p>	<p>10:00 am – 11:00 am Yuet (Clara) Tran: Library Training</p> <p>11:00 am – 12:00 pm Dr. Brooke Ellison: Conducting Ethical Science</p> <p>12:00 pm – 1:00 pm LUNCH</p> <p>1:00 pm – 2:00 pm Dr. Chulsung Bae</p> <p>2:00 pm – 3:00 pm Dr. Yuefan Deng</p> <p>3:00 pm – 4:00 pm Dr. Jonathan Sokolov: Working with DNA</p>	<p>10:00 am – 11:00 am Dr. Peng Zhang: Modeling Protein Structure</p> <p>11:00 am – 11:30 am Dr. Sima Mofakham: Neurosurgery Research</p> <p>11:30 am – 12:00 pm Dr. Michael Gouzman: Introduction to Electrical Engineering</p> <p>12:00 pm – 1:00 pm LUNCH</p> <p>1:00 pm – 4:00 pm Virtual Lab Tours</p> <ul style="list-style-type: none"> - LB Trough - AFM - UV/VIS Zeta Potential - 3D Printer - Molding/Instron/Impact Tester - Brabender/Pelletizer/Fibers - Contact Angle Goniometer - Confocal Microscope - Hydrogen Fuel Cell Test Station - Rheometer & Bioprinter - Cell Lab

Summer Scholar Schedule of Weekly Activities

Each day starts with a mandatory group meeting at 10 AM!

Daily Schedule: Week of 7/6

MONDAY – 7/6	TUESDAY – 7/7	WEDNESDAY – 7/8	THURSDAY – 7/9	FRIDAY – 7/10
<p>10:00 am – 11:00 am Prof. Eyal Zussman, Technion: Designing Scaffolds for Tissue Engineering</p> <p>11:00 am – 12:00 pm Prof. Richard Clark, MD</p> <p>12:00 pm – 1:00 pm LUNCH</p> <p>1:00 pm – 2:00 pm Prof. Steven Schwarz: Spin-casting Polymers</p> <p>2:00 pm – 3:00 pm Prof. Georgios Romanos</p> <p>3:00 pm – 4:00 pm Prof. Matt Tirrell: Nanomedicine based on block copolymer self- assembly</p> <p>4:00 pm – 4:30 pm Dr. Yuval Shmueli: Excel Tutorial</p>	<p>10:00 am – 10:30 am Jessica Hofflich: Facilities Quiz</p> <p>10:30 am – 11:00 am Yifan Yin: Introduction to the Spin- casting Experiment</p> <p>11:00 am – 11:30 am Dr. Jonathan Sokolov: Ellipsometry</p> <p>11:30 am – 12:00 pm FTIR</p> <p>12:00 pm – 1:00 pm LUNCH</p> <p>1:00 pm – 3:30 pm Experimental Stations with Lab Groups Part I</p> <p>3:30 pm – 4:00 pm Dr. Miriam Rafailovich: Data Analysis I</p>	<p>10:00 am – 11:00 am Prof. Ishi Talmon</p> <p>11:00 am – 3:30 pm Experimental Stations with Lab Groups Part II</p> <p>3:30 pm – 4:00 pm Dr. Miriam Rafailovich: Data Analysis II</p>	<p>10:00 am – 12:00 pm Journal Club Presentations</p> <p>12:00 pm – 1:00 pm LUNCH</p> <p>1:00 pm – 1:30 pm Dr. Michael Gouzman: Electronics & Robotics for those who are Disabled</p> <p>1:30 pm – 2:00 pm Dr. Chandramouli Sadasivan: Brain Aneurysms</p> <p>2:00 pm – 2:30 pm Dr. Xiaojun Bi: Eyegaze Technology</p> <p>2:30 pm – 3:00 pm Likun Wang & Aniket Raut: Hydrogen Fuel Cells</p> <p>3:00 pm – 4:00 pm Data Analysis for Lab Experiments</p>	<p>10:00 am – 10:30 am Dr. Peng Zhang: COVID-19 Projects</p> <p>10:30 am – 11:00 am Yuchen Zhou & Yifan Yin: Perovskite Solar Cells</p> <p>11:00 am – 12:00 pm Anthony Del Valle: DNA Projects</p> <p>12:00 pm – 1:00 pm LUNCH</p> <p>12:30 pm – 1:30 pm NIH: Ongoing COVID-19 Research</p> <p>1:30 pm – 2:00 pm Gurtej Singh & Juyi Li: Autologous Bioprinting</p> <p>2:00 pm – 2:30 pm Kuan-Che/Hiajiao: Printing scaffolds/fogging</p> <p>2:30 pm – 3:00 pm Kao Li: Fibrinogen and P12 Project</p>

Summer Scholar Schedule of Weekly Activities

Each day starts with a mandatory group meeting at 10 AM!

Daily Schedule: Week of 7/13

MONDAY – 7/13	TUESDAY – 7/14	WEDNESDAY – 7/15	THURSDAY – 7/16	FRIDAY – 7/17
<p>10:00 am – 10:30 am Jamie Jerome: From Garcia to Estée Lauder</p> <p>10:30 am – 11:00 am Fan Yang: DISC imaging and nanotoxicology</p> <p>11:00 am – 12:15 pm Ya-Chen Chuang: Dental Pulp Stem Cells</p> <p>12:15 pm – 1:00 pm LUNCH</p> <p>1:00 pm – 1:30 pm Won-Il Lee: Biosensor Projects</p> <p>1:30 pm – 2:00 pm Yu-Chung Lin & Yiwei Fang: 3D Printing Projects</p> <p>2:00 pm – 3:00 pm Dr. Yichen Guo: Nanocomposites</p> <p>3:00 pm – 4:00 pm Dr. Yuval Shmueli: Analysis of 3D printing</p>	<p>10:00 am – 12:00 pm Review of Available Projects Part I</p> <p>12:00 pm – 1:00 pm LUNCH</p> <p>1:00 pm – 4:00 pm Review of Available Projects Part II</p>	<p>10:00 am – 11:00 am Prof. Ishi Talmon: Cryo-microscopy</p> <p>11:00 am – 12:00 pm Dr. Ying Liu: Writing the SOP</p> <p>12:00 pm – 1:00 pm LUNCH</p> <p>1:00 pm – 4:00 pm Writing SOPs with Lab Groups</p>	<p>10:00 am – 11:00 am Isaac Cohen: Estée Lauder</p> <p>4:00 pm – 4:30 pm Dara Tayrien: Yoga for Young Adults</p> <p>Research and lunch as coordinated by project</p>	<p>10:00 am – 12:00 pm Spin-casting Presentations: Groups 5-10</p> <p>1:30 pm – 2:00 pm Marcia Simon: Cell Moduli and Aging</p> <p>Research and lunch as coordinated by project</p>

Summer Scholar Schedule of Weekly Activities

Each day starts with a mandatory group meeting at 10 AM!

Daily Schedule: Week of 7/20

MONDAY – 7/20	TUESDAY – 7/21	WEDNESDAY – 7/22	THURSDAY – 7/23	FRIDAY – 7/24
<p>10:00 am – 11:00 am Prof. Ed Palermo, RPI: Anti-bacterial Polymers</p> <p>4:00 pm – 4:30 pm Dara Tayrien: Yoga for Young Adults</p>	<p>10:00 am – 10:30 am Dr. Sarika Sharma: Lab Report Review</p> <p>10:30 am – 11:00 am Dr. Clement Marmorat: Chip Manufacture at Intel</p> <p>12:00 pm – 4:00 pm Dr. Jerome Cymerman: Endodontic Research</p>	<p>10:00 am – 11:00 am Spin-casting Presentations: Groups 1-4</p> <p>4:00 pm – 4:30 pm Dara Tayrien: Yoga for Young Adults</p>	<p>10:00 am – 11:00 am Prof. Stephen Walker: Microbiology</p> <p>11:00 am – 11:30 am Briefing on COVID-19, P12, and Fibrinogen Research</p> <p>3:30 pm – 4:00 pm Dr. Jonathan Sokolov: ImageJ Tutorial</p>	<p>10:00 am – 11:00 am General Meeting & Student Presentations:</p> <ul style="list-style-type: none"> - Contact angle & wetting of droplets - DISC for mental cognition - Anti-microbial coatings
<p>Research and lunch as coordinated by project</p>	<p>Research and lunch as coordinated by project</p>	<p>Research and lunch as coordinated by project</p>	<p>Research and lunch as coordinated by project</p>	<p>Research and lunch as coordinated by project</p>

Summer Scholar Schedule of Weekly Activities

Each day starts with a mandatory group meeting at 10 AM!

Daily Schedule: Week of 7/27

MONDAY – 7/27	TUESDAY – 7/28	WEDNESDAY – 7/29	THURSDAY – 7/30	FRIDAY – 7/31
<p>10:00 am – 11:00 am Prof. Perumal Ramasamy: Nanocomposites</p> <p>11:00 am – 11:15 am Student Presentations: - DNA</p> <p>3:00 pm – 4:00 pm Anantha Desikan: Science in the Chemical Industry</p> <p>4:00 pm – 4:30 pm Dara Tayrien: Yoga for Young Adults</p>	<p>10:00 am – 10:45 am Mariah Geritano: 3D printing the surgical arena</p> <p>10:45 am – 11:45 am Dr. Anna Silverstein: P-values & Statistical Analysis</p> <p>11:45 am – 12:00 pm Student Presentations: - Nanocomposites - Flame retardant</p>	<p>10:00 am – 11:00 am General Meeting & Student Presentations: - Phase segregation & nanocomposites</p> <p>4:00 pm – 4:30 pm Dara Tayrien: Yoga for Young Adults</p>	<p>10:00 am – 10:30 am Dr. Dennis Galanakis, MD</p> <p>10:30 am – 11:30 am Student Presentations: - Biosensors - P12 fiber formation</p>	<p>10:00 am – 10:30 am Group Picture Day: CAMERAS ON!!!</p> <p>10:30 am – 11:30 am Student Presentations - Fogging - Theory and modeling groups - Virus structure on surfaces</p>
Research and lunch as coordinated by project	Research and lunch as coordinated by project	Research and lunch as coordinated by project	Research and lunch as coordinated by project	Research and lunch as coordinated by project

Summer Scholar Schedule of Weekly Activities

Each day starts with a mandatory group meeting at 10 AM!

Daily Schedule: Week of 8/3

MONDAY – 8/3	TUESDAY – 8/4	WEDNESDAY – 8/5	THURSDAY – 8/6	FRIDAY – 8/7
<p>10:00 am – 11:00 am Science Video Blow Out Showcasing of at-home experiments!</p> <p>11:00 am – 12:00 pm Dr. Shlomo Magdassi: From the Gutenberg Bible to 4D printing</p> <p>4:00 pm – 4:30 pm Dara Tayrien: Yoga for Young Adults</p>	<p>10:00 am – 11:00 am General Meeting & Student Presentations: - Fuel cells - Dental research</p> <p>3:30 pm – 4:30 pm Marcia Simon: Review of plaque assay protocol</p>	<p>10:00 am – 11:00 am Prof. Nitin Padture: Perovskite Photovoltaics</p> <p>11:00 am – 12:00 pm Student Presentations: - All bioprinting groups - Brain aneurysm - Gerontology</p> <p>4:00 pm – 4:30 pm Dara Tayrien: Yoga for Young Adults</p>	<p>10:00 am – 11:00 am Prof. Abraham Ulman: Self-Assembly</p> <p>11:00 am – 11:30 am Student Presentations: - All electronics groups - Eyegaze technology</p>	<p>10:00 am – 11:00 am James Centino: Filing for Patents</p> <p>11:00 am – 11:30 am Student Presentations - Neurogenic differentiation - Graphene oxide - Cyberarm technology</p> <p>1:00 pm – 1:15 pm Prof. Maurie McInnis, President of Stony Brook University: Welcome</p>
<p>Research and lunch as coordinated by project</p>	<p>Research and lunch as coordinated by project</p>	<p>Research and lunch as coordinated by project</p>	<p>ABSTRACTS DUE @ 8 pm</p> <p>Research and lunch as coordinated by project</p>	<p>SYMPOSIUM ON MONDAY</p> <p>Research and lunch as coordinated by project</p>

Summer Scholar Schedule of Weekly Activities

Each day starts with a mandatory group meeting at 10 AM!

Daily Schedule: Week of 8/10

MONDAY – 8/10

THE END OF THE 7 WEEKS AT GARCIA!

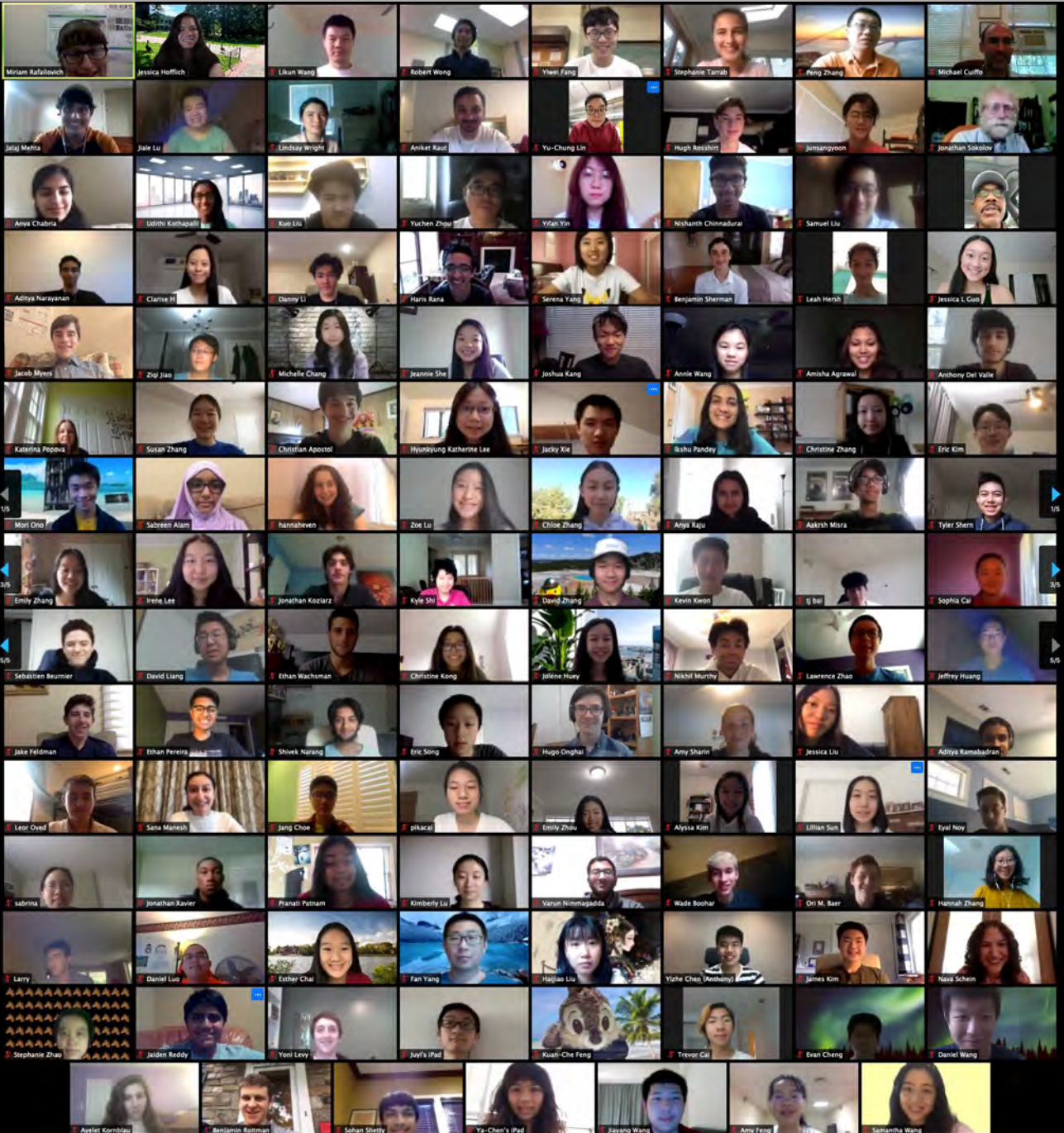
10:00 am – 12:00 pm
Garcia Symposium:
Music quintet followed by
student presentations



You are cordially invited to attend
the
Garcia 2020 Research Symposium
10:00-11:30 AM

Monday, August 10, Via Zoom:

<https://stonybrook.zoom.us/j/94613288338?pwd=WXZmY2MvMWZ5K1E0UkRVWEt1bGxhdz09>
Meeting ID: 946 1328 8338, Password: 650265





The Garcia Research Scholar program continued this summer with a brave and dedicated cohort of students who survived a pandemic, a hurricane, and power outages... and yet worked hard to produce world class research, guided by ethical principles, on stem cell biology, nanocomposites, energy, computer modeling, robotics, and COVID-19 . Their love of science is matched only by their talent in music, and the performing arts.
Please sit back and enjoy this program that they have prepared for you.

10:00	Wind Quartet: Prof. John Luckner Jerome and Garcia Students Arrangement: Jamie Jerome
10:10 AM-10:20AM	Ethical consideration in the response to COVID-19: Chairs: Jessica Guo , Ward Melville High School & Sebastien Beurnier , Stuyvesant High School
	<i>Hospital Triage</i> Lingzi (Susan) Zhang , The Hockaday School, Dallas, TX Jessica Guo , Ward Melville High School, East Setauket, NY
	<i>Telehealth</i> Jolene Huey , Arcadia High School, Arcadia, CA Hugo Onghai , Earl L. Vandermeulen High School, Port Jefferson, NY Jeannie She , Walt Whitman High School, Bethesda, MD Amisha Agrawal , University High School, Johnson City, TN Anya Chabria , The Wheatley School, Old Westbury, NY Clarise Han , Mission San Jose High School, Fremont, CA Tyler Shern , Mission San Jose High School, Fremont, CA Lillian Sun , Thomas Jefferson High School for Science and Technology, Alexandria, VA Serena Yang , Dougherty Valley High School, San Ramon, CA Joshua Kang , Westwood High School, Austin, TX

Logo courtesy Samantha (Jing) Wang: The grey dots represent coronavirus, but they are shot through by white lines, which are the spears of human wisdom, especially scientists' hard work. These lines can also be viewed as internet connections, which linked Garcia program to us in this special summer.



Virtual
Symposium
2020

	<p><i>Remote Learning</i></p> <p>Jeffrey Zhang, Centerville High School, Centerville, OH Luisa Pan, The Harker School, San Jose, CA Annie Wang, Central Bucks High School East, Doylestown, PA Emily Zhang, General Douglas MacArthur High School, Levittown, NY Emily Zhou, The Harker School, San Jose, CA</p>
10:20AM	Science Video I
10:22AM–10:40AM	<p>SARS COV-2: Simulation and Experiment Chairs: Esther Chai, <i>Harvard University</i> & Jacob Myers, <i>The University of Scranton</i></p>
	<p><i>Coarse-Grained Modeling For Simulation of SARS-CoV-2 Spike Glycoprotein</i></p> <p>David Zhang, Fremont High School, Sunnyvale, CA Aditya Narayanan, College Station High School, College Station, TX Aditya Ramabadran, Lynbrook High School, San Jose, CA</p>
	<p><i>Monte Carlo Simulation Studies of SARS-CoV-2 Spike Glycoproteins</i></p> <p>Clarise Han, Mission San Jose High School, Fremont, CA</p>
	<p><i>Differential behavior of SARS-CoV-2 spike glycoprotein in varying ion concentrations</i></p> <p>Lillian Sun, Thomas Jefferson High School for Science and Technology, Alexandria, VA Amy Feng, Pittsford Sutherland High School, Pittsford, NY</p>
	<p><i>Defining respiratory droplet characteristics on different surfaces - implications for viral transmission</i></p> <p>Junsang Yoon, Cupertino High School, Cupertino, CA Anand Srinivasan, The Westminster Schools, Atlanta, GA Jacob F Myers, The University of Scranton, Scranton, PA</p>
	<p><i>Fogging B. Atrophaeus, E. Coli, and E. Faecalis to Determine the Efficacy of Hypochlorous Solution for COVID-19 Applications</i></p> <p>Jessica Liu, Northwood High School, Irvine, CA Kuo Liu, The High School Affiliated to Renmin University of China, Beijing, China Sana Manesh, Sage Hill School, Newport Coast, CA Esther Chai, Harvard University, Cambridge, MA Christine Kong, University of Pennsylvania, Philadelphia, PA</p>
	<p><i>Refining Synthesis of Copper Nanoparticles Formed in Situ on Polylactic Acid Composites for Antimicrobial Applications</i></p> <p>Zoe Lu, Thomas Jefferson High School for Science and Technology, Alexandria, VA Katerina Popova, Hackley School, Tarrytown, NY Sabrina Su, Poolesville High School, Poolesville, MD Serena Yang, Dougherty Valley High School, San Ramon, CA</p>



	<p><i>Molecular Imprinted Biosensor for SARS-CoV-2 Detection</i> Michelle Chang, Seoul International School, Seoul, South Korea Nishanth Chinnadurai, East Meadow High School, East Meadow, NY Jolene Huey, Arcadia High School, Arcadia, CA James Kim, Great Neck South High School, Great Neck, NY Udithi Kothapalli, Saint Anthony's High School, Melville, NY Hugo Onghai, Earl L. Vandermeulen High School, Port Jefferson, NY Jeannie She, Walt Whitman High School, Bethesda, MD</p>
	<p><i>Machine Learning for Long-Term Molecular Dynamics of SARS-CoV-2 Spike Glycoproteins</i> Larry Huang, University of Pennsylvania, Philadelphia, PA David Liang, Ward Melville High School, Stony Brook, NY</p>
10:40AM–10:47AM	<p>Nucleic acids and proteins on surfaces: Chairs: Anthony Del Valle, Stony Brook University & Ikshu Pandey, Johns Hopkins University</p>
	<p><i>Transfer printing of DNA molecules from PDMS (polydimethylsiloxane) to hydrophilic PAA (polyacrylic acid) surfaces for application to sequencing</i> Aakrsh Misra, Dana Hills High School, Dana Point, CA Anya Raju, Basis Independent Silicon Valley, San Jose, CA Daniel Wang, Huron High School, Ann Arbor, MI Eyal Noy, Rochelle Zell Jewish High School, Deerfield, IL Hyunkyung Katherine Lee, Conestoga High School, Berwyn, PA Leor Oved, HAFTR High School, Cedarhurst, NY Samarjit Kaushik, Tesla STEM High School, Redmond, WA Qianyi (Stephanie) Zhao, Princeton International School of Mathematics and Science, Princeton, NJ</p>
	<p><i>Minimizing Surface-Initiated Thrombogenesis Using the Fibronectin-Derived Peptide P12</i> Sabreen Alam, Portola High School, Irvine, CA Ori Baer, Hebrew Academy of Nassau County High School, Plainview, NY Sebastien Beurnier, Stuyvesant, Manhattan, NY Jang Choe, Ed W Clark High School, Las Vegas, NV Kevin Kwon, Niskayuna High School, Schenectady, NY Nikhil Murthy, Archbishop Mitty High School, San Jose, CA Ikshu Pandey, Johns Hopkins University, Baltimore, MD</p>
	<p><i>Enhancing the Action of Cellulase on Biomass</i> Nava Schein, HAFTR High School, Cedarhurst, NY</p>



Virtual
Symposium
2020

10:47AM– 10:55AM	Stem Cell Differentiation in Skin and Dentistry Chair: Kimberly Lu , <i>Stony Brook University</i>
	<i>Effect of Fibrinogen-Gelatin Scaffolds on Dental Pulp Stem Cell Differentiation</i> Tianjian Bai , Huron High School, Ann Arbor, MI Evan Cheng , Syosset High School, Syosset, NY Jake Feldman , Plainview-Old Bethpage John F. Kennedy High School, Old Bethpage, NY Alyssa Kim , New Hyde Park Memorial High School, New Hyde Park, NY
	<i>Effects of Aging and Seacret Broth on Cell and ECM Modulus of Keratinocytes</i> Lingzi (Susan) Zhang , The Hockaday School, Dallas, TX Irene Lee , Jericho High School, Jericho, NY Chloe Zhang , Jericho High School, Jericho, NY Haris Rana , Southside High School, Fort Smith, AR
	<i>Cytotoxicology of Bone Graft Materials</i> Senhuang Cai , Queens College, Queens, NY
	<i>Investigating the Effect of Bioprinting of Organotypic Skin and Angiogenesis Under Confinement</i> Leah Hersh , Central High School, Hollis, NY Joshua Kang , Westwood High School, Austin, TX Mori Ono , Community High School, Ann Arbor, MI Qianyi (Stephanie) Zhao , Princeton International School of Mathematics and Science, Princeton, NJ Annie Wang , Central Bucks High School East, Doylestown, PA Samantha Wang , Saint Mark's School, Southborough, MA Jonathan Xavier , Valley Stream North High School, Franklin Square, NY Kimberly Lu , Stony Brook University, Stony Brook, NY
	<i>Regulating Substrate Mechanics to Achieve Neurogenic Differentiation of Dental Pulp Stem Cells Using Polybutadiene and Graphene/Graphene Oxide Thin Films</i> Samuel Liu , Olathe North High School, Olathe, KS Shivek Narang , Stanford Online High School, Fremont, CA
10:55AM	Science Video II
10:57AM– 11:05AM	Modalities for the Human/Computer Interface Chair: Amisha Agrawal , <i>University High School</i>
	<i>Analytical Method for Eye Gaze Trajectory Calibration</i> Trevor Cai , Canyon Crest Academy, San Diego, CA Jaiden Reddy , Ed W Clark High School, Las Vegas, NV Jiayang Wang , Trinity-Pawling School, Pawling, NY Hannah Zhang , Canyon Crest Academy, San Diego, CA



	<p><i>Recognizing Facial Nerve Innervation for Establishing Reaction Times Using Digital Image Skin Correlation</i></p> <p>Amisha Agrawal, University High School, Johnson City, TN Sophia Cai, Barrington High School, Barrington, IL Wade Boohar, Olathe North High School, Olathe, KS</p>
	<p><i>The Implementation of a Distant Computer Controlled Robotic Arm for the Aid of the Disabled</i></p> <p>Ethan Pereira, West Windsor-Plainsboro High School North, Plainsboro, NJ Hugh Rosshirt, South Side High School, Rockville Centre, NY Ethan Wachsman, Roslyn High School, Roslyn Heights, NY Ayelet Kornblau, Samuel H Wang High School, Bayside, NY Yonatan Levy, HANC Highschool, Uniondale, NY</p>
11:05AM-11:12AM	<p>Nanocomposites: Flame retardants, 3-D printing, and Diffusion Chair: Larry Huang, University of Pennsylvania</p>
	<p><i>Enhancing the Flame Retardancy of Biodegradable and Tough Polymer/Clay Nanocomposites</i></p> <p>Christian Apostol, Ward Melville, East Setauket, NY Lawrence Zhao, University Laboratory High School, Urbana, IL Jiale Lu, Princeton International School of Mathematics and Science, Princeton, NJ</p>
	<p><i>Investigating and Comparing the Resistance to Tensile Testing of Molded and 3D Printed PLA/PP Polymer Blends</i></p> <p>Daniel Luo, Monroe Woodbury High School, Central Valley, NY</p>
	<p><i>Simulating the Diffusion and Adsorption of Gas through UiO-66 and NU-1000 Metal-Organic Frameworks using the Lattice-Boltzmann Method</i></p> <p>Eric J. Kim, Stuyvesant High School, New York, NY Kevin Gu, Deerfield Academy, Deerfield, MA Jalaj Mehta, Hauppauge High School, Hauppauge, NY</p>
11:12AM	Science Video III
11:14AM-11:20AM	<p>Hydrogels Chairs: Ikshu Pandey, Johns Hopkins University & Jeffrey Huang, University of Pennsylvania</p>
	<p><i>Using Coarse-Grained Molecular Dynamics to Model Hydrogel Viscosity</i></p> <p>Hannah Even, Staples High School, Westport, CT Kyle Shi, Dublin High School, Dublin, CA Eric Song, Vernon Hills High School, Vernon Hills, IL</p>



Virtual
Symposium
2020

	<p><i>Developing Thermally Responsive Polymer Gels for Aneurysm Occlusion</i> Anya Chabria, The Wheatley School, Old Westbury, NY Jessica Guo, Ward Melville High School, East Setauket, NY Varun Nimmagadda, Novi High School, Novi, MI Tyler Shern, Mission San Jose High School, Fremont, CA Stephanie Tarrab, Yeshivah of Flatbush Joel Braverman High School, Brooklyn, NY Jeffrey Zhang, Centerville High School, Centerville, OH Emily Zhou, The Harker School, San Jose, CA Jeffrey Huang, University of Pennsylvania, Philadelphia, PA Ikshu Pandey, Johns Hopkins University, Baltimore, MD</p>
11:20AM– 11:30AM	<p>Renewable energy: Solar Fuel Cells Chair: Christine Kong, <i>University of Pennsylvania</i></p>
	<p><i>Using and optimizing cellulose filter paper proton exchange membranes for hydrogen fuel cells</i> Jonathan Koziarz, South Side High School, Rockville Centre, NY Jacky Xie, Harborfields High School, Greenlawn, NY</p>
	<p><i>Enhancing the Performance of Anion Exchange Membrane Fuel Cells by Coating Membranes with Graphene Oxide</i> Amy Sharin, Lawrence High School, Cedarhurst, NY Sohan Shetty, Half Hollow Hills High School East, Melville, NY Lindsay Wright, Del Norte High School, San Diego, CA Emily Zhang, General Douglas MacArthur High School, Levittown, NY</p>
	<p><i>Size Optimization of Gold Nanoparticles Functionalized on PEMFC Interfaces to Increase Power Efficiency</i> Ziqi Jiao, Princeton Int'l School of Maths & Sci., Princeton, NJ Danny Li, Jericho High School, Jericho, Long Island, NY Benjamin Sherman, George W. Hewlett High School, Hewlett, NY Christine Zhang, Saratoga High School, Saratoga, CA</p>
	<p><i>Study of the Formation of Different Electron Transport Layer (ETL) Materials and the Impact on Perovskite Solar Cell Performance</i> Yizhe (Anthony) Chen, Shanghai Pinghe School, Shanghai, China Luisa Pan, The Harker School, San Jose, CA Pranati Patnam, Herricks High School, New Hyde Park, NY Benjamin Roitman, SAR High School, Bronx, NY</p>
11:30AM	Science Video IV and Closing Remarks



Ethical consideration in the response to Covid-19 – Full Projects
<p><i>Community-Focused Data to Drive Reform in Suffolk County Police Department</i> Jeannie She, Walt Whitman High School, Bethesda, MD</p>
<p><i>Stem Cell Policy in India; Hospital Triage Policy in Texas during COVID-19</i> Lingzi (Susan) Zhang, The Hockaday School, Dallas, TX</p>
<p><i>Medical Legal Partnerships in the Greater New York Area - Effective Implementation</i> Jolene Huey, Arcadia High School, Arcadia, CA Hugo Onghai, Earl L. Vandermeulen High School, Port Jefferson, NY Jeannie She, Walt Whitman High School, Bethesda, MD</p>
<p><i>An Examination of Hybrid Remote Learning Models to Optimize Student Academic and Social Performance</i> Luisa Pan, The Harker School, San Jose, CA Annie Wang, Central Bucks High School East, Doylestown, PA Emily Zhang, General Douglas MacArthur High School, Levittown, NY</p>
<p><i>Bioethical Analysis of New York Hospital Triage Policies in the Age of COVID-19; Ethical Analysis of New York State Ventilator Allocation Policies in Relation to Those with Disabilities in the Age of COVID-19</i> Jessica Guo, Ward Melville High School, East Setauket, NY</p>
<p><i>Japan’s Stance on Stem Cell Research Policies</i> Amisha Agrawal, University High School, Johnson City, TN Anya Chabria, The Wheatley School, Old Westbury, NY Clarise Han, Mission San Jose High School, Fremont, CA Mori Ono, Community High School, Ann Arbor, MI Haris Rana, Southside High School, Fort Smith, AR Tyler Shern, Mission San Jose High School, Fremont, CA Lillian Sun, Thomas Jefferson High School for Science and Technology, Alexandria, VA Stephanie Tarrab, Yeshivah of Flatbush Joel Braverman High School, Brooklyn, NY Daniel Wang, Huron High School, Ann Arbor, MI Serena Yang, Dougherty Valley High School, San Ramon, CA</p>
<p><i>Optimizing Remote Learning for Low-Income Students</i> Jeffrey Zhang, Centerville High School, Centerville, OH Emily Zhou, The Harker School, San Jose, CA</p>
<p><i>Ethics of Telehealth in Psychology</i> Amisha Agrawal, University High School, Johnson City, TN Anya Chabria, The Wheatley School, Old Westbury, NY Clarise Han, Mission San Jose High School, Fremont, CA</p>



Virtual
Symposium
2020

<p>Tyler Shern, Mission San Jose High School, Fremont, CA Lillian Sun, Thomas Jefferson High School for Science and Technology, Alexandria, VA Serena Yang, Dougherty Valley High School, San Ramon, CA</p>
<p><i>The Effect of Neonatal Telehealth on Early Release and Remote Monitoring - A Comprehensive Study</i> Jolene Huey, Arcadia High School, Arcadia, CA Joshua Kang, Westwood High School, Austin, TX</p>
<p><i>Role of U.S. Government in Accessibility of Assistive Technology for People with Disabilities</i> Amisha Agrawal, University High School, Johnson City, TN Varun Nimmagadda, Novi High School, Novi, MI Mori Ono, Community High School, Ann Arbor, MI Daniel Wang, Huron High School, Ann Arbor, MI Serena Yang, Dougherty Valley High School, San Ramon, CA</p>
<p><i>Special Education in Remote Learning - Shortcomings and Solutions</i> Junsang Yoon, Cupertino High School, Cupertino, CA David Zhang, Fremont High School, Sunnyvale, CA</p>

Garcia 2020 Logo designed by Samantha (Jing) Wang

We gratefully acknowledge support from the Louis Morin Charitable Trust

SARS COV-2 SIMULATION AND EXPERIMENT

*Haijiao Liu, Robert Wong, Ziji
(Jason) Zhang, Won-Il Lee
and Kuan-Che Feng*

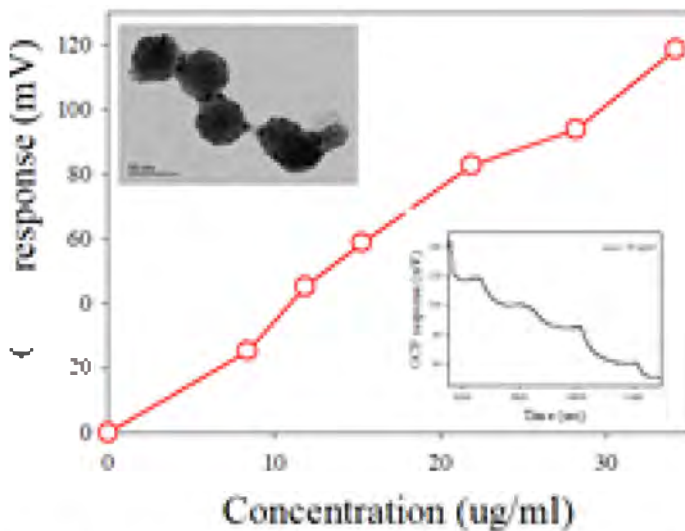


Fig. 1: Average potentiometric response for increasing concentration of hemoglobin.
Inset: TEM image of H1N1 (Top), displays the OCP response in terms of time (bottom).

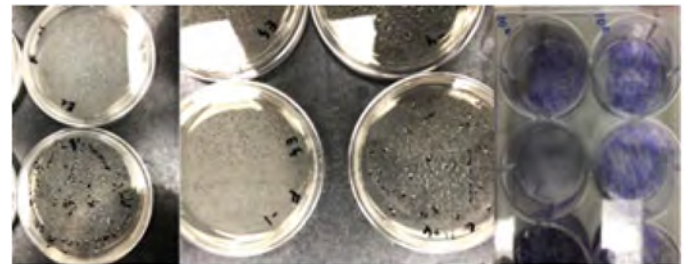


Figure 1: Fogged and Control *E. Coli*.

Figure 2: Fogged and Control *E. Faecalis*.

Figure 3: 10^{-2} dilutions for plaque assay calibration.

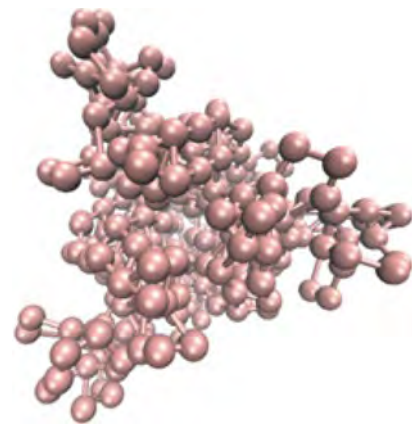


Fig 1: SBCG Model

Coarse-Grained Modeling For Simulation of SARS-CoV-2 Spike Glycoprotein

David Zhang¹, Aditya Narayanan², Aditya Ramabadrans³, Ziji (Jason) Zhang⁴, Peng Zhang⁴

¹Fremont High School, Sunnyvale, CA, 94087; ²College Station High School, College Station, TX, 77845; ³Lynbrook High School, San Jose, CA, 95129; ⁴Department of Applied Mathematics and Statistics, Stony Brook University, NY, 11794

Molecular dynamics is a powerful computational tool for studying the physical movements of and interactions between macromolecules such as proteins. All-atom, fine-grained models are frequently used for molecular dynamics simulations as they are known to provide accurate results¹; however, simulating these models can be quite expensive in computing time and resources.

Coarse-grained (CG) models offer a cheaper alternative to all-atom models, using a few number of particles known as “beads” to represent macromolecules. We developed two types of CG models for the 6VXX SARS-CoV-2 spike glycoprotein² in a closed state and evaluated the robustness of our CG models with comparison to atomic-scale simulation. The two coarse-graining techniques of interest are shape-based coarse graining (SBCG) and residue-based coarse graining (RBCG). SBCG models assign beads to represent the overall topology of the protein, while RBCG models assign beads to represent individual protein residues.

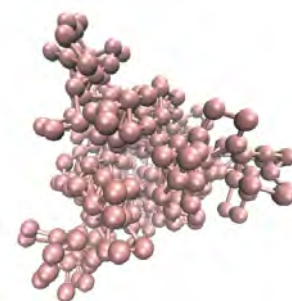


Fig 1: SBCG Model

The SBCG model (Fig. 1) consists of 355 beads, with approximately 150 atoms per bead. In order to provide accurate results with this model, nonbonded Lennard-Jones and bonded interaction parameters had to be generated from an existing all-atom simulation. The bonded interaction parameters were tuned until the stiffness constants deviated less than 25% from those derived from the all-atom simulation.

The RBCG model (Fig. 2) consists of 6498 beads, with approximately 7 atoms per bead. We built the model using VMD's CG Builder GUI³ along with the RBCG 2007 topology file inside the Martini force field. We then solvated the model with Martini water and ionized the model with Na⁺ and Cl⁻ ions.



Fig 2: RBCG Model

Then, after minimizing potentials for 10,000 steps, we successfully ran

NAMD⁴ simulations with multiple runs of incrementally increasing timesteps up to 14 fs.

To determine the robustness of our CG models, we will run verification and validation simulations and compare their results to a control all-atom simulation. The setup will involve a single 6VXX protein solvated in a water box with neutralizing ions at a temperature of 310 K. Finally, we will compare the RMSD values from the CG simulations to the ground truth values from an atomic scale simulation.

¹ Gunsteren, W. F., Dolenc, J., & Mark, A. E. (2008). Molecular Simulation as an aid to experimentalists [Abstract]. *Current Opinion in Structural Biology*, 18(2). doi:https://doi.org/10.1016/j.sbi.2007.12.007

² Walls, A. C., Park, Y., Tortorici, M. A., Wall, A., McGuire, A. T., & Veesler, D. (2020). Structure, Function, and Antigenicity of the SARS-CoV-2 Spike Glycoprotein. *Cell*, 181(2). doi:10.1016/j.cell.2020.02.058

³ Humphrey, W., Dalke, A. and Schulten, K., "VMD - Visual Molecular Dynamics", *J. Molec. Graphics*, 1996, vol. 14, pp. 33-38.

⁴ James C. Phillips, David J. Hardy, Julio D. C. Maia, John E. Stone, Joao V. Ribeiro, Rafael C. Bernardi, Ronak Buch, Giacomo Fiorin, Jerome Henin, Wei Jiang, Ryan McGreevy, Marcelo C. R. Melo, Brian K. Radak, Robert D. Skeel, Abhishek Singharoy, Yi Wang, Benoit Roux, Aleksei Aksimentiev, Zaida Luthey-Schulten, Laxmikant V. Kale, Klaus Schulten, Christophe Chipot, and Emad Tajkhorshid. Scalable molecular dynamics on CPU and GPU architectures with NAMD. *Journal of Chemical Physics*, 153:044130, 2020. doi:10.1063/5.0014475

Monte Carlo Simulation Studies of SARS-CoV-2 Spike Glycoproteins

Clarise Han¹, Karin Hasegawa², Peng Zhang³, Miriam Rafailovich⁴

¹Mission San Jose High School, Fremont, CA 94539

²Department of Applied Mathematics and Statistics, Stony Brook University, Stony Brook, NY 11794

³Department of Biomedical Engineering, Stony Brook University, Stony Brook, NY 11794

⁴Department of Materials Science and Engineering, Stony Brook University, Stony Brook, NY 11794

Given the severity of the COVID-19 pandemic caused by the novel SARS-CoV-2 coronavirus, it is of the utmost importance to develop effective approaches for treatment and prevention. Efforts to develop drugs to attenuate viral function are underway, but a challenge has been the identification of suitable protein targets for disruption due to our sparse understanding of the underlying mechanisms by which the virus binds to receptors¹. The development of personal protective equipment (PPE) especially for people working in clinical environments also relies on comprehensive binding analysis of surface stability and binding intensity of the virus on certain substrates². In this study, we aimed to answer such questions through the investigation of conformational transitions of SARS-CoV-2 spike glycoproteins during binding using computer simulations.

Two main methods for such computer simulations are molecular dynamics (MD) and Monte Carlo (MC). MD simulations are based on trajectories determined by Newton's equations of motion and use small time steps typically on the order of femtoseconds, thus making the simulations computationally expensive. MC simulations generate random movements based on probability distributions at each step, which has often been found to be more computationally efficient. As such, we employ MC methods as implemented in the Cassandra³ and GOMC (GPU-optimized MC)⁴ softwares.

Initial simulations of pentane in its vapor and liquid phases under a grand canonical ensemble were run using Cassandra and calculations of properties such as internal system density and number of molecules are shown in Fig. 2. GOMC is employed for simulations of the closed state 6vxx SARS-CoV-2 spike glycoprotein⁵. Our system configuration consists of a 6vxx protein solvated in a water box as seen

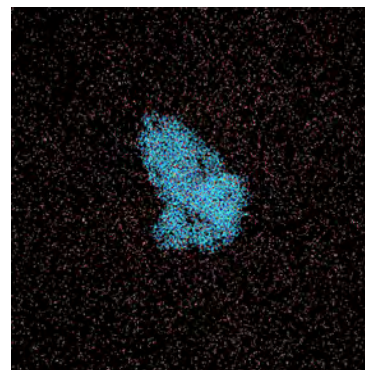


Figure 1. 6vxx spike glycoprotein solvated in a water box viewed using VMD

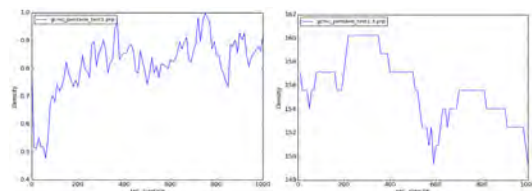


Figure 2. Density profiles across MC sweeps. Left. Pentane in the vapor phase. Right. Pentane in the liquid phase

in Fig. 1 to replicate the real-world system of the virus in a water droplet. Simulations are run in an NPT ensemble under conditions of 1 atm and room temperature, 297 Kelvins. Scripts were developed to randomly generate the initial positions of the protein and water molecules and atomic and molecular movements like translations and rotations based on probability distributions. After obtaining a suitable parameter file, we plan to implement it into the input control file to complete the simulation.

Ultimately, we aim to efficiently simulate conformational changes of SARS-CoV-2 spike glycoproteins during binding in order to allow scientists to make more informed decisions on developments of drugs and PPE to treat and prevent infection.

¹ Sanders JM, Monogue ML, Jodlowski TZ, Cutrell JB. Pharmacologic Treatments for Coronavirus Disease 2019 (COVID-19): A Review. *JAMA*. 2020;323(18):1824–1836. doi:10.1001/jama.2020.6019

² Stewart CL, Thornblade LW, Diamond DJ, Fong Y, Melstrom LG. Personal Protective Equipment and COVID-19: A Review for Surgeons. *Ann Surg*. 2020;10.1097/SLA.0000000000003991. doi:10.1097/SLA.0000000000003991

³ Shah JK, Marin-Rimoldi E, Mullen RG, et al. Cassandra: An open source Monte Carlo package for molecular simulation. *J Comput Chem*. 2017;38(19):1727-1739. doi:10.1002/jcc.24807

⁴ Nejahi Y, Barhaghi MS, Mick J, Jackman B, Rushaidat K, Li Y, Schwiebert L, Potoff J. GOMC: GPU Optimized Monte Carlo for the Simulation of Phase Equilibria and Physical Properties of Complex Fluids. *SoftwareX* 2019;9:20-27. doi: 10.1016/j.softx.2018.11.005

⁵ Walls AC, Park YJ, Tortorici MA, Wall A, McGuire AT, Veesler D. Structure, Function, and Antigenicity of the SARS-CoV-2 Spike Glycoprotein. *Cell*. 2020;181(2):281-292.e6. doi:10.1016/j.cell.2020.02.058

Differential behavior of SARS-CoV-2 spike glycoprotein in varying ion concentrations

Amy Feng¹, Lillian Sun², Kaitlyn Swayze³, Peng Zhang⁴

¹Pittsford Sutherland High School, Pittsford, NY 14534, ²Thomas Jefferson High School for Science and Technology, Alexandria, VA 22312, ³Stony Brook University, NY 11794

Previous studies have uncovered the protein structure of the SARS-CoV-2 spike glycoprotein [1]. In addition, it has been shown that the ion concentration of a solution has significant effects on protein behavior [2]. Understanding the changes that different ion concentrations induce on a protein's structure has important clinical impact, such as aiding in disease diagnosis, prognosis, and development of therapeutics for SARS-CoV-2.

In this study, we aimed to investigate structural changes in the SARS-CoV-2 spike glycoprotein when placed in varying ion concentrations. We simulated the protein's behavior using molecular dynamics (MD). The protein was simulated in two concentrations, a control and 0.6M. We extracted the root-mean-square deviation (RMSD) for analysis.

We fitted an Autoregressive Integrated Moving Average (ARIMA) model on the RMSD data to evaluate the trends in the two concentrations. ARIMA is a class of linear models that can be used to forecast future values after being trained on the past values in the data. In this case, we trained ARIMA on the first 70% of the datasets and evaluated the forecast on the remaining 30% by comparing it to the actual data. The model has a less accurate forecast in the 0.6M concentration than the control (Fig. 1). Furthermore, the increasing trend in the 0.6M is longer than the increasing trend in the control, indicating that the protein is less stable in the 0.6M concentration than the control.

In the 0.6M concentration, more time is needed for the spike protein to stabilize. This study used 237 ns of simulation data. For the future, we will simulate the protein in higher concentrations for a longer period of time. In addition, we will conduct principal component analysis (PCA) and other analysis methods on the data.

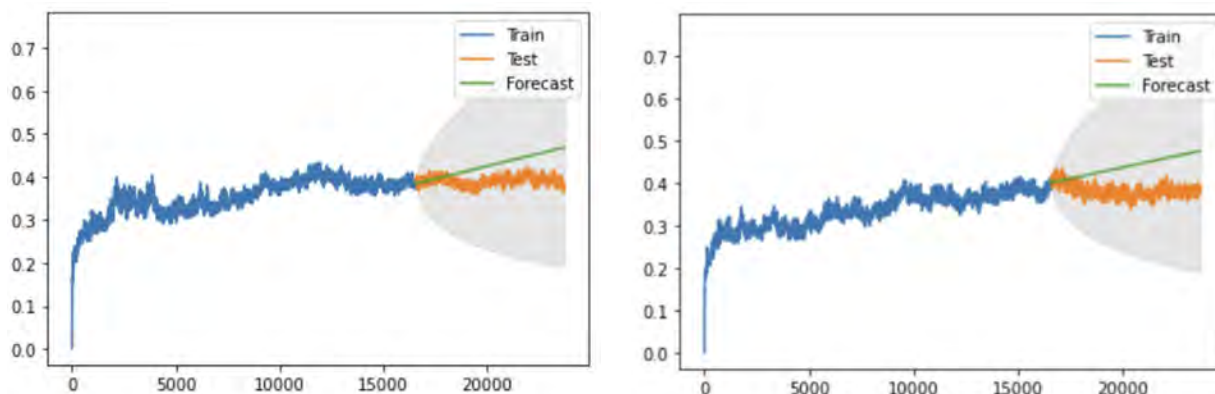


Fig. 1. a) ARIMA forecast on control simulation data. **b)** ARIMA forecast on 0.6M simulation data.

[1] Walls, Alexandra C., et al. "Structure, Function, and Antigenicity of the SARS-CoV-2 Spike Glycoprotein." *Cell*, vol. 181, no. 2, 2020, doi:10.1016/j.cell.2020.02.058.

[2] Batoulis, H., Schmidt, T., Weber, P. *et al.* Concentration Dependent Ion-Protein Interaction Patterns Underlying Protein Oligomerization Behaviours. *Sci Rep* 6, 24131 (2016). <https://doi.org/10.1038/srep24131>

Defining respiratory droplet characteristics on different surfaces: implications for viral transmission

Junsang Yoon¹, Anand Srinivasan², Jacob Myers^{3,4}, Fan Yang⁴, Miriam Rafailovich⁴

¹Cupertino High School, CA, 95051; ²The Westminster Schools, GA, 30324; ³Department of Chemistry, The University of Scranton, PA, 18510; ⁴Department of Materials Science and Chemical Engineering, Stony Brook University, NY, 11794

SARS-CoV-2 (CoV) has sickened millions and killed hundreds of thousands since emerging less than a year ago. Aerosol transmission of CoV in respiratory droplets is well-established, but its capacity for fomite transmission is not well understood^{1, 2}. Previous studies dealing with fomite transmission often test viruses in solutions that fail to account for the complexity of respiratory droplets, which include a complex mixture of salts, proteins and surfactants. Using an accurate respiratory droplet when studying the viability of viruses on surfaces is important because previous work has indicated significantly longer survival time in human respiratory droplets than in a substitute life cell media³. Different droplet compositions could also influence a virus' hydration over time, affecting its viability. Moreover, as CoV containing respiratory droplets dry, the increasing concentration of salts, surfactants, and proteins can lead to the destruction of the viral envelope and inactivation of the virus. Thus, this study aims to better model virus viability by simulating human respiratory droplets.

To simulate real life surface-droplet interactions, droplets of distilled water, saline, DMEM + 10% FBS, rabbit lung fluid, and human saliva, with volumes ranging from 0.25 - 1.5 μL , were deposited onto paper, glass, polylactic acid (PLA), and aluminum. All samples were analyzed using contact angle goniometry; the change in droplet volume and contact angle over time were recorded, from which the concentration and evaporation rate were determined, as shown in figure 1.

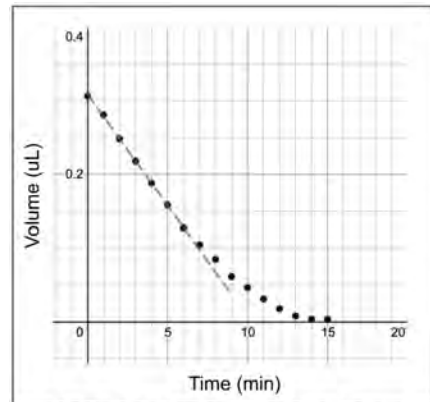


Fig. 2: Volume of saline droplet on PLA surface over time. After 6 mins, the drying becomes nonlinear.

Results indicated that both the surface and the composition of the droplet affected the drying rate [figure 1]. Most droplets

dried fastest on glass and slowest on paper. The rabbit lung fluid dried significantly faster on glass than water, saline, and DMEM + 10% FBS droplets on any surface. Two different drying mechanisms were observed. Some droplets dried at a linear rate, in others, a drying mechanism with an initial linear decrease in volume followed by a slower non-linear decrease was observed, such as with the saline-PLA interaction [figure 2]. Droplets with the second mechanism implies that viruses could be hydrated for a much longer time than could be predicted, possibly contributing to a lengthened virus survivability. The lung surfactant and saliva droplets did not show a slower non-linear section of drying, but this may be due to the goniometer not being able to collect recordings for volumes under about 0.5 μL for these trials.

These findings will be used to produce an in-silico model of the environment inside a drying droplet which can be used to better understand the effects of drying for CoV. Further research with plaque assays will hopefully lead to a better understanding of the relationship between viral susceptibility and droplet evaporation.

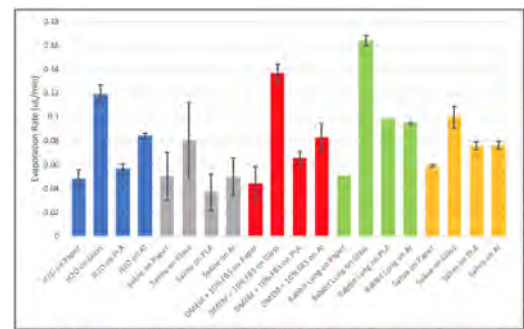


Fig. 1: Drying rates of H2O, saline, DMEM + 10% FBS, rabbit lung, and saliva on paper, glass, PLA, and aluminum

¹ Aboubakr HA, Sharafeldin TA, Goyal SM. Stability of SARS-CoV-2 and other coronaviruses in the environment and on common touch surfaces and the influence of climatic conditions: A review. *Transboundary and emerging diseases*. Published online July 14, 2020. doi:10.1111/tbed.13707

² Firquet, S., Beaujard, S., Lobert, P. E., Sané, F., Caloone, D., Izard, D., & Hober, D. (2015). Survival of Enveloped and Non-Enveloped Viruses on Inanimate Surfaces. *Microbes and environments*, 30(2), 140–144. <https://doi.org/10.1264/jmsme2.ME14145>

³ Thomas Y, Vogel G, Wunderli W, et al. Survival of Influenza Virus on Banknotes. *Applied and Environmental Microbiology* 2008;74(10):3002-07 doi: 10.1128/aem.00076-08

Fogging *B. Atrophaeus*, *E. Coli*, and *E. Faecalis* to Determine the Efficacy of Hypochlorous Solution for COVID-19 Applications

Jessica Liu¹, Kuo Liu², Sana Manesh³, Esther Chai⁴, Christine Kong⁵,
Haijiao Liu⁶, Kuan-Che Feng⁶, Stephen G. Walker⁷ Miriam Rafailovich⁶

¹Northwood High School, Irvine, CA, 92620, ²High School Affiliated to Renmin University of China, Beijing, China, ³Sage Hill School, Newport Coast, CA 92657, ⁴Harvard University, Cambridge, MA, 02138, ⁵University of Pennsylvania, Philadelphia, PA, 19104, ⁶Department of Materials Science and Chemical Engineering, Stony Brook University, Stony Brook, NY 11790, ⁷Department of Oral Biology and Pathology, Stony Brook University, Stony Brook, NY 11790

As COVID-19 spreads across the nation, proper disinfection in public spaces and offices is pivotal to stop the spread of infection. Hypochlorous acid is an effective liquid-based disinfectant¹. Studies on norovirus determined that exposing surfaces to hypochlorous solution for 10 minutes reduced the infectivity and RNA titers of several noroviruses by over 99.9% and exposing surfaces to hypochlorous fog reduced the infectivity and RNA titers of several noroviruses by at least 99.9%². Hypochlorous acid fogging is beneficial when disinfecting large spaces, such as offices and classrooms because aerosols are airborne for longer periods of time². In this project, our focus is on determining the amount of time a surface needs to be fogged to disinfect it of several different bacteria strains and of H1N1 virus.

Measurement of bacterial killing: 50 μ L of 1×10^9 *E. Faecalis* / mL and 50 μ L of 1×10^9 *E. Coli* / mL were each plated on two pieces of aluminum and left to dry for 1 hour. Then, one sample plated with *E. Faecalis* and one sample plated with *E. Coli* were fogged on a Contronics HU-45 Humidifier with Ecological 0.046% hypochlorous solution for 1 hour, while the other two samples serving as controls were left on the bench. Afterwards, the samples were all given 1 additional hour to dry before being submerged in 10 mL of PBS solution and vortexed to remove all bacteria. The new bacterial solution with PBS underwent 1:10 serial dilution from 10^{-1} to 10^{-6} and then were plated onto agar plates in triplicates. The plates were placed in the incubator and left to grow overnight. The plates containing colonies within the range of 30-300 were then counted and recorded the next day.

Measurement of infectious virus: To calibrate infectious virus a plaque assay was carried out using MDCK-II cells grown on 6-well plates to 90%-100% confluency. The medium used comprised 25 mL of 1 x MEM, 12.5 mL of tragacanth gum, 12.5 mL of 2x DMEM, 0.2% BSA, and 0.5% of TrypLE Select. 2 mL of plaque medium was aliquoted into each well and cultures incubated for 4 days. Then, 1 mL of a dye containing 1% crystal violet, 50% methanol, and 4% formaldehyde was added to each well. The wells were placed on the rocker for 15 minutes, and then the supernatant was aspirated off.

Our preliminary results for fogging the bacteria, as shown in Table 1, show that although the chlorine content is lost during the fogging (600ppm to less than 200 ppm), it is still an effective disinfectant. For *E. Coli*, there was an average of $1.966 \pm 0.306 \times 10^6$ bacteria total on the control surfaces and less than 1,000 bacteria total on the fogged surfaces,



Figure 1: Fogged and Control *E. Coli*.

Figure 2: Fogged and Control *E. Faecalis*.

Figure 3: 10^{-2} dilutions for plaque assay calibration.

Table 1: *E. Coli* Colonies on Aluminum Surface in 10^{-3} Dilution

Control	188	132	172	$1.966 \pm 0.306 \times 10^6$ bacteria total
Fogged	No colonies found across all dishes			<100 bacteria in 1 mL* <1,000 bacteria total *

Table 2: *E. Faecalis* Colonies on Aluminum Surface in 10^{-4} Dilution

Control	115	95	85	$3.26 \pm 0.6 \times 10^5$ bacteria total
Fogged	No colonies found across all dishes			<100 bacteria in 1 mL* <1,000 bacteria total *

resulting in a 99.95% bacterial reduction (Table 1). For *E. Faecalis*, there was an average of $3.26 \pm 0.6 \times 10^5$ bacteria total on the control surfaces and less than 1,000 bacteria total on the fogged surfaces, resulting in a 99.6% bacterial reduction (Table 2). The experiment is restricted by the detection limit of the bacterial assay. In future experiments, the surfaces will be seeded with a greater number of bacteria to better see the bacterial reduction and additional surfaces and fogging times will be assessed.

* Limitation of assay.

¹ Block MS, Rowan BG. Hypochlorous Acid: A Review [published online ahead of print, 2020 Jun 25]. *J Oral Maxillofac Surg*. 2020;S0278-2391(20)30672-8. doi:10.1016/j.joms.2020.06.029

² Park GW, Boston DM, Kase JA, Sampson MN, Sobsey MD. Evaluation of liquid- and fog-based application of Sterilox hypochlorous acid solution for surface inactivation of human norovirus. *Appl Environ Microbiol*. 2007;73(14):4463-4468. doi:10.1128/AEM.02839-06

Refining Synthesis of Copper Nanoparticles Formed in Situ on Polylactic Acid Composites for Antimicrobial Applications

Zoe Lu¹, Katerina Popova², Sabrina Su³, Serena Yang⁴, Michael Cuiffo⁵, Miriam Rafailovich⁵

¹Thomas Jefferson High School for Science and Technology, Alexandria, VA 22312 ²Hackley School, Tarrytown, NY 10591

³Poolesville High School, Poolesville MD 20837 ⁴Dougherty Valley High School, San Ramon, CA 94582 ⁵Department of Materials Science & Chemical Engineering, Stony Brook University, Stony Brook, NY 11794

In previous studies, silver nanoparticles (NPs) have demonstrated antibacterial and antiviral properties [1]. It is hypothesized that copper nanoparticles (Cu NPs) will have similar effects. The theories for the cause of antimicrobial activity and cytotoxicity are the same for metal NPs deposited in situ [2]. Polylactic acid (PLA) is an organic polymer that is used in Fused Deposition Modelling (FDM) and biomedical scaffolding, as it is biodegradable, biocompatible, and immunologically inert [3]. PLA structures were used as substrates for the Cu NP synthesis in this study.

The primary goal of this research was to synthesize smaller Cu NPs for antiviral and antibacterial properties as a possible application against COVID-19. This study explores Cu NP deposition techniques onto FDM 3D printed PLA samples and molded PLA samples. Some of the 3D printed PLA samples were pre-treated with pure acetone then rinsed with deionized (DI) water to alter the surface chemistry and possibly allow for more NP adhesion. The PLA samples were first submerged in a hot water bath for 20-30 minutes to soften the PLA and allow for better surface adhesion of NPs. The NPs were then synthesized by submerging the PLA samples in a sodium borohydride and copper (II) nitrate solution, which was placed in a water bath with an ultrasonicator. The Cu NP synthesis parameters, such as the solution concentrations, solution ratios, and the temperature and duration of the water bath were adjusted to optimize for smaller and more evenly spread NPs.

Various analytical techniques such as optical microscopy, Fourier-Transform Infrared Spectroscopy (FTIR), X-ray Photoelectron Spectroscopy (XPS), Ultraviolet-Visible Spectroscopy (UV-Vis), and X-ray Fluorescence (XRF) were used to analyze physical characteristics (shape and size) of the NPs after specific parameter changes, as well as chemical changes of our PLA surfaces with the Cu NPs as compared to PLA without Cu NPs.

Optical microscopy showed that NPs were unevenly distributed on molded PLA samples, as seen in Fig. 1. Changing the concentrations of the sodium borohydride and copper (II) nitrate solutions did not have a significant effect. XRF reports showed that acetone pre-treated PLA had greater and more even distribution of Cu NPs than the molded and the regular 3D printed PLA, as seen in Table 1. The contact angle of our samples showed they were less hydrophobic compared to regular PLA, but not yet hydrophilic.

In summary, this study showed that acetone treated PLA allowed for greater and more even distribution of Cu NPs on the PLA. Future research includes bacterial and viral testing to see the antimicrobial efficacy of the samples, followed by applications, such as face shields, based on results of the testing.

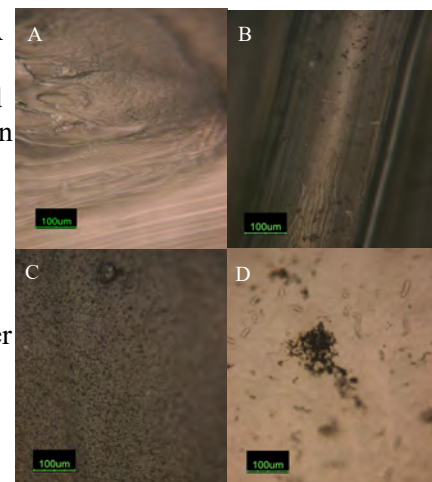


Fig. 1 - Optical microscopy images of PLA samples
A) printed PLA B) printed PLA with NP
C) acetone printed PLA with NP D) molded PLA with NP

Material	Cu (ppm)
Molded PLA (spot 1)	15, 206.792
Molded PLA (spot 2)	2, 246.179
Printed PLA (acetone, spot 1)	133, 735.438
Printed PLA (acetone, spot 2)	118, 586.016
Regular PLA (spot 1)	221, 543.938
Regular PLA (spot 2)	73, 393.328

Table 1: XRF data for various PLA samples.

[1] Galdiero, Stefania et al. "Silver nanoparticles as potential antiviral agents." *Molecules (Basel, Switzerland)* vol. 16, 10 8894-918. 24 Oct. 2011, doi:10.3390/molecules16108894

[2] Ingle, Avinash P., et al. "Bioactivity, Mechanism of Action, and Cytotoxicity of Copper-Based Nanoparticles: A Review." *Applied Microbiology and Biotechnology*, vol. 98, no. 3, 2013, pp. 1001-1009., doi:10.1007/s00253-013-5422-8.

[3] Cuiffo, Michael et al. "Impact of the Fused Deposition (FDM) Printing Process on Polylactic Acid (PLA) Chemistry and Structure." *ProQuest*, 3 Apr. 2017, doi:10.20944/preprints201704.0010.v1

Molecular Imprinted Biosensor for SARS-CoV-2 Detection

Won-il Lee¹, Robert Wong¹, Michelle Chang², Nishanth Chinnadurai³, Jolene Huey⁴, James Kim⁵,
Udithi Kothapalli⁶, Hugo Onghai⁷, Jeannie She⁸, Miriam Rafailovich¹

¹Department of Materials Science and Chemical Engineering, Stony Brook University, NY 11794, ²Seoul International School, South Korea, ³East Meadow High School, NY 11554, ⁴Arcadia High School, CA 91006, ⁵Great Neck South High School, NY 11020, ⁶Saint Anthony's High School, NY 11747, ⁷Earl L. Vandermeulen High School, NY 11777, ⁸Walt Whitman High School, MD 20817

The COVID-19 pandemic has changed the world drastically, causing numerous infections and deaths. Although many testing methods have been developed to detect SARS-CoV-2, a more accessible technique is desired due to current methods requiring an extensive amount of time to process results (up to one week) and potentially unavailable equipment. We are developing an electrochemical biosensor, capable of detecting entire virions or virion-associated proteins, which can be applied for rapid point-of-care detection of SARS-CoV-2. This type of sensor was previously demonstrated to be successful in the detection of Zika virus, with excellent discrimination between Zika and Dengue viruses [1]. Since both Zika and Dengue are flaviviruses and have similar dimensions as the Coronavirus, we believe that this mechanism will be applicable to SARS-CoV-2 as well. The advantages of this method are: (a) rapid results using readily available instrumentation such as a simple potentiometer, now available on cell phones; (b) high sensitivity and specificity, even in the presence of other proteins, and hence can be used with almost any bodily fluid, blood or saliva.

Our electrochemical biosensor uses the molecular imprinting (MI) technique on top of a gold substrate with hydroxyl-terminated alkanethiol chains to form a self-assembled-monolayer (SAM) and crystallize to the specific shape of a virion. The initial steps of the technique are dependent on the chance that a virion will settle into a cavity; however, after settling, the hydrophobic sulfur end of the thiol chemically binds to the exposed gold surface and the hydrophilic hydroxyl end of the thiol forms hydrogen bonds with the analyte's surface proteins. The biosensor's specificity can be attributed to the cavities formed in the thiol layer based upon the size, orientation, and hydrophilicity of the analyte. After MI, the remaining analytes are washed with a succession of DI water, a sodium chloride solution, and DI water again, leaving footprint-like cavities in the crystallized

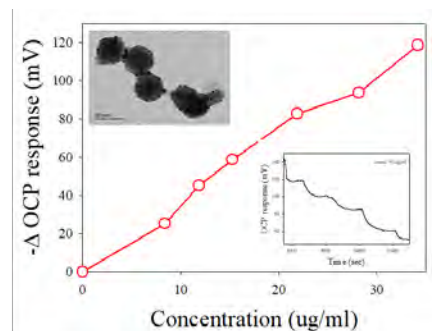


Fig. 1: Average potentiometric response for increasing concentration of hemoglobin.
Inset: TEM image of H1N1 (Top), displays the OCP response in terms of time (bottom).

thiol SAM layer. When used for detection, the imprinted chip attaches to the working electrode in a 3-electrode system. An OCP response is observed when pipetting the sample for re-adsorption [Fig. 1]. Samples were made by deposition of Au/Ti on both the electropolished and the rough surfaces of Si wafers. Ideally, the roughness of the gold chip should correlate with the size of the analyte used; this would promote maximum conformity. TEM and AFM were used to characterize roughness. Virions of the Zika, H1N1, and COVID-19 viruses have a diameter of roughly 50 - 100 nm [Fig. 1 inset]. The most successful imprints of Zika virus have been with the rough gold chip, indicating that rough gold chips would be most appropriate for imprinting virions of comparable size. Likewise, the relatively smaller protein size of Hemoglobin (Hb) and SARS-CoV-2 Spike protein (S-protein) would optimally imprint on a smooth chip.

The efficacy of the smooth chips was tested with bovine Hb at an imprinting concentration of 30 $\mu\text{g}/\text{mL}$. Hb protein molecules are roughly 5 nm in diameter and have a positive charge; both crucial characteristics for MI. After re-adsorption, the limit of detection (LOD) was found at $\sim 2 \mu\text{g}/\text{mL}$ and the saturation point at $\sim 18 \mu\text{g}/\text{mL}$. Further investigation will yield imprinting smooth chips with the SARS-CoV-2 S protein and imprinting rough chips with H1N1 and SARS-CoV-2 virions for real-world application. Since the S protein has a comparable size and charge to the bovine Hb, we infer that the suggested accuracy and efficacy of the Hb biosensor can correlate with potential success in an S-protein biosensor.

[1] Ricotta, Vincent, et al. "A Chip-Based Potentiometric Sensor for a Zika Virus Diagnostic Using 3D Surface Molecular Imprinting." *The Analyst*, vol. 144, no. 14, 2019, pp. 4266–4280., doi:10.1039/c9an00580c.

Machine Learning for Long-Term Molecular Dynamics of SARS-CoV-2 Spike Glycoproteins

Larry Huang¹, David Liang², Meichen Song³, Ziyuan Niu³, Peng Zhang³, Miriam Rafailovich⁴

¹University of Pennsylvania, Philadelphia, PA, 19104, ²Ward Melville High School, East Setauket, NY 11733, ³Stony Brook University, Stony Brook, NY 11790, ⁴Department of Mat. Sci. & Chem. Eng., Stony Brook University, Stony Brook, NY 11790

As the SARS-CoV-2 pandemic continues to spread, the effects of environmental factors, such as temperature and pH, on the molecular level remain unclear. While molecular dynamics (MD) simulations are a widely-used technique in modeling complex nanoscale interactions, its high computation requirements limit capabilities in long-term modeling. This work explores a machine learning (ML) solution to predicting microsecond, second, and minute properties of SARS-CoV-2 spike glycoproteins through the analysis of nanosecond RMSD (root-mean-square deviation) and RMSF (root-mean-square fluctuation) MD simulation data. RMSD values are particularly useful in the analysis of protein flexibility and movement as the values represent the measure of the deviation between the position of two structures, while the RMSF values refer to the average RMSD over time. The changes in structure and shape as time progresses is key to understanding the behavior and functionality of the virus under specific conditions.^[1]

Our data processing is characterized primarily with the smoothing of the trends, along with the utilization of rolling averages, fast Fourier transforms (FFT), and wavelets. FFTs are utilized in converting the RMSD time-series data from its time-domain representation to a frequency domain representation, which is particularly useful in the identification of cyclic trends and the evaluation of stability. Statistical modes such as the autoregressive integrated moving average (ARIMA) models were used as a basic prediction model on the RMSD time-series data, as shown in Figure 1, achieving a coefficient of determination (R^2) of 0.50. Furthermore, recurrent neural networks (RNN) were utilized to predict time series trends.^[2] Early predictions of the long-short term memory (LSTM) RNN models achieved a high extrapolation coefficient of determination (R^2) of 0.95 as compared to the MD simulation data. Relatively low RNN training times ranging from seconds to several minutes combined with high R^2 suggest an alternative to the weeks of supercomputer usage required of MD simulations. The validity of the ML models for long-term predictions will be corroborated once lab bench experiment results are analyzed. Moreover, the RMSF data can be used in identifying key residues and clustering similar trends.

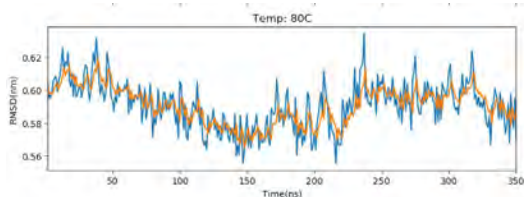


Figure 1: Time-series plot of RMSD values (blue), along with the ARIMA in-sample predictions (orange) for 80C.

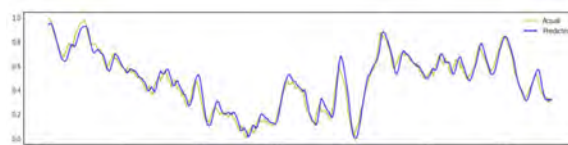


Figure 2: Time-series plot of RMSD values with a LSTM network prediction model for 80C.

^[1]Tan, Jinzhi et al. “pH-dependent conformational flexibility of the SARS-CoV main proteinase (M(pro)) dimer: molecular dynamics simulations and multiple X-ray structure analyses.” *Journal of molecular biology* vol. 354,1 (2005): 25-40. doi:10.1016/j.jmb.2005.09.012

^[2]Ho, S. L. et al. “A comparative study of neural network and Box-Jenkins ARIMA modeling in time series prediction.” (2002). doi:10.1016/S0360-8352(02)00036-0

Nucleic Acids and Proteins on Surfaces

*Kao Li, Rebecca Isseroff, and
Anthony Del Valle*

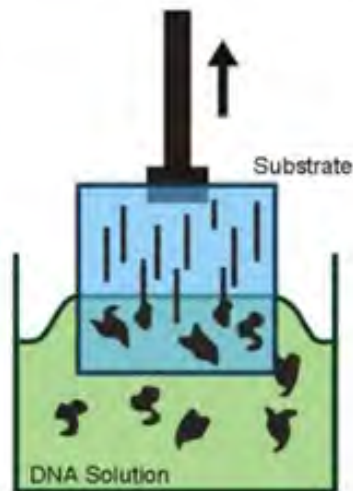


Fig. 1: (left) Apparatus for dip-coating (“combing”) DNA molecules onto a substrate by withdrawal from solution. (right) Schematic of stretching and straightening of DNA on the surface by preferential end adsorption

Transfer printing of DNA molecules from PDMS (polydimethylsiloxane) to hydrophilic PAA (polyacrylic acid) surfaces for application to sequencing

Aakrsh Misra¹, Anya Raju², Daniel Wang³, Eyal Noy⁴, Hyunkyung Katherine Lee⁵, Leor Oved⁶, Samarjit Kaushik⁷, Stephanie Zhao⁸, Jonathan Sokolov⁹, Anthony Del Valle⁹

¹Dana Hills High School, Dana Point, CA 92629 ²Basis Independent Silicon Valley High School, San Jose, CA 95126 ³Huron High School, Ann Arbor, MI 48105 ⁴Rochelle Zell Jewish High School, Deerfield, IL 60015 ⁵Conestoga High School, Berwyn, PA 19312 ⁶HAFTR High School, Cedarhurst, NY 11516 ⁷Tesla STEM High School, Redmond, WA 98053 ⁸Princeton International School of Mathematics and Science, Princeton, NJ 08540 ⁹Department of Materials Science and Chemical Engineering, Stony Brook University, Stony Brook, NY 11794

Next generation DNA sequencing technologies have made rapid advances in improving sequencing accuracy and efficiency but require the random fragmentation of DNA, and the subsequent computational reassembly is costly, time-consuming, and often fails to capture nucleotide repeats or other structural complexities in the DNA sequence.¹ The primary goal of this experiment is to enable ordered cutting of DNA on polymer surfaces to improve sequencing efficiency. Polyacrylic acid (PAA) is a uniquely suitable surface as it can be made both water insoluble, for DNA deposition, and water soluble, for DNA fragment removal, by immersion in ionic solutions.²

Silicon wafers (10 mm by 10 mm or 10 mm by 20 mm) were cut with a scribe and breaker and cleaned with 5% HCl. PAA-water solutions of 10%, 5%, and 2.5% were spincoated onto the silicon wafers at 2500 rpm for 30 seconds. The samples were heated in a vacuum oven at 130 degrees Celsius and an ellipsometer was used to measure the film thickness of the samples. The samples were soaked in 1M CaCl₂ solution for 1 minute to make the PAA water-insoluble. A contact angle goniometer measured the contact angles of the samples with water, MES:NaOH buffer, NEB Buffer 3.1, and NEB DNase I Reaction Buffer. As visualized in Fig. 1, the PAA-coated samples were dipped in a lambda DNA solution (48502 bp) with buffer and dye and slowly withdrawn to “comb” the DNA onto the PAA surface. DNA combing onto PAA was also attempted by evaporating drops of DNA solution at various temperatures, spincoating DNA onto the PAA surface, and sliding DNA solution down an inclined plane.

The contact angles for water, MES:NaOH buffer, NEB Buffer 3.1, and NEB DNase I Reaction Buffer on the PAA surface were measured to be $17^\circ \pm 5^\circ$, $20^\circ \pm 5^\circ$, 20° , and 20° respectively, indicating that the PAA was strongly hydrophilic, which likely led to the unsuccessful results of various combing methods for the PAA surface showing incomplete or irregular deposition.

We then attempted DNA deposition onto PDMS for “contact printing” onto the PAA. Three concentrations of DNA in NEB Buffer 3.1 were deposited by dipping and withdrawal (Fig. 1) at various speeds, as well as drop evaporation. The deposited DNA on the PDMS stamp was dried and then transferred to the PAA surface by pressing the stamp onto the PAA surface for 1 minute.

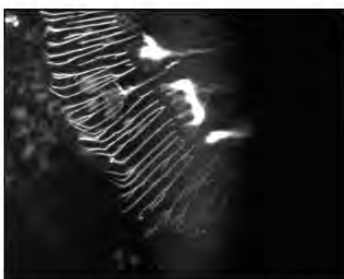


Fig. 2: DNA transferred from PDMS to PAA-coated Si wafers, showing some undesirable branching

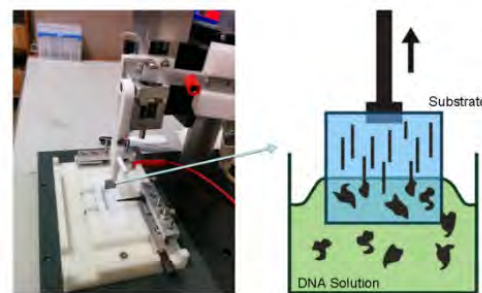


Fig. 1: (left) Apparatus for dip-coating (“combing”) DNA molecules onto a substrate by withdrawal from solution. (right) Schematic of stretching and straightening of DNA on the surface by preferential end adsorption

The combing on the PDMS showed branching rather than the desired regular deposition. We attempted heating the DNA solutions to 60°C to prevent clumping, as well as adding NaCl, using different buffers, and varying the rate of deposition. Reduced but still present branching was observed. However, the DNA was successfully transferred to the PAA (Fig. 2). After testing several samples, we suspect the lambda DNA may be the problem, and new DNA tested shows slightly better results.

The PDMS transfer method has yielded promising results. However, better combing of DNA is still required to reduce DNA branching and deposit the fragments at a convenient density. Although further research is needed to cut the DNA on the PAA surface and remove the fragments into a water-based buffer for sequencing, transfer printing of DNA onto a PAA surface is a valid candidate for ordered cutting of DNA fragments on a polymer surface with a goal of improving sequencing efficiency.

¹ Goodwin, S., McPherson, J. & McCombie, W. “Coming of age: ten years of next-generation sequencing technologies.” *Nature Reviews Genetics* 17, 333–351 (2016). <https://doi.org/10.1038/nrg.2016.49>

² Linder, Vincent, et al. “Water-Soluble Sacrificial Layers for Surface Micromachining.” *Small*, vol. 1, no. 7, 2005, pp. 730–736., doi:10.1002/smll.200400159.

Minimizing Surface-Initiated Thrombogenesis Using the Fibronectin-Derived Peptide P12

Sabreen Alam¹, Ori Baer², Sebastien Beurnier³, Jang Choe⁴, Kevin Kwon⁵, Nikhil Murthy⁶, Ikshu Pandey⁷, Kao Li⁸, M.Rafailovich⁸
¹Portola High School, Irvine, CA, 92618; ²Hebrew Academy of Nassau County High School, Plainview, NY, 11803; ³Stuyvesant High School, Manhattan, NY, 10282; ⁴Ed W Clark High School, Las Vegas, NV, 89102; ⁵Niskayuna High School, Niskayuna, NY, 12309; ⁶Archbishop Mitty High School, San Jose, CA, 95129; ⁷Johns Hopkins University, Baltimore, MD 21218; ⁸Department of Mat. Sci. & Chem. Eng., Stony Brook University, NY, 11790

Fibrinogen is a soluble glycoprotein present in the human blood plasma, and is responsible for the formation of blood clots. Fibrinogen's functionality is largely dependent on the exposure of the protein's Alpha-C domains where the recruitment and binding of fibrinogen molecules occurs [3]. Previous studies have shown that high levels of fibrinogen and clotting are present in critically ill COVID-19 patients [1,2], which could lead to strokes, pulmonary embolisms and deep-vein thromboses if left untreated. Mechanistically, we hypothesized that COVID-19 turns surfaces in the body hydrophobic, potentially resulting in complications even after the patient recovers from the virus, as adsorption to hydrophobic surfaces exposes the alpha-c domains and leads to polymerization without normal triggers like thrombin [4]. P12 is a fibronectin-derived oligopeptide that antagonistically binds to the Alpha-C domains of fibrinogen, and has previously shown to be effective in the healing of burns by limiting clotting [5]. In this study, we aimed to determine if P12 could be an effective localized anti-clotting peptide to minimize surface-induced thrombogenesis in COVID-19 patients. To study the effects of P12 on clotting, we first analyzed fibrin formation on polystyrene, a hydrophobic polymer, to determine the optimal experimental conditions and concentration of fibrinogen to conduct further tests and analyze fiber formation. Polystyrene was spun-cast onto silicon wafers. After annealing the wafers in a vacuum oven at 130°C to evenly distribute the polymer, the wafers were placed into wells with various solutions of fibrinogen in phosphate buffered saline (PBS) and deionized (DI) water. The wafers were then washed at intervals of 30 minutes, 1 hour, 2 hours, and overnight, before images were taken via optical microscopy. Concentrations of 2 mg/mL, 3 mg/mL, and 4 mg/mL were tested, of which the optimal fibrinogen solution for inducing fiber formation was determined to be 3 mg/mL with the use of a 2D rocker. This solution was used to test the effectiveness of a 50 μ M solution of cyclic P12 at intervals of 1 hour and 2 hours. 300 μ l of fibrinogen solution and 3 μ l of P12 solution were deposited onto our experimental samples. Various parameters including fiber and aggregate concentration, fiber orientation, fiber length, and fiber radius were analyzed. Atomic Force Microscopy was also employed to further characterize fiber formation. The results of our image analysis on the 2-hour samples displayed that fiber and aggregate formation in the P12 samples were reduced by a factor of 205.2 and 1.327 respectively when compared to the control, with most images showing little to no fiber formation (Figure 1). This indicates that P12 was effective in preventing fiber formation, although further trials will have to be performed to determine the statistical significance of the data. Future directions would include additional trials of the current concentration of fibrinogen and P12 on polystyrene, observing the effects of P12 inhibition within H1N1-infected cell cultures to mimic COVID-19, and observe the effects of P12 on fiber formation in rabbit aorta tissue.

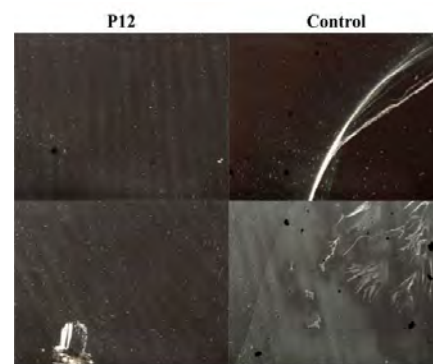


Figure 1: Representative Optical Microscopy Images of the Effect of P12 on Fibrinogen Fiber Formation on Spincast Polystyrene

[1]Klok, F A et al. "Incidence of thrombotic complications in critically ill ICU patients with COVID-19." *Thrombosis research* vol. 191 (2020): 145-147. doi:10.1016/j.thromres.2020.04.013

[2]Ranucci, M., Ballotta, A., Di Dedda, U., Bayshnikova, E., Dei Poli, M., Resta, M., Falco, M., Albano, G. and Menicanti, L. (2020), The procoagulant pattern of patients with COVID-19 acute respiratory distress syndrome. *J Thromb Haemost*, 18: 1747-1751. doi:10.1111/jth.14854

[3] Weisel, John & Litvinov, Rustem. (2017). Fibrin Formation, Structure and Properties. 10.1007/978-3-319-49674-0_13.

[4] Zhang, Liudi & Casey, Brendan & Galanakis, Dennis & Marmorat, Clement & Skoog, Shelby & Vorvolakos, Katherine & Simon, Marcia & Rafailovich, Miriam. (2017). The influence of surface chemistry on adsorbed fibrinogen conformation, orientation, fiber formation and platelet adhesion. *Acta Biomaterialia*. 54. 10.1016/j.actbio.2017.03.002.

[5] Lin, Fubao et al. "Fibronectin peptides that bind PDGF-BB enhance survival of cells and tissue under stress." *The Journal of investigative dermatology* vol. 134,4 (2014): 1119-1127. doi:10.1038/jid.2013.420

Enhancing the Action of Cellulase on Biomass

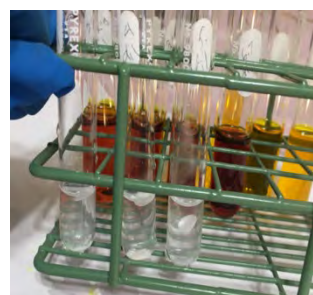
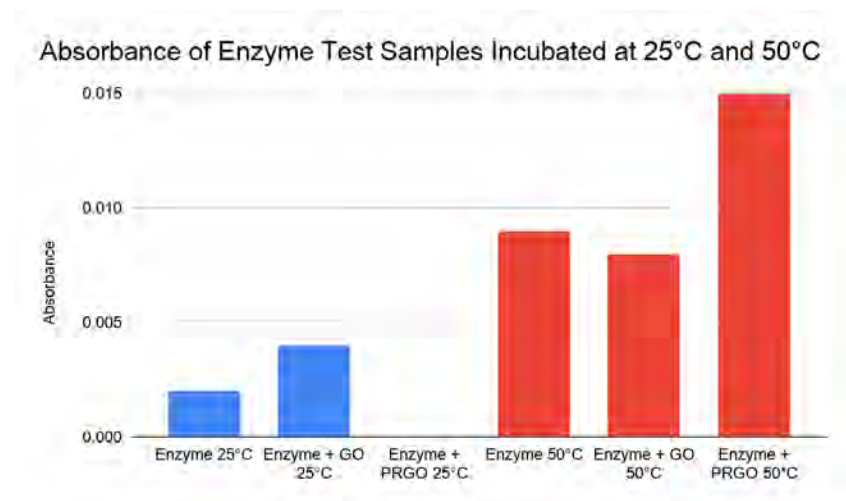
Nava Schein¹, Rebecca Isseroff², Dr. Miriam Rafailovich²

¹HAFTR High School, Cedarhurst, NY, ² Stony Brook University, Stony Brook, NY³

There is a strong motivation to develop methods of converting biomass into liquid fuels. The challenge is to create a technology for converting cellulose, hemicellulose, and lignin into their constituent sugar monomers. Cellulases are enzymes that break up cellulose into sugars and can give nearly 100% yields of glucose. However, the rate of reaction is slow. Acid hydrolysis of cellulose has a much faster reaction rate but also produces products such as levulinic acid which cannot be converted to fuel by fermentation.¹

This project investigates methods of increasing the catalytic actions of cellulase on cellulose. Partially reduced graphene oxide (PRGO) has already been demonstrated to increase the rate of cross-linking gelatin by microbial transglutaminase and it is tested here to see if it can increase the action of cellulase on cellulose². We compared the glucose production of both cellulase/Graphene Oxide (GO) as well as PRGO/cellulase from a circle of a Whatman filter to that of a control sample of cellulase alone.

Results suggest that PRGO enhances the activity of cellulase on paper, by displaying an increase in the amount of glucose generated at 50°C as compared either enzyme alone or enzyme plus GO incubated at that temperature. Future work includes using freshly-synthesized GO and PRGO, which should display not only more activity but also greater water solubility, thus increasing contact with the dissolved enzyme. In addition, PRGO can be functionalized with metal nanoparticles, and will be investigated as a possible catalyst for the conversion of sugars into ethanol, hydrogen and/or small alkanes.



¹ Gates, Bruce C., et al. "Catalysts for Emerging Energy Applications." *MRS Bulletin*, vol. 33, no. 4, 2008, pp. 429–435., doi:10.1557/mrs2008.85.

² Isseroff, Rebecca; Reyes, Jerry; Reddy, Roshan; Williams, Nicholas; Rafailovich, Miriam. (2019). The Effects of Graphene Oxide and Partially Reduced Graphene Oxide on the Enzymatic Activity of Microbial Transglutaminase in Gelatin. *MRS Advances*. 4. 1-9. 10.1557/adv.2019.89.

Stem Cell Differentiation in Skin and Dentistry

*Ya-Chen Chuang, Kao Li, Fan
Yang, Haijiao Liu,
Juyi Li and Kuan-Che Feng*

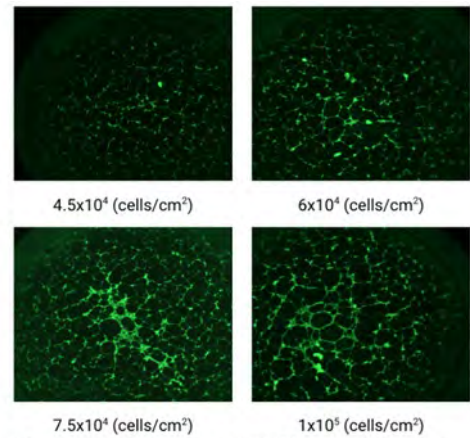
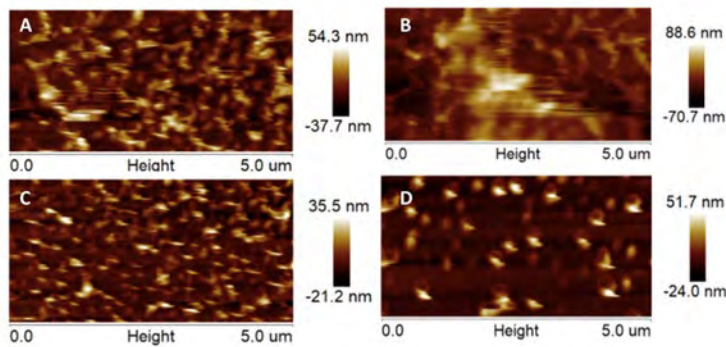


Figure 1. EVOS microscope images of the HUVEC samples of different densities.

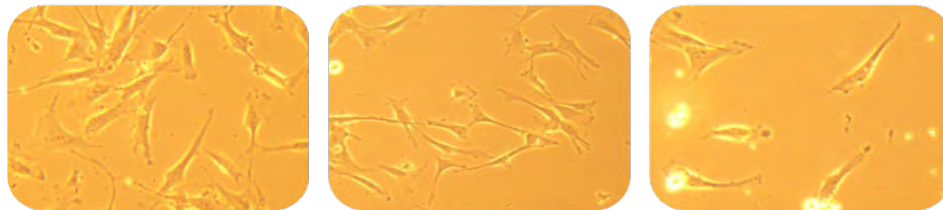


Figure 3. Cells in each group after day 2. (Left) Control (Middle) with Hydroxylapatite (Right) Bio-Oss

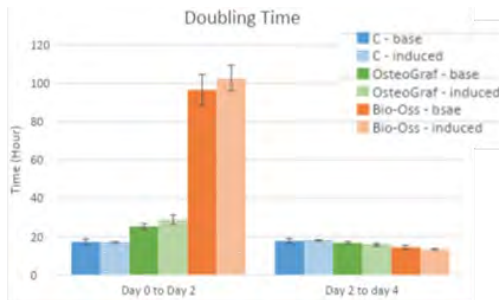
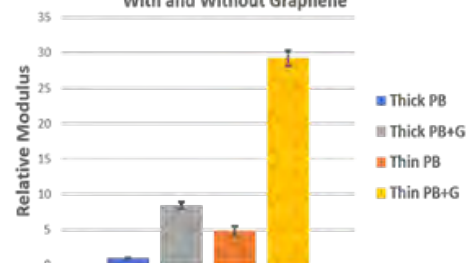


Figure 2: The doubling time of each cell culture on Day 0, 2, and 4

Fig 2: Relative Modulus of Thin and Thick PB Films With and Without Graphene



Effect of Fibrinogen-Gelatin Scaffolds on Dental Pulp Stem Cell Differentiation

Tianjian Bai¹, Evan Cheng², Jake Feldman³, Alyssa Kim⁴, Kao Li⁵, Miriam Rafailovich⁵, Marcia Simon⁶

¹Huron High School, Ann Arbor, MI 48105 ²Syosset High School, Syosset, NY 11791 ³Plainview-Old Bethpage John F. Kennedy High School, Old Bethpage, NY 11804 ⁴New Hyde Park Memorial High School, New Hyde Park, NY 11040 ⁵Department of Materials Science & Engineering, Stony Brook University, Stony Brook, NY 11794 ⁶Department of Oral Biology & Pathology, Stony Brook University, Stony Brook, NY 11794

Advances in tissue engineering present a prospect for the biologic regeneration of damaged dental tissue through the use of a scaffold, growth factors, and dental pulp stem cells (DPSCs) as an alternative to traditional endodontic therapy, which has several limitations such as a loss of sensitivity in the tooth and greater susceptibility to postoperative fractures and infections¹. DPSCs are chosen due to their ability to differentiate along an odontogenic lineage and their relative accessibility. Furthermore, gelatin, derived from collagen, has been found to be suitable for tissue growth²; Lovelace *et al.* demonstrated intracanal bleeding can successfully assist in dental tissue regeneration³, potentially due to fibrinogen. This study evaluates fibrinogen-gelatin scaffolds as viable substrates for DPSC differentiation.

DPSCs were cultured and harvested, then seeded in well plates at a density of ~1500 cells/cm² on crosslinked gelatin hydrogels. By varying the amount of mTG added to the hydrogel, we produced hard and soft gelatin gels in both fibrinogen and non-fibrinogen varieties for each with the addition of bovine fibrinogen. Thrombin was added to the fibrinogen gels in order to polymerize the fibrinogen into fibrin. As controls, DPSCs were seeded directly onto tissue culture plates without any gel, and gels were prepared in the absence of DPSCs.

RT-PCR was used on a previously seeded set of replicate cell samples in order to examine the gene expression of osteocalcin (OCN), a marker protein of early biomineralization and dentin formation. Gels with fibrinogen, both hard and soft, demonstrated the greatest OCN expression on days 14 and 30, respectively (Fig 1). By day 30, the relative proximity of the OCN expression for the hard and soft gels with fibrinogen indicates that stiffness of the substrate may not have an appreciable effect on DPSC growth, corroborating Bhatanagar *et al.*⁴. Both fibrinogen gels also displayed the greatest upregulation in OCN expression between day 0 and day 30 compared to the non-fibrinogen gels, suggesting the fibrinogen had a positive effect on DPSC differentiation (Fig 2).

Further investigations will continue to use RT-PCR to measure the mRNA expression of OCN and dentin sialophosphoprotein (DSPP), another protein indicative of terminal odontogenic differentiation. Alizarin red staining, confocal and SEM microscopy, and EDX analysis will also be used to examine the morphology and elemental composition of the DPSCs and biomineralized deposits.

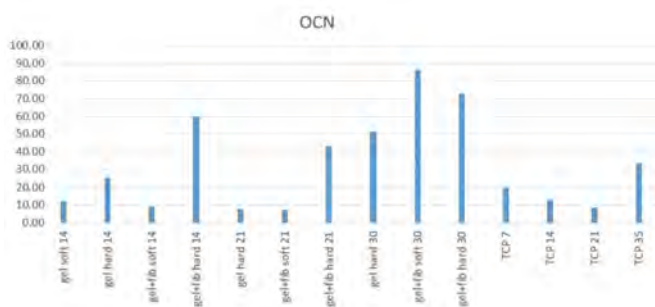


Fig 1 Relative OCN expression of DPSCs by gel type and day.

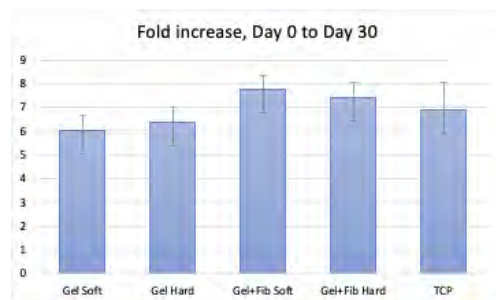


Fig 2 RT-PCR fold increase of different gel types, day 0 to day 30

¹Paduano, Francesco et al. "Odontogenic Differentiation of Human Dental Pulp Stem Cells on Hydrogel Scaffolds Derived from Decellularized Bone Extracellular Matrix and Collagen Type I." *PLoS one* vol. 11,2 e0148225. 16 Feb. 2016, doi:10.1371/journal.pone.0148225

²Marmorat, Clement, et al. "Cryo-Imaging of Hydrogels Supermolecular Structure." *Scientific Reports*, vol. 6, no. 1, 2016, doi:10.1038/srep25495.

³Lovelace TW, Henry MA, Hargreaves KM, et al. Evaluation of the delivery of mesenchymal stem cells into the root canal space of necrotic immature teeth after clinical regenerative endodontic procedure. *J Endod* 2011; 37: 133–138.

⁴Bhatanagar, D.; Bherwani, A. K.; Simon, M.; Rafailovich, M. H.. Biomineralization on Enzymatically Cross-linked Gelatin Hydrogels in the Absence of Dexamethasone. *Journal of Materials Chemistry B*. *Journal of Materials Chemistry B* 2015, pp 5210–5219.

Effects of Aging and Seacret Broth on Cell and ECM Modulus of Keratinocytes

Lingzi (Susan) Zhang¹, Irene Lee², Chloe Zhang², Haris Rana³, Dr. Ya-Chen Chuang⁴, Dr. Miriam Rafailovich⁴

¹The Hockaday School, Dallas, TX, 11600; ²Jericho High School, Jericho, NY, 11753; ³Southside High School, Fort Smith, AR, 72903;

⁴Department of Material Science and Chemical Engineering, Stony Brook University, Stony Brook, NY, 11794

Studying the biomechanics of skin is important for understanding skin and its functions, such as wound healing¹. Different factors can impact skin mechanics, especially aging. Aging has a significant effect on the function, structure, and mechanical properties of skin cells and the surrounding extracellular matrix (ECM). Most notably, aging directly affects the most important structural component of the ECM— collagen— in two significant ways². Firstly, aging increases cross-linking of collagen fibers, resulting in a thicker ECM network³. Secondly, dehydration of the ECM results in weakened collagen fibers³. As a result, older cells are generally more rigid than their younger counterparts: extracellularly, due to the aforementioned increase in cross-linking, and intracellularly, due to higher density and thickness of cytoskeleton fibers such as actin.

To investigate the relationship between biochemistry and biomechanics of keratinocytes, young (DO33, age ~25) and old (DO36, age ~50-60) cells were first cultured on sulfonated polystyrene (SPS) and polybutadiene (PB) thick (200 nm) and thin (20 nm) films spin-casted on silicon wafers at a density of $\sim 2 \times 10^4$ cells per well. In addition, Seacret broth, a drug used in skincare products, was added to some of the cultures to test its effect on modulus and morphology. The cell and ECM modulus of treated and untreated cells were measured using atomic force microscopy (AFM) on PB and SPS films, respectively. Afterwards, ECM morphology was imaged via AFM.

ECM modulus and morphology data revealed that both aging and Seacret broth affect ECM composition, mainly fiber density. In general, the fiber density of DO33 ECM is higher than that of DO36 (Fig.1). Such results signify that older cells synthesize less ECM proteins. Furthermore, based on calculations, DO33 ECM generally has a higher relative modulus than DO36 ECM, indicating that ECM becomes softer as the cell ages (Fig. 2A). The driving versus response amplitude graphs obtained from AFM testing of ECM indicate that Seacret Broth made DO33 ECM tougher (able to endure the impact of higher force or pressure) while it had a slight effect DO36 ECM toughness, for the curves of the Seacret-treated DO33 ECM did not yield as amplitude exerted by AFM cantilevers increased whereas the DO36 curves did. Cell modulus testing on PB thick and thin films indicates that Seacret broth also affects cytoskeleton structure. Data for cells on PB thick films may not accurately represent the actual modulus of the cells, for testing was done on day 3 after plating and the cells might not have fully attached to the surface by that point. However, cells plated on PB thin film were tested on day 7, and results showed that Seacret-treated cells had higher relative moduli than untreated ones (Fig. 2B). Such data indicates that intracellular structural proteins become stiffer in the presence of this drug. Confocal microscopy of cells and ECM will be conducted in the future in order to confirm modulus results and analyze the effects of aging and

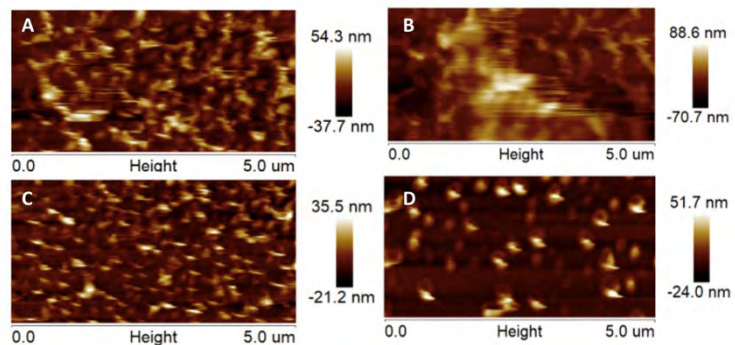
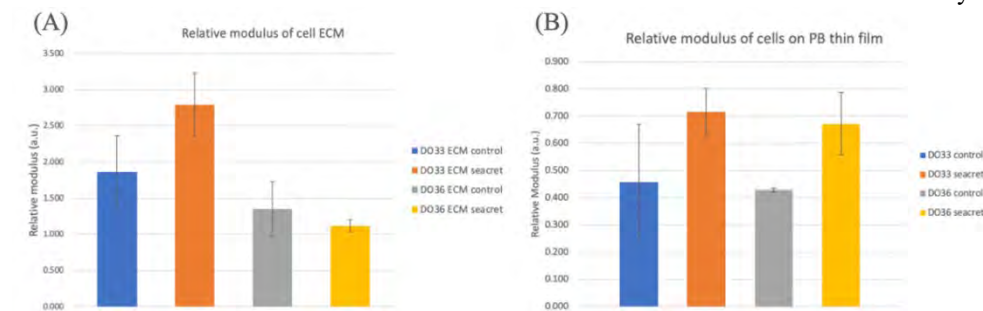


Figure 1. AFM height sensor images of (A) untreated DO33, (B) untreated DO36, (C) Seacret-treated DO33, and (D) Seacret-treated DO36.



Seacret broth on protein structure and density.

Figure 2. Relative modulus of (A) ECM of DO33 and DO36 untreated and treated with Seacret on SPS films (mean \pm 1 SD), (B) DO33 and DO36 cells untreated and treated with Seacret on PB thin (20 nm) films (mean \pm 1 SD).

¹ Hussain, S., et al. "The Biomechanical Properties of the Skin." *Dermatologic Surgery*, vol. 39, no. 2, Feb. 2013, pp. 193-203, doi: 10.1111/dsu.12095.

² Uitto, J. "Biochemistry of the Elastic Fibers in Normal Connective Tissues and Its Alterations in Diseases." *Journal of Investigative Dermatology*, vol. 72, no. 1, 1979, pp. 1-10, doi:10.1111/1523-1747.ep12530093.

³ Berdyeva, T. K., et al. "Human Epithelial Cells Increase Their Rigidity with Ageing In Vitro: Direct Measurements." *Physics in Medicine and Biology*, vol. 50, no. 1, 2004, pp. 81-92, doi:10.1088/0031-9155/50/1/007.

Cytotoxicology of Bone Graft Materials

Senhuang Cai¹, Fan Yang², and Anthony Mendez¹

¹Queens College, Flushing, NY 11367, ²Department of Materials Science and Chemical Engineering, Stony Brook University NY 11794-2275

Bone grafting is a procedure to make up for lost bone after the tooth removal process to allow for the implantation of new teeth.¹ Recently, some bone graft materials have been found to be toxic to dental pulp stem cells². For this experiment, we performed a lab to analyze the effects of two bone grafting materials, OsteoGraf LD 300 hydroxyapatite and Bio-Oss bone graft materials on dental pulp stem cells in vitro. This study will help determine the impact OsteoGraf LD 300 hydroxyapatite and Bio-Oss material on bone grafting in dentistry.

MEM Alpha supplemented with fetal bovine serum, ascorbic acid, and β -glycerol phosphate was used as the base medium to provide nutrition for the dental pulp stem cell cultures for determining the effects of Graf LD 300 hydroxylapatite and Bio-Oss bone graft material. Our experiments evaluated two groups, one in the base medium and one in base medium with dexamethasone, a known inducer of osteogenesis and odontogenesis. Each 6-well plate contained dental pulp stem cell cultures in which 2 were mixed with OsteoGraf LD 300 hydroxyapatite cultures, 2 mixed with Bio-Oss, and 2 served as control. Cell counts for each and every combination were counted with the optical microscope every two days for a total of three datasets Day 0, Day 2, and Day 4 (Figure 1, 2, 3).

Cultures with OsteoGraf LD 300 hydroxyapatite and Bio-Oss bone graft material yielded lower cell counts at the end of the 4-day period. Compared to the control, they appeared to release material that limited the proliferation of dental pulp stem cells. Additionally, we found that the Bio-Oss limited proliferation more effectively than OsteoGraf LD 300 hydroxyapatite (Figure 2 and 3). However, after a single medium change, the dental pulp stem cells in all culture conditions began proliferating (Figure 1, 2). The identity of the compound(s) responsible for initially limiting proliferation is the subject of further research.

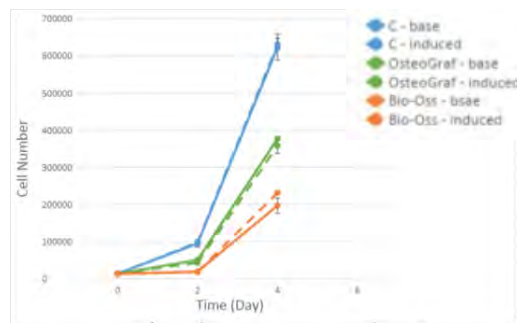


Figure 1: The cell numbers in each environment on Day 0, 2, and 4

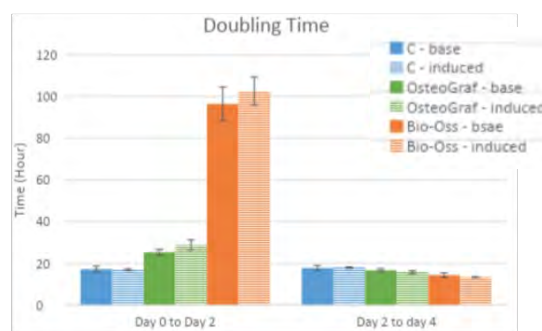


Figure 2: The doubling time of each cell culture on Day 0, 2, and 4

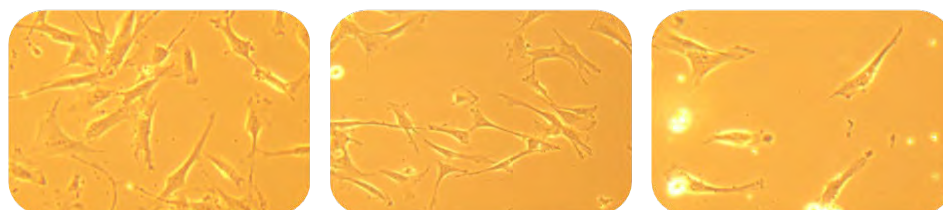


Figure 3. Cells in each group after day 2. (Left) Control (Middle) with Hydroxylapatite (Right) Bio-Oss

¹ Midtown Dentistry Dentistry. (2013, Sep 16). What is a dental bone graft?.mp4. www.youtube.com/watch?v=956l-T9CMX0

² Modi, P. K., Prabhu, A., Bhandary, Y. P., Shenoy P, S., Hegde, A., ES, S. P., ... & Rekha, P. D. (2019). Effect of calcium glucoheptonate on proliferation and osteogenesis of osteoblast-like cells in vitro. *PLoS one*, 14(9), e0222240.

Investigating the Effect of Bioprinting Organotypic Skin and Angiogenesis Under Confinement

Leah Hersh¹, Joshua Kang², Kimberly Lu³, Mori Ono⁴, Annie Wang⁵, Samantha Wang⁶, Qianyi Zhao⁷, Jonathan Xavier⁸, Juyi Li³, Marcia Simon⁹, Miriam Rafailovich³

¹Central High School, Hollis, NY 11423 ²Westwood High School, 12400 Mellow Meadow Dr, Austin, TX 78750 ³Department of Materials Science and Chemical Engineering, Stony Brook University, Stony Brook, NY 11790 ⁴Community High School, Ann Arbor, MI, 48104 ⁵Central Bucks High School East, Doylestown, PA 18902, ⁶St. Mark's School, Southborough, MA 01772, ⁷Princeton Int'l School of Math and Science, Princeton, NJ ⁸Valley Stream North High School, Franklin Square, NY 11010, 08540, ⁹Department of Oral Biology and Pathology, Stony Brook University, NY 11794

Skin tissue, compared to other organs in high demand, is known for its convenient versatility and its regenerative potential. However, despite its relatively high level of accessibility, over 300,000 deaths¹ result annually from severe burn injuries, and autologous grafts are not always an option for time-constricted situations. 3D bioprinters have been used to create engineered human bilayer skin, providing an alternative to traditional grafting methods. Angiogenesis plays a crucial role in achieving full function of engineered organotypic skin for grafting purposes. Our study focused on finding the optimal conditions for angiogenesis.

In preparation for spincasting, silicon wafers were coated with polystyrene (PS), polymethyl methacrylate (PMMA), poly 4-vinylpyridine (P4VP), and polybutadiene (PB) solutions. Once spincast, the substrates were annealed at 170°C, received drops of matrigel, and were topped with human umbilical vein endothelial cells (HUVECs) before being incubated at 37°C for 16h. Contact angles were then measured using a goniometer and HUVEC network tube formation was measured using a fluorescent microscope. The resulting data was cross-analyzed to relate contact angle and proliferation success.

To prepare the skin, human dermal fibroblasts were incubated until the desired cell density was achieved. The first layer of collagen was either printed with a cellink bioprinter or plated in the insert of a 6-well plate. After gelation, a second layer of collagen with fibroblasts was then bioprinted or plated into each well. Metal rings were added after three days to preserve the structures' integrity. Next, keratinocyte cells were bioprinted or plated into each well. Since then, the media has been replenished regularly.

The results of comparing contact angle and connection number suggest a negative correlation between the two; substrates with highest average contact angles produced the lowest numbers of connections. Additional data will be necessary to validate and support these conclusions.

To determine the optimal HUVEC density, four different cell densities (4.5×10^4 , 6×10^4 , 7.5×10^4 , and 1×10^5 cells/cm²) were plated and their proliferation measured in the number of junctions formed. As shown by the correlated Fig. 2, the optimal cell density was determined to be 7.5×10^4 cells/cm².

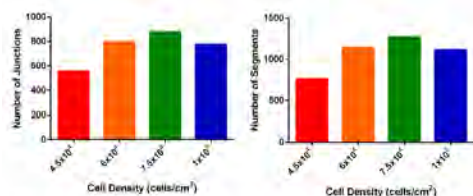


Figure 2. As the cell density increased, network proliferation generally increased.

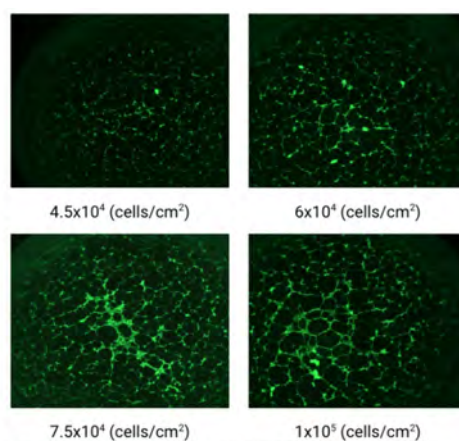


Figure 1. EVOS microscope images of the HUVEC samples of different densities.

Successful angiogenesis in bioprinted skin would be an important step for the therapeutic use of bioprinted skin. Additionally, angiogenesis in bioprinted skin would indicate its potential to be implemented in other bioprinted organs as the field progresses.

¹ Peck, Michael. "Epidemiology of burns throughout the world. Part I: Distribution and risk factors." *Burns: Journal of the International Society for Burn Injuries*, vol. 37, no. 1, 2011, pp. 1087-100.

Regulating Substrate Mechanics to Achieve Neurogenic Differentiation of Dental Pulp Stem Cells Using Polybutadiene and Graphene/Graphene Oxide Thin Films

Samuel Liu¹, Shivek Narang², Kuan-Che Feng³, Haijiao Liu³, Marcia Simon⁴, Miriam Rafailovich³

¹Olathe North High School, KS, 66061; ²Stanford Online High School, CA, 94345; ³Department of Materials Science and Chemical Engineering, Stony Brook University, NY, 11794 ⁴Department of Oral Biology and Pathology, School of Dental Medicine, Stony Brook University, Stony Brook, NY 11794

Injuries to the nervous system can critically disrupt the function and survival of humans and animals. Currently, the central nervous system is unable to effectively repair itself or regenerate neurons when affected by damage. Dental pulp stem cells (DPSCs) are pluripotent stem cells which have exhibited the ability to differentiate into neurons¹. DPSCs are promising candidates in neuroregenerative medicine due to their neurogenic ability and accessibility via human third molars². Polybutadiene (PB) is a biocompatible polymer, whose modulus can be regulated substrate modulus by changing film thickness or adding inorganic particles³. Previously substrate mechanics have been shown to affect stem cell differentiation. Graphene (G) and reduced graphene oxide (GO) have both been shown to be beneficial in neurogenic differentiation, potentially due to their conductive properties, which may enhance synaptic communication between neurons⁴. Graphene oxide has also been shown to enhance stem cell proliferation and differentiation via interactions with key biomolecules. This study investigates the role of substrate mechanics and graphene/graphene oxide in the neurogenic differentiation of DPSCs. To create thin films of different thicknesses, solutions of 3 mg/mL (thin) and 20 mg/mL (thick) PB were spun cast at 2500 RPM for 30 seconds onto cleaved silicon wafers, with and without the presence of 3% graphene. The surface morphology and relative modulus of the films were analyzed with AFM imaging and Nanoscope Analysis software. **Figure 1** shows the effect of graphene particles on PB film topography. Graphene particles were much more prevalent in the thin films compared to the thick films. **Figure 2** shows that the thin films and films with incorporated graphene have significantly higher relative modulus compared to the thick films and films without graphene. Following the procedure described in Arthur et al., the wells were first coated with 0.01 % stock Poly-L-Ornithine diluted in PBS in a 1:3 ratio and incubated overnight at room temperature, washed twice with water, then coated with laminin (5 μg/mL) and incubated overnight at 37 °C.¹ The wells were then washed with phosphate buffered saline (PBS) and growth medium. The spin casted

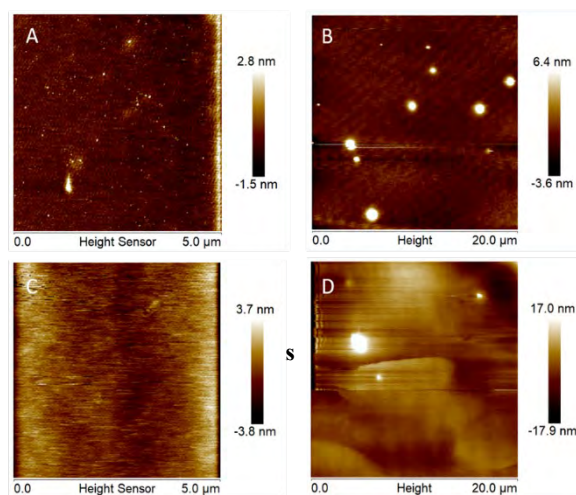
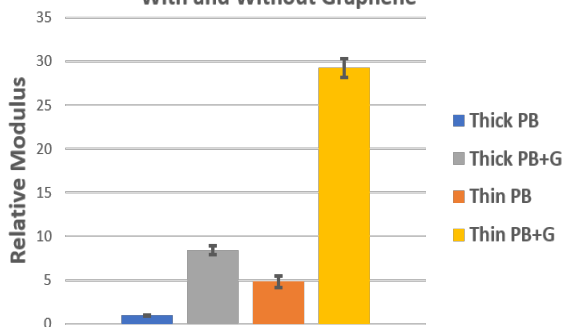


Figure 1. AFM surface morphology images A) Thin PB, B) Thin PB+G, C) Thick PB, D) Thick PB+G

Fig 2: Relative Modulus of Thin and Thick PB Films With and Without Graphene



using confocal microscopy. After 21 days, the DPSCs will be harvested and RNA will be isolated using QIAzol lysis reagent RT-PCR will be conducted in order to quantify the expression of neuromarkers Nestin (early), β-Tubulin-III (intermediate), and NEFM (mature). Day 21 neuromarker expression will then be compared to initial expression.

- Arthur, Agnes, et al. "Adult Human Dental Pulp Stem Cells Differentiate Toward Functionally Active Neurons Under Appropriate Environmental Cues." *Stem Cells*, vol. 26, no. 7, 2008, pp. 1787–1795., doi:10.1634/stemcells.2007-0979.
- Anitua, Eduardo, et al. "Progress in the Use of Dental Pulp Stem Cells in Regenerative Medicine." *Cytotherapy*, vol. 20, no. 4, 12 Feb. 2018, pp. 479–498., doi:10.1016/j.jcyt.2017.12.011.
- Chang C et al. "Entangled Polymer Surface Confinement, an Alternative Method to Control Stem Cell Differentiation in the Absence of Chemical Mediators." *Ann J Materials Sci Eng.* 2014;1(3): 7.
- Guo, Rongrong, et al. "Accelerating Bioelectric Functional Development of Neural Stem Cells by Graphene Coupling: Implications for Neural Interfacing with Conductive Materials." *Biomaterials*, vol. 106, Nov. 2016, pp. 193–204., doi:10.1016/j.biomaterials.2016.08.019.

Modalities for the Human/Computer Interface

Fan Yang and Zhi Li

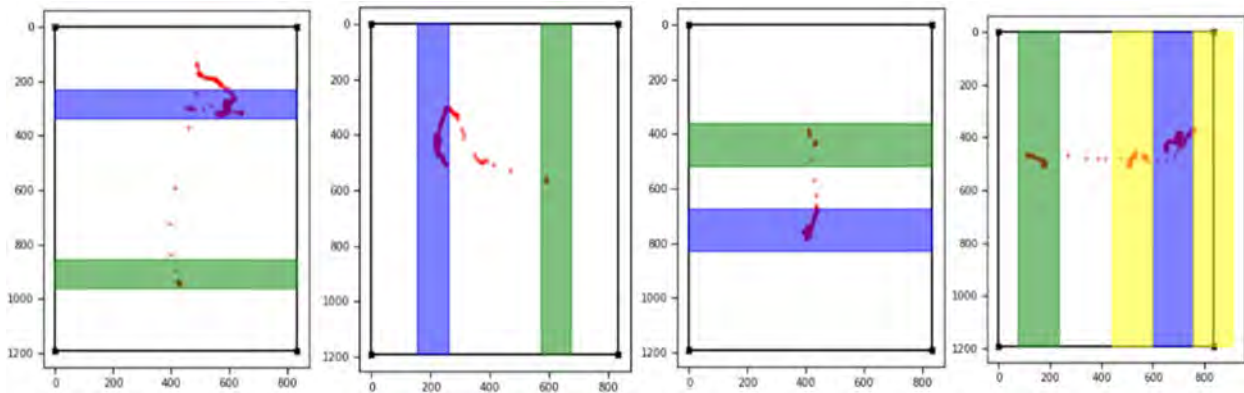


Figure 1: Heat map of face after viewing a "happy" slide. The warmer the color, the stronger the displacement at a single point.



Figure 1: View from camera system for external user to

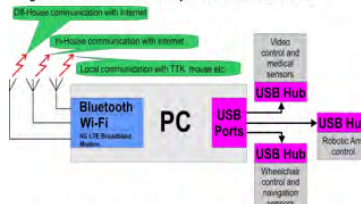


Figure 2: Diagram of inputs and outputs of wheelchair system

Analytical Method for Eye Gaze Trajectory Calibration

By Trevor Cai¹, Jaiden Reddy², Jiayang Wang³, Hannah Zhang¹, Zhi Li⁴, Xiaojun Bi⁴

¹ Canyon Crest Academy, San Diego, California; ² Ed W Clark High School, Las Vegas, NV; ³ Trinity-Pawling School, Pawling, NY; ⁴ Department of Computer Science, Stony Brook University, Stony Brook, NY

The use of eye gaze tracking through iPads allows those with physical disabilities to access technological devices, communicate with others, and access online resources, even with a limited range of movement.¹ To further progress towards this goal, a focus was placed on eye-gaze tracking calibration. Using a currently available eye tracking device, eye gaze trajectories between the corners of the screen were collected to visualize the discrepancy between camera reading and actually reported input, recording all data through coordinates. While many current calibration methods involve anatomical scans, the method used here was purely analytical.

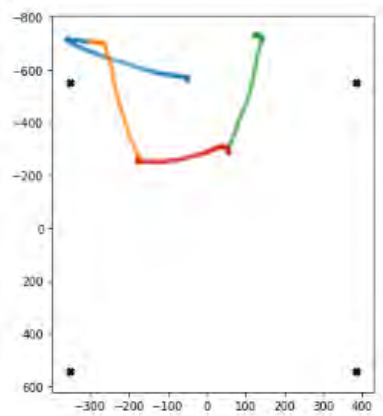


Figure 1: Graph of eye-tracking on iPad

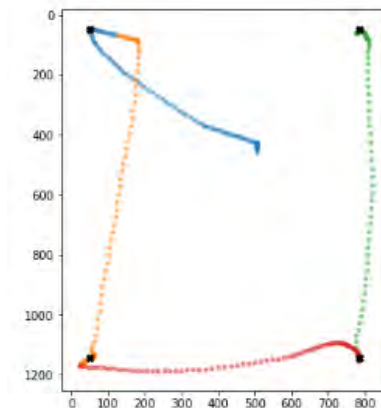


Figure 2: Trajectory from Fig 1 Calibrated

The calibration method used involved the identification of four measured points that corresponded to the four known points the users reported looking at, which can be seen in **Figure 1**. In order to identify these points, an algorithm that identifies a point with the highest density of points in a scatter plot was applied. This algorithm works as a direct result of the tendency of eye gaze movement to saccade during movement between points and fixates once they've reached a target. From there, four linear regressions were created to predict coordinates of all points between the user reported points. A grid was created in which each square of the grid was transformed into another square, resulting in the calibration shown in **Figure 2**. This method had a high level of accuracy but was computationally inefficient. While efforts were made to reduce the level of computation necessary for this method, even with said methods, the amount of time necessary for calibration would make this method difficult for real-time user cursor calibration. Still, further experimentation to increase computational efficiency will occur.

Attempts to implement other methods were made to identify a similarly accurate, but more computationally efficient way to calibrate user inputs. Homography has been implemented in two ways, one of which was successful, although less so than the one previously described. The first involved developing a homography matrix using only the four user reported points and the four corresponding points gathered experimentally, applying the matrix to the entire dataset. The second involved developing a homography matrix using all points gathered by eye-tracking and creating target points as arrays evenly spaced between user reported points. The first method was successful, but existing inaccuracies were not solved through the second method. Further development of the method, such as RANSAC, is planned.

¹ K. Pfeuffer, M. Vidal, J. Turner, A. Bulling, and H. Gellersen, "Pursuit Calibration: Making Gaze Calibration Less Tedious and More Flexible," in *Cite Seer X*, doi.

Analytical Method for Eye Gaze Trajectory Target Selection

By Trevor Cai¹, Jaiden Reddy², Jiayang Wang³, Hannah Zhang¹, Zhi Li⁴, Xiaojun Bi⁴

¹ Canyon Crest Academy, San Diego, California; ² Ed W Clark High School, Las Vegas, NV; ³ Trinity-Pawling School, Pawling, NY; ⁴ Department of Computer Science, Stony Brook University, Stony Brook, NY

The use of eye gaze tracking through iPads allows those with physical disabilities to fully access technological devices, even with a limited range of movement. To further progress towards this goal, a focus was placed on eye gaze target selection. Current selection methods for eye gaze, such as dwell time-based target selection (DTBTS), require extended periods of intense user focus and, as a result, ultimately cause asthenopia for the user. Alternative methods were investigated in order to outperform DTBTS in both selection accuracy and time.

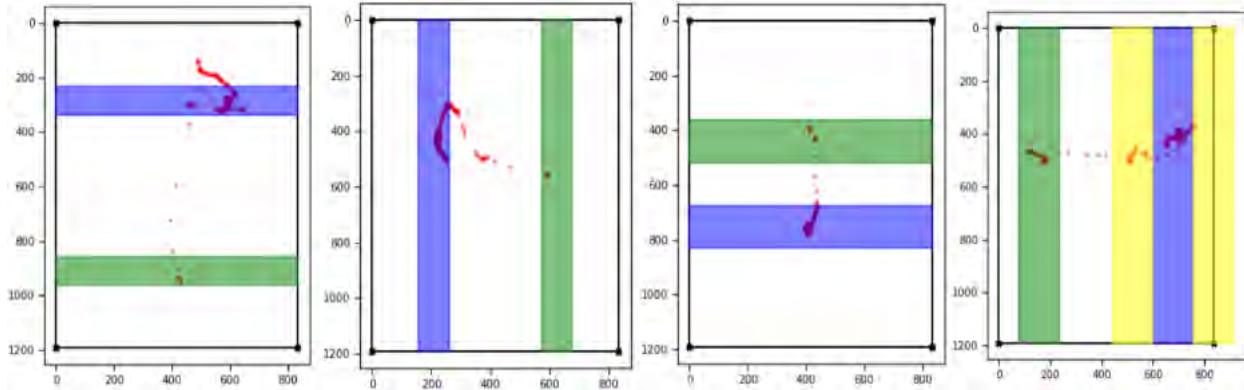


Figure 1 For the first three seconds, the four participants looked at the preparation button on the iPad screen, causing the button to turn green. Then, users shift their gaze to the target button and maintain their gaze for five seconds. The orientation of the preparation and target buttons were adjusted for a robust data set. The four figures above are examples of eye tracking trajectory plotted as red coordinates.

When testing the methods in this experiment, distractor buttons were placed on either side of the target button to simulate a realistic environment. It should be noted that the data was observed to have an underlying problem in which a number of the graphs contained fixation of points, typically indicating the biological response to the selection of the target button, in locations that the distractor buttons laid. This means all results obtained may not be accurate as it could lead to methods failing when they typically should work and is an issue that needs to be solved before definite conclusions can be made.

We added algorithms to DTBTS to improve the selection time and the selection rate. The sliding window, or the required amount of time to keep gazing at the target to perform an action, for DTBTS was 1 second. However, because users tend to gaze out of the target button, DTBTS was unable to select the target button for much of the data. To increase the selection rate, instead of resetting the window, the new method tracks time backwards when the user's gaze drifts out of the target button. Thus, the user can continue the process by quickly shifting their gaze back.

Acceleration of the selection process was also implemented. By detecting the distance between consecutive gaze points, the algorithm applies a threshold in which the magnitude of time is multiplied in order to reach 1 second faster. This "acceleration" is applied to succeeding timestamps until the distance exceeds the threshold or the user's gaze moves out of the target button. The acceleration algorithm is specifically designed for datasets with distractor buttons presenting. In a majority of cases, the distance between gaze points in the distractor buttons was more scattered than gaze points in the target button. Therefore, the gaze points in the distractor button are less likely to trigger the acceleration process, which allows a larger sliding window size for gaze points in the distractor button and thus harder to be selected. Still, this algorithm is highly dependent on the scatter of the user's gaze trajectory as it only improves the selection rate when gaze points are relatively scattered.

Another approach that was taken was to look at the standard deviation of the points in a given window in order to find when the gaze was fixated and thus was looking at and selecting the target button. While this method was able to improve the data for the first dataset, it became apparent the spread of points for each user was different and thus a generalized method of evaluating the standard deviations might not be as effective. Further work for this method as well as looking into the use of LSTM recurrent neural networks is planned.

Recognizing Facial Nerve Innervation for Establishing Reaction Times Using Digital Image Skin Correlation

Amisha Agrawal¹, Sophia Cai², Wade Boohar³, Fan Yang⁴, Miriam Rafailovich⁴

¹University High School, Johnson City, TN 37614, ²Barrington High School, Barrington, IL 60010, Olathe North High School, Olathe, KS 66061, ⁴Department of Materials Science and Chemical Engineering, Stony Brook University, Stony Brook, NY 11790

Digital Image Skin Correlation (DISC) is a method used to recognize the movement of facial muscles by analyzing skin pores. Because it tracks one's microexpressions, DISC is a more viable form for analysis of movement imperceptible to the human eye. This method evaluates individual images for displacement from a reference image and yields a facial deformation map that indicates changes in facial muscles and subsequently, microexpressions resulting from changes in mood¹. This can then be used to generate reaction time plots that may suggest the point at which an individual reacts based on their microexpressions. Since each person's microexpressions are unique to them, DISC can be used to accurately recognize a person's face².

This study first analyzed our own facial movement in response to happy and sad images. A series of heat and vector maps were produced after running the DISC analysis on the individual frames of each video (Figure 1); these maps reflected the displacement of our facial muscles compared to the neutral first photo. The results demonstrated a greater amount of movement in the lower half of the face when observing happy images and more movement in the upper half when observing sad images.

To collect reaction times, the DISC program plotted the average displacement of each pore, creating a graph that can be interpreted to find the moment of reaction (Figure 2). In order to track reaction times, we recorded our observations to word searches, in which only one word was hidden, to determine if there was a noticeable reaction to the discovery of that word as well as the speed of that reaction.

By looking at the derivative of displacement and finding areas on the graph where the displacement changes by a significant margin relative to the rest of the graph, we can narrow down the points where the reaction may have occurred. This can be seen in Figure 2, where the displacement drastically decreases just a few frames before the participant physically indicates that they have found the correct word.

Overall, these methods of DISC may be utilized as a form of mood assessment for psychological purposes, determining the consciousness of comatose patients, as well as other applications within psychology and neuroscience. The next step for this study would be to test the reaction time process on other participants, potentially with materials other than word searches, evaluate the efficacy of our approach, and continue improving our methods.

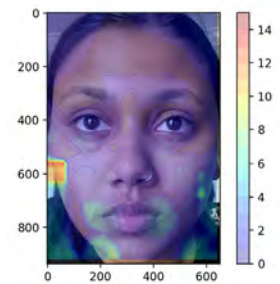


Figure 1: Heat map of face after viewing a "happy" slide. The warmer the color, the stronger the displacement at a single point.

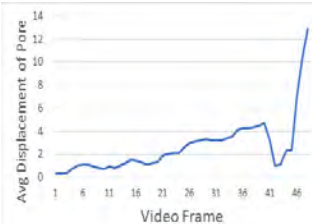


Figure 2: Graph of the average displacement of each pore versus the frame number of the image. The participant signaled that they found the hidden word at frame number 40.

[1] Staloff, Isabelle Afriat et al. "An in vivo study of the mechanical properties of facial skin and influence of aging using digital image speckle correlation." *Skin research and technology : official journal of International Society for Bioengineering and the Skin (ISBS) [and] International Society for Digital Imaging of Skin (ISDIS) [and] International Society for Skin Imaging (ISSI)* vol. 14,2 (2008): 127-34. doi:10.1111/j.1600-0846.2007.00266.x

[2] Pamudurthy, Satprem, et al. "Dynamic approach for face recognition using digital image skin correlation." *International Conference on Audio-and Video-Based Biometric Person Authentication*. Springer, Berlin, Heidelberg, 2005.

The Implementation of a Distant Computer Controlled Robotic Arm for the Aid of the Disabled

Ethan Pereira¹, Hugh Rosshirt², Ethan Wachsmann³, Ayelet Kornblau⁴, Yoni Levy⁵, Michael Gouzman⁶

¹West Windsor-Plainsboro High School North, NJ, 08536; ²South Side High School, NY, 11570; ³Roslyn High School, NY, 11577; ⁴Samuel H Wang Highschool, NY, 11423 ; ⁵Hebrew Academy of Nassau County High School, NY, 11553; ⁶ Stony Brook University, NY, 11794

For many within the disabled community, accomplishing even the simplest of tasks can seem impossible. Despite the current advances in technology, control methods for those with severe disability are still difficult to use and inefficient. Our goal is to establish a method such that a robotic arm with approximately 10 different movements may be controlled by a simple control pad such as a tongue touch keyboard (TTK). With the easy control this method provides, tetraplegics and other disabled persons will be able to live far more self-reliant lives. However, this method of control still takes immense effort and concentration. For this reason, we intend on making a wirelessly connected and controlled wheelchair, where the wheelchair components, including the robotic arm, can be controlled wirelessly (Bluetooth, WIFI, 4G broadband) by either the disabled person, or with the help of certified professionals situated anywhere in the world. This connection enables people with disabilities to complete everyday tasks with significantly greater ease due to the help they receive. In carrying out this research, we set up a multi view camera system so that a more comprehensible view of the arm's movements are visible to the person in control of it. Our goal is to create a user interface that will be simple for ease of control. As such, we plan to set up the TTK as a "computer mouse" capable of changing the x, y, z coordinates of the robotic arm through a Bluetooth connection to the PC. We will be measuring our success through a series of dexterity tests: sorting objects, drawing simple shapes, turning the pages of a book, and feeding a person food. So far, our progress has been setting up the robotic arm and usb cameras all connected to the main PC, which receives an input from a mouse currently to manipulate the arm's movements. Due to the current circumstances, we use TeamViewer² to access the PC remotely from our personal computers. A primary issue encountered with this setup was the CPU overload caused by all these programs (camera display, Dobot³ robotic arm software, TeamViewer) running in tandem with each other, causing the computer to crash. This drew importance to the computing power needed for these tasks, and we plan on upgrading our CPU and RAM in further iterations for smoother and more responsive feedback and control. We also plan to adapt the PC to establish Bluetooth connections to the TTK, as well as add a broadband connection to connect to remote computers all around the world. Although previous research has covered similar topics, they were all high cost (\$30,000+), bulky, and focused on more complex yet not entirely efficient devices such as neural interfacing.¹ The TTK, being both simple and efficient, provides arguably the best method of control, and with the expiration of its patent it is possible to freely research its boundless potential.



Figure 1: View from camera system for external user to

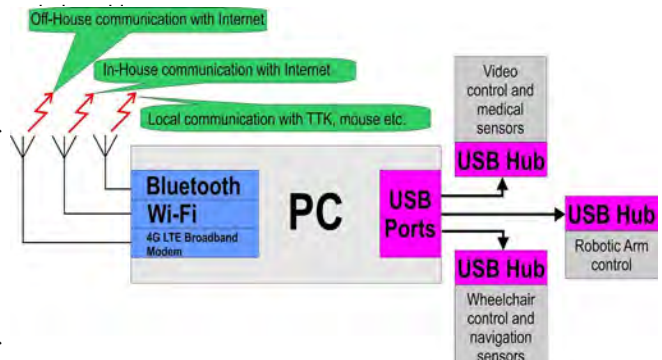


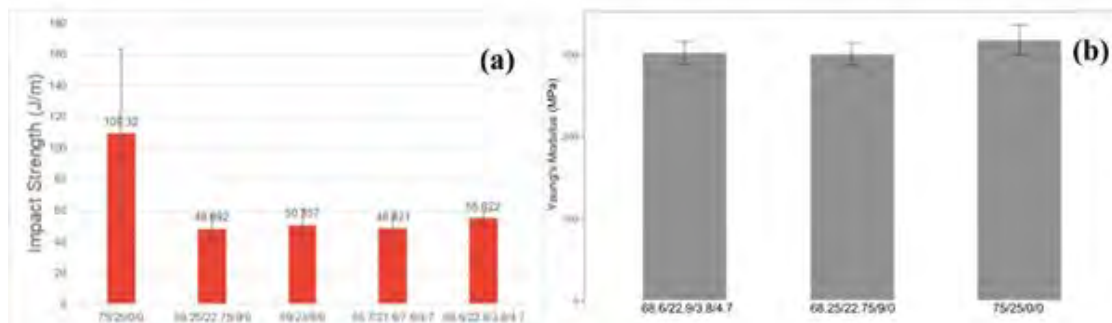
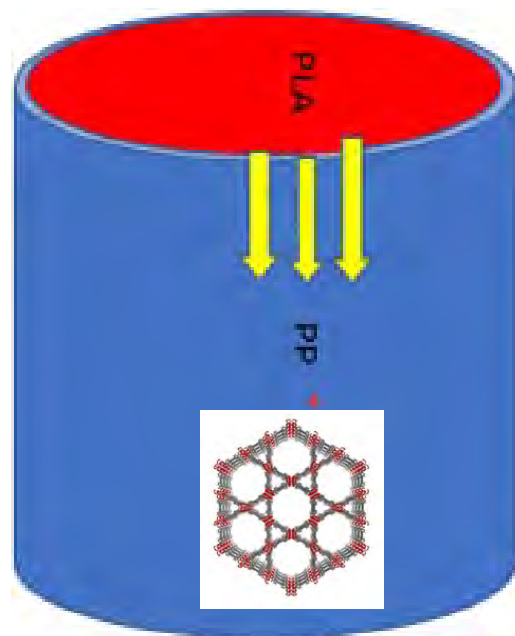
Figure 2: Diagram of inputs and outputs of wheelchair system

1. "KINOVA JACO Assistive Robotic Arm." Kinova, www.kinovarobotics.com/en/products/assistive-technologies/kinova-jaco-assistive-robotic-arm. "The Remote Desktop Software." TeamViewer, www.teamviewer.com/en-us/.

2. Vaudel, Cedric. "Dobot Magician Robotic EDU EDITION." RobotLAB, www.robotlab.com/store/dobot-robotic-arm.

Nanocomposites: Flame retardants, 3-D printing, and Diffusion

Yiwei Fang, Yu-Chung Lin, Hongyu Li



Enhancing the Flame Retardancy of Biodegradable and Tough Polymer/Clay Nanocomposites

Authors: Christian Apostol¹, Lawrence Zhao², Jiale Lu³, Yiwei Fang⁴, Miriam Rafailovich⁴

¹Ward Melville High School, East Setauket, NY ²University Laboratory High School, Urbana IL ³Princeton International School of Mathematics and Science, NJ ⁴Department of Material Science and Engineering, Stony Brook University, NY

Poly(lactic acid) (PLA) has received significant attention for its biodegradability and good mechanical properties. However, PLA's flammability limits its potential applications in areas like electronics. Recently, various studies have investigated thermoplastic blends of polybutylene adipate terephthalate (PBAT), another biodegradable polymer, and PLA, resulting in greater toughness.³ This study focused on nanocomposites with PLA/PBAT blends in a 3:1 ratio. The primary goal of this research was to engineer a biodegradable nanocomposite with optimal flame retardancy and toughness.

Research has shown that the addition of either ammonium polyphosphate (APP) and resorcinol bis(diphenyl phosphate) (RDP) enhances the flame retardancy of PLA.² APP acts as an intumescent flame retardant as during combustion it decomposes, forming phosphoric acid that catalyzes char formation. RDP serves as a compatibilizer that improves the dispersion of APP particles within the PLA/PBAT interface.² Therefore, APP and RDP (9:1) acted as the flame-retardant agent. Previous findings have shown that the introduction of organoclays, such as Cloisite-30B, also improves the dispersion of the flame retardant substances in the polymer interface, which in turn improves flame retardancy.¹ Sodium clay also enhances the miscibility of PLA/PBAT blends and lowers the PLA/PBAT interfacial energy.¹ Therefore, sodium clay coated with RDP (C-RDP) (1:1) was added to the nanocomposites.

Samples (% PLA/PBAT/APP-RDP/C-RDP)	t ₁	t ₂	Dripping?	Cotton Condition	Grade
68.25/22.75/9/0	<1s	<1s	Yes (slight)	No Fire	V-0
71.25/23.75/5/0	<1s	<1s	Yes (heavy)	Burnt	V-2
65.7/21.9/7.6/4.7	1s	<1s	Yes (slight)	No Fire	V-0
68.6/22.9/3.8/4.7	<1s	3-4s	Yes	No Fire	V-0
67.65/22.55/7.8/2	<1s	2-5s	Yes	No Fire/Burnt	V-2
69/23/3/5	<1s	3-4s	Yes	No Fire/Burnt	V-0/V-2

Fig 1. UL-94 flame test results of nanocomposites.

The flame retardancy of nanocomposites were tested using the UL-94 flame test protocol. The most common result of each sample is shown (Fig. 1). Molded polymer samples that achieved a V-0 grade were subject to impact testing to determine toughness (Fig. 2a). The results indicate that decreasing the amount of APP/RDP present in the blend, which allows an increase in the % of PLA/PBAT, restores toughness. In addition, clay appeared to have a negligible effect on impact strength, as samples with comparable amounts of APP/RDP differed by 2 J/m. While clay likely decreased the PBAT domain size in PLA, the addition of clay also decreased the overall proportion of PLA/PBAT. The nanocomposite with 3.8% APP-RDP and 4.7% C-RDP had the best overall performance, with low loading of APP-RDP leading to restored impact strength (55.022 J/m) and a V-0 flame retardant rating. Tensile measurements (Fig. 2b) also indicate that this nanocomposite has a comparable Young's modulus to the original PLA/PBAT (3:1) blend. Currently, the morphology and structure of the nanocomposites are being investigated using scanning electron microscopy (SEM) and Raman spectroscopy.

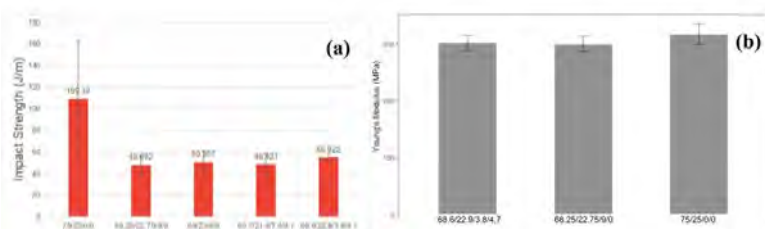


Figure 2. (a) Izod impact test results for nanocomposites that achieved a V-0 UL-94 rating. (b) Instron tensile test results for selected nanocomposites. In both figures, the impact strength of a PLA/PBAT (3:1) blend is a control.

¹Guo, Yichen, et al. "Engineering Flame Retardant Biodegradable Polymer Nanocomposites and Their Application in 3D Printing." *Polymer Degradation and Stability*, vol. 137, 2017, pp. 205–215., doi:10.1016/j.polymerdegradstab.2017.01.019.

²Xue, Yuan, et al. "Enhanced Flame Retardancy of Poly(Lactic Acid) with Ultra-Low Loading of Ammonium Polyphosphate." *Composites Part B: Engineering*, vol. 196, 2020, p. 108124., doi:10.1016/j.compositesb.2020.108124.

³Zhao, Hongwei, et al. "Blends of Poly(Butylene Adipate-Co-Terephthalate) (PBAT) and Stereocomplex Poly(lactide) with Improved Rheological and Mechanical Properties." *RSC Advances*, vol. 10, no. 18, 2020, pp. 10482–10490., doi:10.1039/c9ra10827k.

Investigating and Comparing the Resistance to Tensile Testing of Molded and 3D Printed PLA/PP Polymer Blends

Daniel Luo¹, Yu-Chung Lin², Miriam Rafailovich³

¹Monroe-Woodbury High School, Central Valley, NY 10917; ²Department of Material Science and Engineering, Stony Brook University, Stony Brook, NY 11794; ³Department of Material Science and Engineering, Stony Brook University, Stony Brook, NY 11794

In the process of 3D printing, the quick cooling rate of PLA does not allow enough time for the filament to properly penetrate across an interface.¹ This property inhibits adhesion and reduces the overall strength of prints. This study aims to tackle this problem by adding low concentrations of polypropylene (PP) to PLA to create a 3D-printing filament with improved interlayer diffusion.² Our hypothesis is that when a PLA/PP blend is formed either through 3D printing, its lower surface energy and lower glass transition temperature causes the PP to migrate to the surface of the filaments, forming a core-shell structure (as seen in Fig. 1) that can potentially fuse deformed fibers, producing a “self-healing” effect.² This effect is due to the lower surface tension of PP as compared to PLA (30.7 mN/m vs 44 mN/m)⁵, so PP will travel to the surface of the fibers when extruded, displacing possible air pockets formed when the fibers crack.^{3,4} Previous testing has shown that 1% PP blends are the most resistant to tensile testing. This study seeks to determine if the PP/PLA blend produced by molding or 3D printing is more effective in this regard, and which concentration of PP is most resistant to tensile testing.

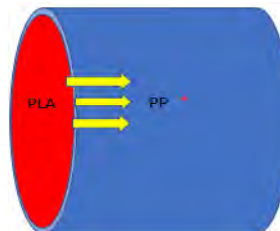


Fig. 1: Core shell structure of the PLA/PP blends when extruded as a filament. The PP goes to the surface and promotes “self-healing” if the fibers are deformed.

In this study, 5 groups differing in PP % by weight were used to compare which concentration of PP in a PLA/PP blend could best resist tensile testing: 0%, 0.5%, 1%, 2.5%, and 5%. After all of the samples were successfully prepared, the Young’s Modulus, UTS (Ultimate Tensile Strength), and Elongation at Break were analyzed. Fig. 2 shows the comparisons of the Young’s Modulus of each of the molded samples, and it indicates that the Pure PLA was had the highest Young’s Modulus, meaning that the molded samples did not exhibit the “self-healing” effect. Fig. 3 shows the comparison between the Young’s Moduli of the 0.5% PP, 1% PP, 2.5 % PP, 5% PP, and Pure PLA for the 3D printed samples. The results indicate that the 0.5% PP has a higher Young’s Modulus compared to the 1% and Pure PLA, making it a more efficient blend for 3D printing. Contact angle was also measured in Fig. 4, showing that even a small amount of PP added to PLA in a blend can produce a contact angle similar to pure PP, meaning adding the PP makes the surface tension of the blend much lower, meaning that the 3D printed blends will have PP travel to the surface of the fibers and will produce a self-healing effect. In conclusion, this study shows that the optimal concentrations for making a PLA/PP blend for 3D printing is 99.5% PLA/0.5% PP. It also shows that compared to the 3D printed blends, the molded blends do not strengthen the blends to the same extent during tensile testing.

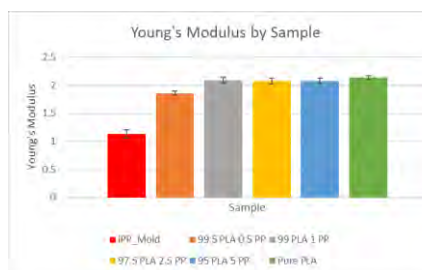


Fig. 2: Graph of the differing Young’s Moduli of all of the molded samples. Pure PLA still has the best Young’s Modulus, meaning that the molded samples do not exhibit the “self-healing” effect.

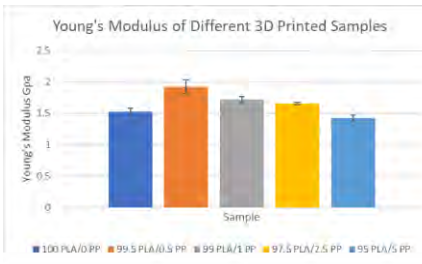


Fig. 3: Comparison of the Young’s Modulus of Pure PLA, 99.5% PLA, 99% PLA, 97.5% PLA, and 95% PLA. 99.5% PLA produced the highest Young’s Modulus, meaning that it is even better than 99% for 3D Printing.

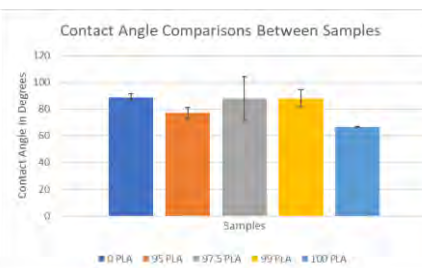


Fig. 4: Contact Angle Measurements for each sample. As you can see, adding a small amount of PP to PLA produces about the same angle as pure PP, meaning that the samples will exhibit self-healing.

1 Liu, Zengguang, et al. “A Critical Review of Fused Deposition Modeling 3D Printing Technology in Manufacturing Polymeric Parts.” International Journal of Advanced Manufacturing Technology, vol. 102, no. 9-12, Springer Science and Business Media LLC, 2019, pp. 2877–89, doi:10.1007/s00170-019-03332-x.

2 Peng, Fang, et al. “3D Printing with Core–Shell Filaments Containing High or Low Density Polyethylene Shells.” ACS Applied Polymer Materials, vol. 1, no. 2, American Chemical Society, Feb. 2019, pp. 275–85, doi:10.1021/acsapm.8b00186.

3 Mehrabi Mazidi, Majid, et al. “Highly-Toughened Poly(lactide- (PLA)) Based Ternary Blends with Significantly Enhanced Glass Transition and Melt Strength: Tailoring the Interfacial Interactions, Phase Morphology, and Performance.” Macromolecules(51, 4298-314), 2018

4 “Polymer Properties Database.” Surface Tension, polymerdatabase.com/polymer%20physics/sigma.html.

5 Guo, Yichen, et al. “Enhancing Impact Resistance of Polymer Blends via Self-Assembled Nanoscale Interfacial Structures.” Macromolecules, vol. 51, no. 11, American Chemical Society, June 2018, pp. 3897–910, doi:10.1021/acs.macromol.8b00297.

Simulating the Diffusion and Adsorption of Gas through UiO-66 and NU-1000 Metal-Organic Frameworks using the Lattice-Boltzmann Method

Eric J. Kim^a, Kevin Gu^b, Jalaj Mehta^c, Hongyu Li^d, Dilip Gersappe^d, Miriam Rafailovich^d

^aStuyvesant High School, New York, NY 10282; ^bDeerfield Academy, Deerfield, MA 01342; ^cHauppauge High School, Hauppauge, NY, 11788; ^dDepartment of Materials Science and Chemical Engineering, Stony Brook University, Stony Brook, NY 11794

There are numerous methods for modeling the flow of fluids through metal-organic frameworks including molecular dynamics and computational fluid dynamics. However, the most efficient and accurate method for coarse-grained molecular dynamics modeling is the Lattice Boltzmann Method, which can effectively simulate complex systems and is able to utilize parallel computing.¹ We used Palabos to write C++ scripts and XCode and ran our simulations on the server and used Paraview to visualize the data and employed MatLab for analysis.

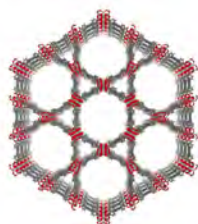


Figure 1. NU-1000 Lattice Structure

We modeled the diffusion of CO₂ through NU-1000, as shown in Figure 1, and UiO-66 metal-organic frameworks in an attempt to differentiate between pure diffusion and diffusion with adsorption defects in the two materials using a modified version of the Boltzmann Transport Equation that employed the Bhatnagar-Gross-Krook operator as the collision function for pure diffusion and the Langmuir adsorption model for diffusion with adsorption and desorption.

Additionally, Fick's second law with a planar Dirac initial condition at the origin was employed to calculate the diffusion coefficient of CO₂ through the MOFs. This diffusion coefficient was then fitted to the concentration-time curve with timestep t to give a simulation result of the diffusion coefficient. The analysis consisted of a review of the speed in time-steps to reach Maxwell-Boltzmann Equilibrium and the subsequent comparison of said speeds between NU-1000 and UiO-66 as well as an investigation into the speed change between the pure diffusion and diffusion with defects for each MOF, with the defects being accounted for using Polanyi-Wigner equation solved for desorption, which we assume is equal to adsorption.

We plotted the diffusion coefficient versus timesteps for UiO-66 and NU-1000 at 263 K, 273 K, and 293 K (Figure 2) and found that the coefficient changed minimally with temperature in the membrane with adsorption and stayed at about .05 the entire time. For diffusion without adsorption through UiO-66 the diffusion coefficient stayed just under .15, and decreased slowly as the experiment reached its conclusion. The NU-1000 MOF resulted in a diffusion coefficient of .37 without adsorption and .1 with adsorption, assuring the fact that adsorption decreases the diffusion rate.

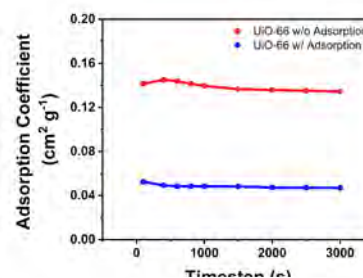


Figure 2. UiO-66 diffusion coefficient with adsorption

¹ Chen, S., & Doolen, G. D. (1998). Lattice Boltzmann Method For Fluid Flows. Annual Review of Fluid Mechanics, 30(1), 329-364. doi:10.1146/annurev.fluid.30.1.329

²Ramsahye, N. A., Gao, J., Jobic, H., Llewellyn, P. L., Yang, Q., Wiersum, A. D., . . . Maurin, G. (2014). Adsorption and Diffusion of Light Hydrocarbons in UiO-66(Zr): A Combination of Experimental and Modeling Tools. *The Journal of Physical Chemistry C*, 118(47), 27470-27482. doi:10.1021/jp509672c

HYDROGELS

*Robert Wong, Shoumik Saha
and Juyi Li*

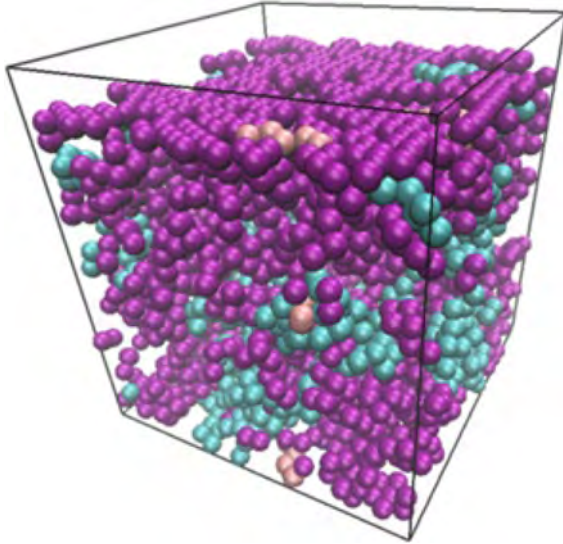


Fig 1. Visualization of a Hydrogel system before shearing. Blue is Polymer A, Purple is Polymer B. Tan is the clay nanocomposite.

Maximum Crosslinking Times vs. Catalyst Concentration for Varying Hydrogel Blends

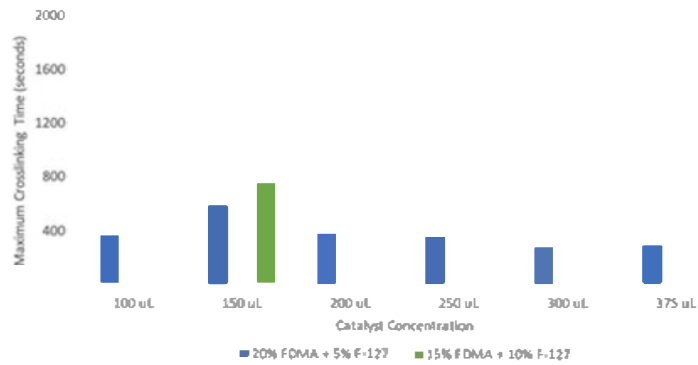


Figure 1: Single frequency time sweeps conducted on various hydrogel blends

Using Coarse-Grained Molecular Dynamics to Model Hydrogel Viscosity

Hannah Even¹, Kyle Shi², Eric Song³, Shoumik Saha⁴, Dilip Gersappe⁴

¹Staples High School, Westport, CT 06880, ²Dublin High School, Dublin, CA 94568, ³Vernon Hills High School, Vernon Hills, IL 60061, ⁴Department of Materials Science & Engineering, Stony Brook University, Stony Brook, NY 11794

Recent experimental studies show that biopolymer-based pore fluids have potential as a substitute for cement in stabilizing soil structures¹. Through physical interactions with clay nanoparticles, these hydrogels can greatly enhance the mechanical strength of the soil. However, while experiments have successfully demonstrated the effect of hydrogels on soil strength, the structure formation process and mechanical properties of such systems are still not well known. Past studies have found a positive relationship between hydrogel viscosity and clay nanocomposite concentration^{2,3} using coarse-grained molecular dynamics simulations with a qualitative stress-autocorrelation function.

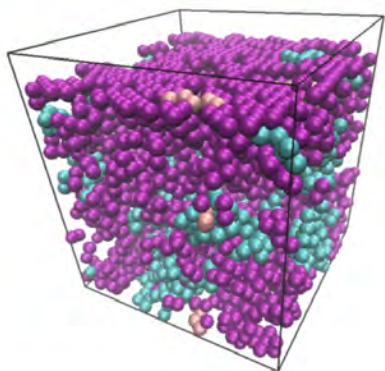


Fig 1. Visualization of a Hydrogel system before shearing. Blue is Polymer A, Purple is Polymer B, Tin is the clay nanocomposite.

This study seeks to verify and improve upon those results by measuring viscosity of various systems under shearing, as well as further optimizing hydrogel composition. Each system consisted of varying ratios of two different biopolymers, clay nanoparticles, and water particles in randomly generated initial positions which were then simulated through a coarse-grain molecular dynamics model with LAMMPS⁴ (Fig 1.). Each system was sheared to obtain a velocity profile for the hydrogels. From there, strain rates were calculated, and the viscosity was found through the formula $\eta = \frac{-p}{\dot{\epsilon}}$, where η is viscosity, p is pressure, and $\dot{\epsilon}$ is strain rate.

Results using sheet-shaped nanoparticles, with 19 monomers each, gave non-linear velocity profiles leading to inaccurate viscosity calculations. Instead, systems with rod-shaped nanoparticles, with 5 monomers each, gave linear velocity profiles (Fig 2.), and therefore more accurate viscosity data. Each system was run with either differing concentrations of biopolymers, fillers, or different shearing speeds to see each's effect on viscosity. Simulations showed a decrease in viscosity as shearing speeds decreased and as the number of nanoparticles decreased.

While current data does show some general trends, future simulations with more timesteps and a more diverse range of biopolymers and nanocomposites are needed for conclusions. We hope to compare our results with the results of previous studies and actual experimental data to verify this method of determining viscosity. Our findings can hopefully provide knowledge on the theoretical aspect of improving hydrogels for better soil stability.

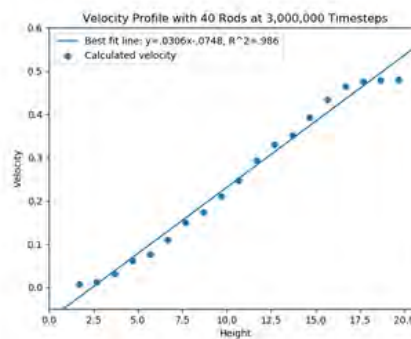


Fig 2. A Linear velocity profile of a Hydrogel with 40 Rods at 3 Million timesteps

¹ Zhao, Zhi, et al. "Biomimetic Hydrogel Composites for Soil Stabilization and Contaminant Mitigation." *Environmental Science & Technology*, vol. 50, no. 22, American Chemical Society, Nov. 2016, pp. 12401–10, doi:10.1021/acs.est.6b01285.

²Xu, D. et. al. "Rheology of Poly(N-isopropylacrylamide)–Clay Nanocomposite Hydrogels." *Macromolecules* Sept. 12 2019

³Xu, D., Gersappe, D. "Structure formation in nanocomposite hydrogels." *Soft Materials* vol. 13, Issue 1853 (2017). Doi: 10.1039/c6sm02543a

⁴S. Plimpton, Fast Parallel Algorithms for Short-Range Molecular Dynamics, *J Comp Phys*, 117, 1-19 (1995)

Developing Thermally Responsive Polymer Gels for Aneurysm Occlusion

Anya Chabria^{1*}, Jessica Guo^{2*}, Varun Nimmagadda^{3*}, Tyler Shern^{4*}, Stephanie Tarrab^{5*}, Jeffrey Zhang^{6*}, Emily Zhou^{7*}, Jeffrey Huang⁸, Ikshu Pandey⁹, Juyi Li¹⁰, Robert Wong¹⁰, Chandramouli Sadasivan¹¹, Miriam Rafailovich¹⁰

¹The Wheatley School, Old Westbury, NY 11568, ²Ward Melville High School, East Setauket, NY 11733, ³Novi High School, Novi, MI 48375, ⁴Mission San Jose High School, Fremont, CA 94539, ⁵Yeshivah of Flatbush Joel Braverman High School, Brooklyn, NY 11230, ⁶Centerville High School, Centerville, OH 45459, ⁷The Harker School, San Jose, CA 95129, ⁸University of Pennsylvania, Philadelphia, PA 19104, ⁹Johns Hopkins University, Baltimore, MD 21218, ¹⁰Department of Mat. Sci. & Chem. Eng., Stony Brook University, Stony Brook, NY 11790, ¹¹Department of Neurological Surgery, Stony Brook University, Stony Brook, NY 11790

*Authors 1-7 contributed equally to this work

Cerebral aneurysms are weak areas in the walls of an artery that, if left untreated, can rupture and lead to strokes or even death. Endovascular coiling using metallic and hydrogel-coated coils has emerged as an optimal method for treating cerebral aneurysms by blocking blood flow and inducing clotting.¹ However, due to the permanence of endovascular coils, this minimally invasive technique can lead to vessel trauma and thrombosis. Additionally, while hydrogel-coated coils result in lower aneurysm recurrence rates, they did not show any significant differences in other favorable outcomes such as functional recovery and mortality when compared to metallic coils.² Therefore, this project focuses on the development of a nonmetallic, biocompatible, and thermally responsive gel solution composed of FDMA and Pluronic® F-127 for aneurysm occlusion.

Combined gels made of Pluronic® F-127, FDMA, and DI Water were mixed in several different concentrations (20% FDMA and 5% F-127, 10% FDMA and 15% F-127, 15% FDMA and 10% F-127). A crosslinker consisting of ammonium persulfate, L-ascorbic acid, and iron (III) chloride was added to samples of the gels in varying volumes to form different ratios of gel to crosslinker. Rheological tests, including single-frequency time sweeps and amplitude sweeps, were conducted on different gel combinations to determine times of cross-linking and maximum elastic moduli and to compare varying incubation and peristaltic flow conditions.

Single frequency time sweep results for the gels were analyzed through plots of maximum chemical cross-linking times vs. catalyst concentration and maximum elastic modulus vs. catalyst concentration. Catalyst concentration to gel ratios that were predicted to result in the target maximum cross-linking time range of 300-360 seconds were selected for future rheological testing, with the results for the 20% FDMA+5% F-127 and 15% FDMA+10% F-127 gels shown in Fig 1. Amplitude sweep results were analyzed following incubation and peristaltic flow to consider the strength of the gels. In terms of both elastic and viscous moduli, the moduli for 3 days of flow are shown to be lower than the results of 3 days incubation and 20-minute incubation for the 10% FDMA+15% F-127 gel (Fig 2). While the elastic modulus is higher after 3 days of incubation than after 3 days of water flow, the viscous modulus is higher after 3 days of water flow than 3 days of incubation. These results indicate that water flow significantly weakens the gel, perhaps due to the washing away of F-127 or the gel's biodegradable qualities. To test the efficacy of the hydrogel blends, a 3D-printed model of a blood vessel containing aneurysms with differing geometries and sizes was designed.

This model will be connected to a water flow apparatus to simulate blood flow and temperature (37°C). This system will then be used to analyze the shear of the hydrogel over long periods of time and determine viability. While improvement is needed to ensure total occlusion, this study shows promise for a novel embolization method. Further testing with FDMA and F-127 to optimize polymer and catalyst concentrations is necessary in order to achieve cross-linking times of 300-360 seconds so that in practice, the hydrogels cross-link only after release from the catheter into the aneurysm. Later studies will design hydrogels that remain in the aneurysm for 6 months and then biodegrade, which offers a less dangerous, more biocompatible alternative to coil embolization. The next step would be to include the thrombin coagulant and fibrinogen in the hydrogels to simulate blood clotting in intracranial aneurysms. As the hydrogel is left in the aneurysm, the F-127 will degrade and pores will form, thus allowing thrombin to induce coagulation with fibrinogen for a controlled thrombosis inside the aneurysm necessary for occlusion. Additionally, binding the RGD peptide to FDMA will cause surrounding endothelial cells to migrate and block off the opening of the aneurysm, contributing to a successful occlusion.

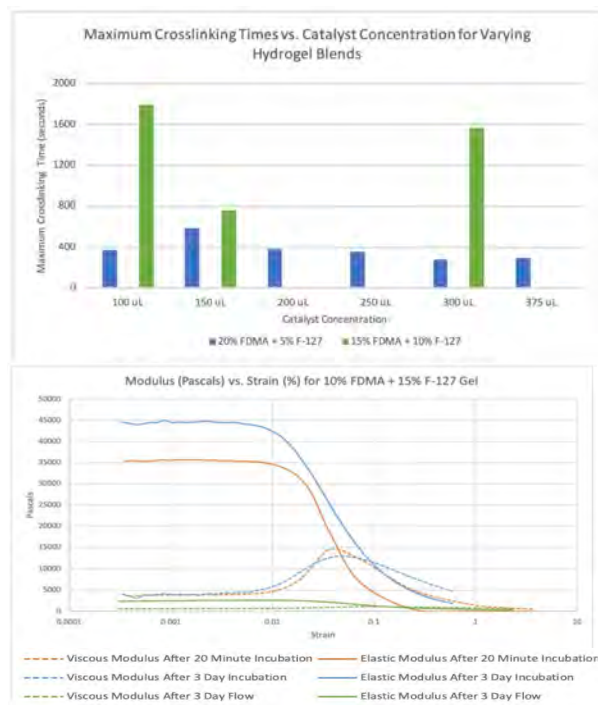


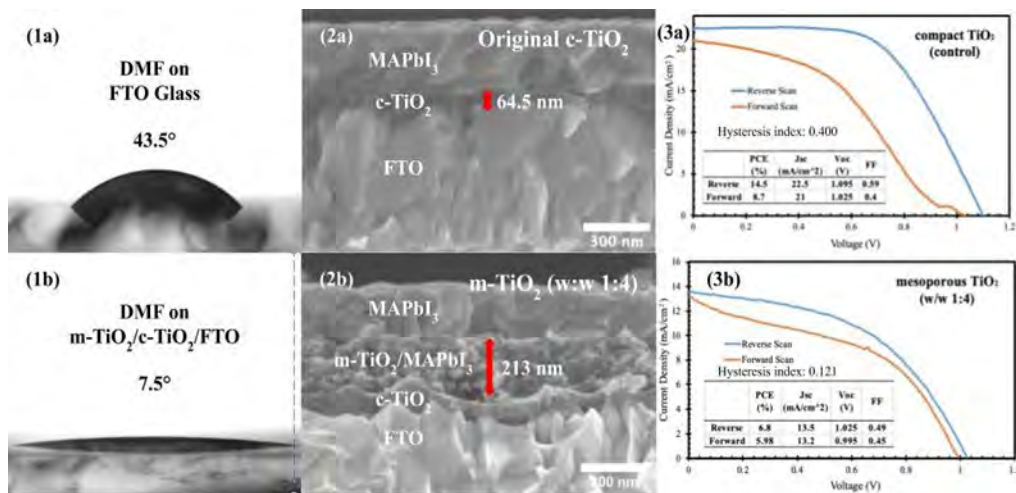
Figure 2: Elastic and viscous moduli graphs of a gel obtained from amplitude sweep

¹ Kieffer, Sara. "Endovascular Coiling for Brain Aneurysms: Treatment: Johns Hopkins Aneurysm Center." *Endovascular Coiling for Brain Aneurysms | Treatment | Johns Hopkins Aneurysm Center*, 8 Dec. 2017. www.hopkinsmedicine.org/neurology_neurosurgery/centers_clinics/aneurysm/treatment/aneurysm_endovascular_coiling.html.

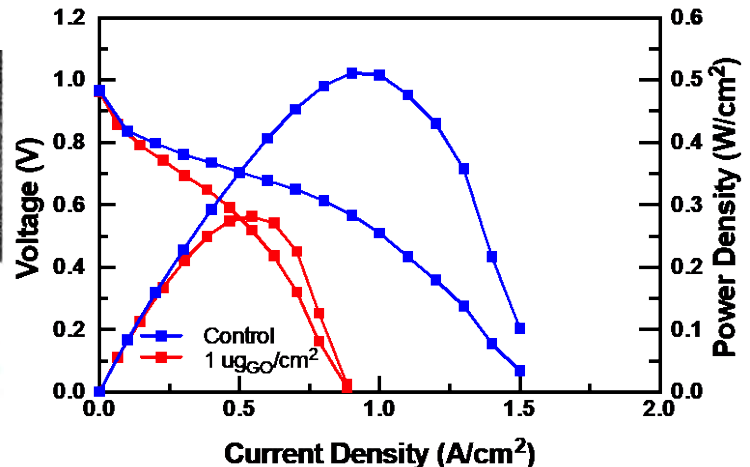
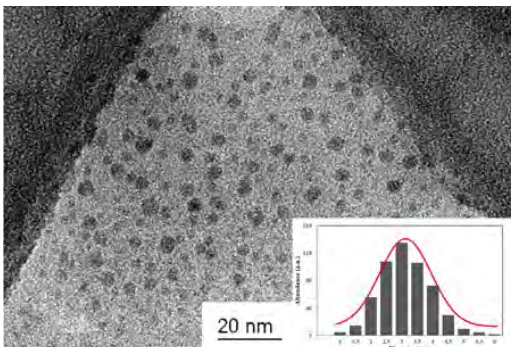
² Xue, T., Chen, Z., Lin, W. et al. Hydrogel coils versus bare platinum coils for the endovascular treatment of intracranial aneurysms: a meta-analysis of randomized controlled trials. *BMC Neurol* 18, 167 (2018). <https://doi.org/10.1186/s12883-018-1171-8>

Renewable Energy: Solar Fuel Cells

Likun Wang, Aniket Raut, Won-Il Lee



Sustainion® Membrane



Using and optimizing cellulose filter paper proton exchange membranes for hydrogen fuel cells

Jonathan Koziarz¹, Jacky Xie², Aniket Raut³, Likun Wang³, Miriam Rafailovich³

¹South Side High School, NY, 11570; ²Harborfields High School, NY, 11740;

³Department of Material Sciences and Chemical Engineering, Stony Brook University, NY, 11794

Hydrogen fuel cells are a promising alternative power source due to their efficiency and clean byproduct, water, however one such type of hydrogen fuel cell which utilizes proton exchange membranes (PEMs) come with the drawback of high cost¹. Searching for more cost efficient materials to replace the nafion typically used has led to experimentation with cellulose filter paper, which is abundant, inexpensive and biodegradable. A previous study looked at the use of a nafion solution and RDP to optimize the performance of the cellulose filter paper proton exchange membrane fuel cell (PEMFC)². This study continues to investigate optimization of cellulose filter paper, using cellulose with RDP as the control samples while the variable samples were immersed in acids of varying molarity, with later samples incorporating nafion solution and a RDP-nafion mix.

For all samples tested, Ahlstrom Munksjö cellulose filter paper was the brand used. The control used Fyrolflex[®] RDP on the filter papers and 6 mol of citric acid was the focus for the effect of acid on the filter paper. Cellulose with nafion and cellulose/RDP/nafion were tested after the control and citric acid. 312.73 mg of nafion solution was added to the cellulose filter paper. For cellulose/RDP/nafion, drops of RDP were added on to the filter paper, followed by 170.7 mg of nafion solution. Each sample of filter paper was placed within the hydrogen fuel cell, hooked up to the test station and the results of the performance at 30°C, 60°C and 80°C were recorded.

The performance of most of the fuel cells can be described as inadequate. With the exception of the nafion sample, no fuel cell had a maximum power density that exceeded 10 mW/cm². For the control/RDP cellulose in this experiment, the highest performing control was tested twice at 30°C and 60°C, with the greatest performance during the first test at 60°C, 3.77 mW/cm² at 11.6 mA/cm² (Fig 1a). The 80°C test was not included in this recording as it resulted in the rapid decrease in performance of the cell, leading to the shutting down of the test station before any data was collected. Much like underperformance, rapid decrease of performance at 80°C was a trend among the other variable samples :6 mol citric acid and cellulose/RDP/nafion. The 6 mol citric acid sample had a maximum power density of 3.87 mW/cm² at 11.64 mA/cm² and 60°C, and cellulose/RDP/nafion a maximum power density of 3.25 mW/cm² at 10 mA/cm² and 30°C. In contrast to the previously mentioned samples, the cellulose with nafion solution exceeded the 10 mW/cm² performance at 30°C, 60°C, and 80°C. The maximum power density for nafion occurred at 80°C and 47.9 mA/cm²: 15.1 mW/cm² (Fig 1b). While this performance was the highest in this study, it still lacks in comparison to the output of nafion PEMFCs, allowing for this area to be further explored. In fact, the underperformance of cellulose/RDP/nafion is rather interesting, and it is theorized that the RDP blocked the pores of the filter paper. The testing of cellulose filter paper immersed in nafion solution and then prepared with RDP is a future step in the optimization of cellulose filter paper as a PEM for hydrogen fuel cells.

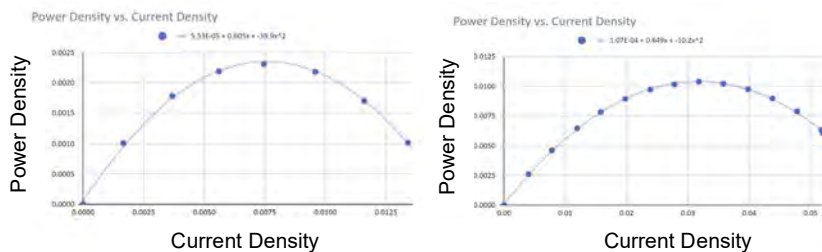


Fig. 1: (1a)(left) Power density vs. current density graph for cellulose control sample at 60°C. (1b)(right) Power density vs. current density graph for cellulose/nafion at 80°C.

¹Whiston, M.M.et al. "Expert assessments of the cost and expected future performance of proton exchange membrane fuel cells for vehicles". *Proceedings of the National Academy of Sciences* 2.25 (2019), doi:10.1073/pnas.1804221116

²Wang, Likun, et al. "Operation of proton exchange membrane (PEM) fuel cells using natural cellulose fiber membranes." *Sustainable Energy & Fuels* 3.10 (2019): 2725-2732.

Enhancing the Performance of Anion Exchange Membrane Fuel Cells by Coating Membranes with Graphene Oxide

Amy Sharin¹, Sohan Shetty², Lindsay Wright³, Emily Zhang⁴, Aniket Raut⁵, Dr. Likun Wang⁵, Rebecca Isseroff¹, Dr. Miriam Rafailovich⁵

¹Lawrence High School, Cedarhurst, NY 11516, ²Half Hollow Hills High School East, Dix Hills, NY 11746, ³Del Norte High School, San Diego, CA 92127, ⁴General Douglas MacArthur High School, Levittown, NY 11756, ⁵Department of Materials Science and Chemical Engineering, Stony Brook University, Stony Brook, NY 11794

Anion exchange membrane fuel cells (AEMFCs) are a source of clean alternative energy that utilize hydrogen and oxygen similar to proton exchange membrane fuel cells (PEMFCs), except that AEMFCs utilize an alkaline pH environment and transport OH^- from the cathode to the anode of the cell.¹ The alkalinity allows AEMFCs to perform using non-precious metal catalysts that would dissolve in PEMFCs, effectively reducing cost of performance. Recent research has focused on improving anion exchange membranes and addressing the shortcomings of AEMFCs including lower mobility of OH^- than H^+ in PEMFCs, management of water from the reactions, and low durability.²

Scientists are exploring potential uses of graphene oxide (GO), a recently discovered compound with similar properties to graphene. GO is polar and disperses better in solution and on surfaces, providing more complete protection than graphene would.³ In this study, membranes were coated with GO to further understand the chemistry of AEMFCs and to improve their performance.

Multiple membranes were tested-- first a control to establish baseline performance and then a membrane with a GO coating. These membranes included the commercial Sustainion[®] 37-50 membrane from Dioxide Materials and the MTPN1-TMA membrane from Dr. Chulsung Bae.⁴ The electrodes for the membrane electrode assembly (MEA) were prepared by cutting 5 cm² of carbon toray paper. A catalyst ink solution with a 75:25 ratio (electrocatalyst:ionomer) was sprayed onto the electrodes to achieve a Pt loading of 0.76 mg/cm², using either Sustainion[®] (5% in ethanol) or TPA-TMA-Br (2% in IPA/Water) for the ionomer for the Sustainion[®] membrane or MTPN1-TMA membrane, respectively. The electrodes and membranes were soaked in 1 M KOH for 1 hour to improve mobilization of OH^- . For the GO tests, a solution of graphene oxide was sprayed onto the surface of the membrane with a concentration of 1 or 2 $\mu\text{g}/\text{cm}^2$. The MEA was assembled with teflon gaskets, the electrodes, and the membrane. The fuel cell stack was connected to the test station and hydrogen and oxygen gas cylinders.

The performance based on peak power density in the MTPN1-TMA membrane exhibited a 7% improvement with GO coating of 1 $\mu\text{g}/\text{cm}^2$ with an increase from 0.416 to 0.445 W/cm² at a current density of 0.800 and 0.571 A/cm², respectively. However, when 2 $\mu\text{g}/\text{cm}^2$ of GO was coated on the membrane, the peak performance declined to 0.309 W/cm² at a current density of 0.58 A/cm². The peak power density of the commercial Sustainion[®] membrane decreased from 0.512 W/cm² at a current density of 0.9 A/cm² to 0.282 W/cm² at a current density of 0.544 A/cm² with a GO coating of 1 $\mu\text{g}/\text{cm}^2$. While there have been some improvements in performance observed, there is still ongoing research testing optimum concentrations of graphene oxide coatings on both of the membranes to reach greater performance and durability. Additionally, research is being done to optimize the test station process of applying current and voltage to collect data.

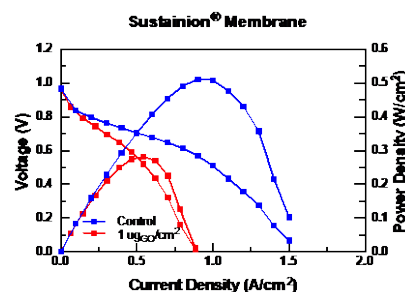


Figure 1 Polarization curve for Sustainion[®] membrane

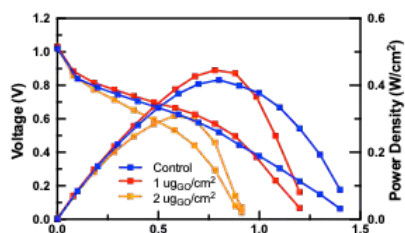


Figure 2 Polarization curve for MTPN1-TMA membrane

¹Dekel, Dario R. "Review of Cell Performance in Anion Exchange Membrane Fuel Cells." *Journal of Power Sources*, vol. 375, 2018, pp. 158-169., doi:10.1016/j.jpowsour.2017.07.117.

²Lee, W., Park, E. J., Han, J., Shin, D. W., Kim, Y. S., & Bae, C. (2017). Poly(terphenylene) Anion Exchange Membranes: The Effect of Backbone Structure on Morphology and Membrane Property. *ACS Macro Letters*, 6(5), 566-570. doi:10.1021/acsmacrolett.7b00148

³Chauhan, Dheeraj Singh et al. "Graphene and Graphene Oxide as a New Class of Materials for Corrosion Control and Prevention." *Process in Organic Coatings*, Volume 147, 105741, October 2020, doi.org/10.1016/j.porgcoat.2020.105741.

⁴Bae, Chulsung. "Welcome to Bae Research Group." Rensselaer Polytechnic Institute, <http://homepages.rpi.edu/~baec/index.html>

Size Optimization of Gold Nanoparticles Functionalized on PEMFC Interfaces to Increase Power Efficiency

Ziqi Jiao¹, Danny Li², Benjamin Sherman³, Christine Zhang⁴, Likun Wang⁵, Won-Il Lee⁵, Miriam Rafailovich⁵

¹Princeton Int'l School of Maths & Sci., Princeton, NJ 08540, ²Jericho High School, Jericho, NY 11753, ³George W. Hewlett High School, Hewlett, NY 11557, ⁴Saratoga High School, Saratoga, CA 95070, ⁵Stony Brook University, Stony Brook, NY 11790

Polymer Electrolyte Membrane Fuel Cells (PEMFCs), or Proton Exchange Membrane Fuel Cells, are efficient electrochemical energy conversion devices that use hydrogen and oxygen as fuel and produce water as exhaust. As a result, they are one of the cleanest energy sources. However, PEMFCs are particularly vulnerable to the carbon monoxide contaminant in hydrogen fuel, which competitively inhibits active sites of the platinum catalyst. This research focuses on incorporating gold nanoparticles in PEMFCs to achieve on-site oxidation of carbon monoxide, preventing the fuel cell from deteriorating.

The gold nanoparticles in this research were synthesized using a two-phase method reported by Brust et al., which incorporated dodecanethiol as growth regulator [1]. Molar ratio of thiol to chloroaurate starting material was used to name each synthesis batch. The product was functionalized onto Nafion 117 membranes using a Langmuir-Blodgett trough, and the membrane was assembled with electrode components to form the Membrane Electrode Assembly (MEA). Hydrogen gas was allowed to flow into the anode while the cathode was left exposed to air. Measurements of voltage and power output were recorded under a series of operating currents. TEM images of the nanoparticles were also taken in order to analyze particle size and distribution.

Voltage and power density were graphed as a function of operating current density, as shown in Figure 1. Results show a 27% increase ($4.34\text{mW}/\text{cm}^2$ to $5.52\text{mW}/\text{cm}^2$) in maximum power output in $\text{Au}_{0.85}$ functionalized Nafion

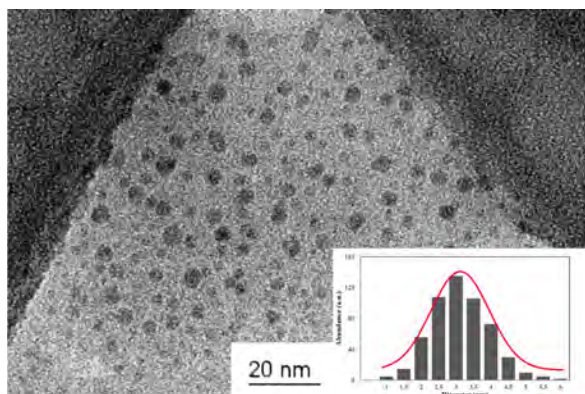


Figure 2: TEM image of $\text{Au}_{0.85}$ batch with distribution curve of particle diameter

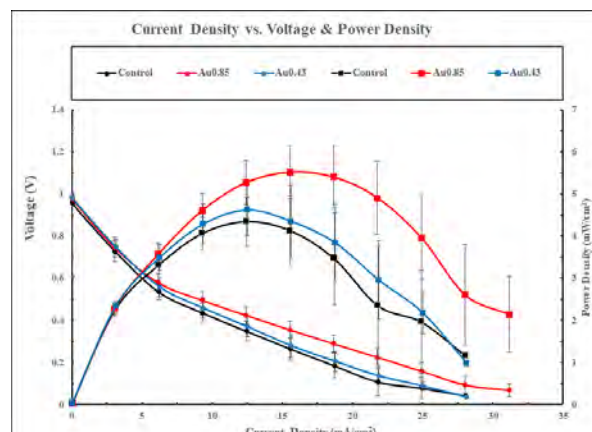


Figure 1: Voltage and power density vs. current density

compared to the control, and a 6% increase ($4.34\text{mW}/\text{cm}^2$ to $4.62\text{mW}/\text{cm}^2$) in $\text{Au}_{0.43}$ functionalized Nafion. We also observed an increase in power output across all operating currents of the fuel cell, showing that gold nanoparticles produce significant increases in cell efficiency especially at smaller sizes. TEM analysis of the $\text{Au}_{0.85}$ batch, as illustrated in Figure 2, shows a distribution of particle diameter with average size $3.37 \pm 0.83\text{nm}$ and $D50$ 3.32nm . The particles were also very monodispersed and homogenous, both crucial properties we aimed to achieve.

Future work includes testing a $\text{Au}_{1.7}$ functionalized Nafion membrane to compare the results. Additionally, functionalization of Nafion under different LB trough settings will be carried out to find the optimal distribution density of nanoparticles. Carbon monoxide gas will also be mixed into the hydrogen fuel flow to evaluate catalyst poisoning suppression ability of the gold nanoparticles.

[1] Brust, Mathias, et al. "Synthesis of Thiol-Derivatised Gold Nanoparticles in a Two-Phase Liquid-Liquid System." *Journal of the Chemical Society, Chemical Communications*, no. 7, 1994, pp. 801–802., doi:10.1039/c39940000801.

A Comprehensive Study of the Formation of Different Electron Transport Layers (ETL) and Its Impact on Perovskite Solar Cell (PSC) Performance

Anthony Chen¹, Luisa Pan², Pranati Patnam³, Benjamin Roitman⁴, Yifan Yin⁵, Yuchen Zhou⁵,
Miriam Rafailovich⁵

¹Shanghai Pinghe School, Shanghai, China 201206, ²The Harker School, San Jose, CA 95129, ³Herricks High School, New Hyde Park, NY 11040, ⁴SAR High School, Bronx, NY 10471, ⁵Department of Materials Science & Engineering, Stony Brook University, Stony Brook, NY 11794

Perovskite solar cells, which are believed to be the core of next-generation solar cells, have had a promising increase in efficiency since its 2009 introduction¹. A typical PSC consists of a photoactive perovskite layer sandwiched between an electron transport layer (ETL) and a hole transport layer (HTL). Despite the rapid progress of PSC performance, the interfacial contact between the ETL and the perovskite layer in the cell often results in the problem of hysteresis, in which the current-voltage scans yield different results due to scan directions². Herein, our main purpose of this project is to investigate different ETL materials to remedy hysteresis in organic-inorganic CH₃NH₃PbI₃ (MAPbI₃) perovskite solar cells.

Compact TiO₂ (c-TiO₂), SnO₂ (0.1M and 0.2M), and mesoporous TiO₂ (m-TiO₂) (1:4 and 1:6 w:w) were deposited as the chosen ETL materials *via* spin-casting and followed by high-temperature annealing. The PSCs were built using FTO as the conductive substrate. MAPbI₃ was deposited as the photoactive layer via the solvent annealing process and spiro-OMeTAD was used as the HTL layer. The gold electrodes (80nm) were deposited on top of the cell through physical vapor deposition.

Compared to the bare FTO, all ETL samples showed smaller contact angles with DMF acting as the droplet, confirming that the ETL layers show more hydrophilic surface properties and help the PSVK precursor spread over the surface when spin-casting. Scanning electron microscopy (SEM) was utilized to take cross-sectional images of the solar cell after depositing the perovskite layer. Higher values in the precursor concentration correlated with increased ETL thickness. Qualitative analysis of the c-TiO₂/m-TiO₂ bilayer SEM image demonstrated that the perovskite layer also effectively diffused into the porous m-TiO₂, which increased the interfacial contact between the perovskite and the ETL. Although the control c-TiO₂ had a PCE of 14.5%, the sample also had a hysteresis index of 0.400. In comparison, the 34 mM TiO₂ sample had a PCE of 11.9% with a hysteresis index of 0.034. Because the hysteresis index indicates the closest forward and reverse scan of the I-V curve, a lower hysteresis index, like the one in the 34mM TiO₂ sample, is desired. The m-TiO₂ bilayer sample, albeit having a PCE of 6.8%, had a hysteresis index of 0.121, suggesting that the mesoporous layer aided in reducing the hysteresis index of the original c-TiO₂ ETL and has potential to improve.

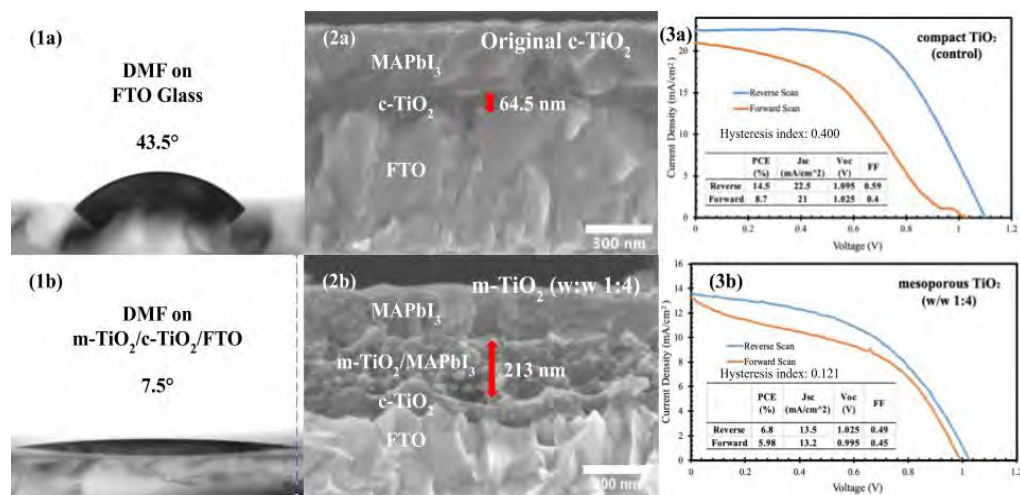


Fig. (1a) contact angle over FTO glass and **(1b)** m-TiO₂ **(2a)** SEM images of original c-TiO₂ and **(2b)** m-TiO₂ (w:w 1:4) **(3a)** I-V curve of original c-TiO₂ sample and **(3b)** mesoporous TiO₂ (w:w 1:4)

¹ Chen, Y., *et al.* "Structure and Growth Control of Organic-Inorganic Halide Perovskites for Optoelectronics: From Polycrystalline Films to Single Crystals." *Advanced Science*, 3.4, 1500392 (2016). doi:10.1002/advs.201500392

² Kang, D., and Park, N. "On the Current-Voltage Hysteresis in Perovskite Solar Cells: Dependence on Perovskite Composition and Methods to Remove Hysteresis." *Advanced Materials*, 31.34, 1805214 (2019). doi:10.1002/adma.201805214

Special Session: Ethical Considerations in our Response to COVID and Other Topics

Prof. Brooke Ellison



An Examination of Hybrid Remote Learning Models to Optimize Student Academic and Social Performance

Luisa Pan¹, Annie Wang², Emily Zhang³

¹The Harker School, San Jose, CA 95129, ²Central Bucks High School East, Doylestown, PA 18902, ³General Douglas MacArthur High School, Levittown, NY 11756

Due to current pandemic circumstances, education at all levels has begun to shift towards remote learning. The foreseeable future points to widespread hybridized and virtual schooling models, and while long-term speculation is extremely uncertain, it is clear that alternatives to complete in-person schooling must be pursued immediately. An increase in technology-related strategies will play an integral role in education for months, if not years. But the oft-critical response¹ to 2020's spring semester demonstrated that the transition to a more digital classroom is nothing if not disorderly. In order to optimize hybridized and remote learning strategies, several measures must be implemented to retain maximal academic drive and performance.

There are several disparities between full in-person education and a hybridized or online model. Students who adjust to remote or hybrid learning encounter a decrease in not only in-person instruction, but also academic structure. Without constant academic enforcement from a teacher that one would typically receive in class, students' intrinsic motivation might understandably decrease. One survey indicated that students were most concerned about their final grades; disquietude over learning itself came secondarily.¹ When such situations arise, the purpose of school becomes distorted: while grades are an important tool to measure academic performance, true learning should be prioritized. It is critical to maintain constant feedback from the student body, recognize when students are more focused on their transcripts than their erudition, and compensate using other tactics as needed.

Another widespread concern has been raised over the amount of time students will be able to attain for the purpose of interacting with their teachers and socializing and emotionally connecting with their peers. The most important factors in overall student perceptions of learning and satisfaction are suggested to be consistent, streamlined course design, feedback from instructors, and active discussion.² A traditional classroom setting might provide room for these factors in the form of discussion, questioning, and small talk, almost all of which are removed from an online setting. To indemnify this loss, teachers can optimize on the advantages of digitalization. In a hybrid setting, a flipped classroom model might be proposed—students would study the bulk of the course content at home with lesson material provided by teachers and return to the school building in order to discourse on crucial concepts while rectifying understanding. Digitalization also provides teachers with a more open avenue to talk to students one-on-one over more flexible calls, which should be capitalized upon to ensure maximum comprehension.

The responsibility of ensuring optimized remote learning falls upon the administration of the school system, who are responsible for ensuring the wellbeing and maximum success for students anyway. The tasks of budgeting for technological improvements, structuring schedules, and informing and educating teachers fall on administration. Meanwhile, as the first link between students and staff, teachers should act as guides to introduce students to this new medium of learning.

As for future implications, one interview with a Levittown high school teacher yielded this insight: despite the critical global exigence for remote learning at this hour, the shift to digital education does not necessarily pertain to only COVID-19 safety measures. Online school is not new -- it has been steadily competing with full-time education since the 1990s.³ Schools that were behind technologically are now being forced to accelerate in a direction that education was perhaps bound to go eventually -- in the digital era of technological innovation, why should education be merely constrained to methods that have existed for centuries? Additionally, the forced process of transitioning to a more technology-based schooling model has helped lay bare the massive digital disparity between socioeconomic tiers of society: those who had poorer access to now-necessities such as internet connection and 1:1 devices for students and staff are now obliged to catch up to reach the same compulsory level for education without the same resources. And although digital education is not a fully formed and researched field, the coming times will serve as a measure of what is and what is not feasible in this novel situation.

¹Lederman, D. (2020, May 20). Inside Higher Ed. Retrieved from <https://www.insidehighered.com/digital-learning/article/2020/05/20/student-view-springs-shift-remote-learning>

²Karen Swan. (2002) Building Learning Communities in Online Courses: the importance of interaction, *Education, Communication & Information*, 2:1, 23-49, DOI: 10.1080/1463631022000005016

³Raven M. Wallace. (2003) Online Learning in Higher Education: a review of research on interactions among teachers and students, *Education, Communication & Information*, 3:2, 241-280, DOI: 10.1080/14636310303143

Bioethical Analysis of New York Hospital Triage Policies in the Age of the Coronavirus

Jessica Guo¹, Brooke Ellison²

¹Ward Melville High School, East Setauket, NY 11733, ²Department of Behavioral and Community Health, Stony Brook University, Stony Brook, NY 11790

As of August 6, 2020, there were 18,614,177 confirmed cases of COVID-19 worldwide [1], including 4,728,239 cases in the United States of America [1], of which 418,225 cases were from New York State alone [4]. Although most Coronavirus patients do not require hospital admission, severe cases can lead to acute respiratory distress syndrome and require invasive mechanical ventilation [2]. As a result of this the demand for life-saving ventilators has skyrocketed, and the ethicality if their distribution has come into question. As a Coronavirus epicenter, New York physicians and policymakers, in particular, have and will continue to make impossible decisions regarding which patients to save. Physicians adhere to the bioethical principles of beneficence (medical workers should act for the benefit of their patients), nonmaleficence (doctors should refrain from harm or induce the least harm possible to produce a beneficial outcome), autonomy (patients have the prerogative to be informed of their options in order to determine the course of their medical care), and justice (the idea that resources should be equally distributed to all groups in society) [4]. This study uses these concepts to analyze whether the 2015 New York State Department of Health Ventilator Allocation Guidelines are ethically just.

In anticipation of an influenza pandemic that would flood the state and exhaust the health system, the New York State Task Force on Life and the Law drafted ventilator allocation guidelines [6] that some hospitals may decide to implement. The guidelines are written with adult, pediatric, neonatal, and legal considerations that follow the primary goal of achieving the lowest possible mortality rate [6]. A patient's likelihood of survival and in turn level of access to ventilator therapy and continuance of treatment is calculated through three procedures [5]. Patients are first screened for exclusion criteria that would deem him/her ineligible for ventilator therapy [5]. Next, patients are given a mortality risk assessment using SOFA (Sequential Organ Failure Assessment), which is a round of clinical evaluations of six crucial organs/conditions- lungs, liver, brain, kidneys, blood clotting, and blood pressure[5]. These two tests determine a patient's level of access to ventilator therapy [5]. SOFA tests are then periodically conducted at 48 and 120 hours to evaluate whether he/she will continue with the treatment [5].

These aforementioned protocols follow a 5-component ethical framework: duty to care, distributive justice, transparency, duty to plan, and duty to steward resources [5]. Although not explicitly stated, some of the 5 components do loosely align with the bioethical fundamentals (beneficence, justice, autonomy, non-maleficence). Duty to care and beneficence are both the obligation for the healthcare provider to care and act in the best interest of the patient; distributive justice and justice both ensure resources are distributed to the population equally; transparency ensures a patient is aware of the allocation protocols, which is relatively similar to autonomy; duty to plan is the responsibility of the government to plan for such crises, which although not included in bioethics, is a proper extension; and duty to steward resources is the need to manage resources in times of scarcity, also relating to justice. No component directly addressed non-maleficence; however, its theory is suggested by the "duty to care" clause.

The purpose of the guideline is to help physicians allocate ventilators in times of emergency, like the coronavirus pandemic. These guidelines closely follow the principles of bioethics, yet this system could be inherently biased because while SOFA is impartial, a human medical staff with emotions is performing the test.

When demand exceeds supply there is no perfect solution, but the allocation protocols are ethical and would likely result in lower mortality rates than if they were not implemented at all, so while there are flaws, during crises such as the coronavirus, these guidelines would effectively mitigate the worst outcomes and save lives.

1. [Coronavirus-Covid19 cases] [Chart]. (n.d.). *World Health Organization*. <https://covid19.who.int/region/amro/country/us>
2. Feinstein, M. M. et al., 2020. Considerations for ventilator triage during the COVID-19 pandemic. *The Lancet. Respiratory medicine*, 8(6), e53. [https://doi.org/10.1016/S2213-2600\(20\)30192-2](https://doi.org/10.1016/S2213-2600(20)30192-2)
3. [NYSDOH COVID-19 Tracker] [Chart]. (n.d.). *New York State Department of Health*. <https://covid19tracker.health.ny.gov/views/NYS-COVID19-Tracker/NYSDOHCOVID-19Tracker-Map?%3Aembed=yes&%3Atoolbar=no&%3Atabs=n>
4. *What are the Basic Principles of Medical Ethics?* (n.d.). Stanford. <https://web.stanford.edu/class/siw198q/websites/reprotech/New%20Ways%20of%20Making%20Babies/EthicVoc.htm#:~:text=Bioethicists%20often%20refer%20to%20the,beneficence%2C%20and%20non%2Dmaleficence>.
5. Zucker, H. A., Adler, K. P., Berens, D. P., & David Bleich, R. J. (n.d.). Ventilator Allocation Guidelines. *New York State Department of Health*. https://www.health.ny.gov/regulations/task_force/reports_publications/docs/ventilator_guidelines.pdf

Community-Focused Data to Drive Reform in Suffolk County Police Department

Jeannie She¹

¹Walt Whitman High School, MD 20817

Racial tensions between Latino residents of Suffolk County, New York and the Suffolk County Police Department (SCPD) reached national exposure after an extensive delay in adequate investigations for the murders of two Latino individuals: Marcelo Lucero in 2008 and José Fermín Sánchez in 2010. Following Lucero's murder, the United States Department of Justice (DOJ) opened an evaluation of the SCPD in 2009 based on "discriminatory policing allegations."¹ Although an agreement for more equitable policing was reached and following DOJ assessments confirmed progress, a lack of trust and demonstration of improvement persists on the local level, according to Irma Solis, the Suffolk County director of the New York Civil Liberties Union.² The SCPD has already established generalized anti-bias policies,³ hired an Ecuadorian immigrant (Lizbeth Carrillo) into the department council,⁴ and created Spanish-language social media,⁵ but this action has proven to be insufficient. Instead, measures that are specific to the minority Latino community in Suffolk County may lead to more effective overall policing.

This proposed community-oriented direction of reform for the SCPD is four-fold: establishment of an understanding of local issues and utilization of community-tailored solutions,⁶ reduction of deportation fears and rhetoric to promote communication and respect, increased awareness of endemic health issues, and collection of empirical data and increased transparency on new policing measures.

First, the SCPD should take note of the housing conditions, employment rate, and other factors within the community that directly correlate with frequent, repeat incidents. A familiarity with the community demographics could lead to more appropriate, tailored solutions that prevent crime proactively rather than address crime reactively. Second, deportation fears have been cited as reasons to interact minimally with the police.⁷ This concern is a barrier to improving the protection of the community and must be addressed. Third, amongst various physical health issues, mental health stigma is a pressing issue amongst the Latino community due to the favoring of privacy in social culture as well as a fear of being labeled crazy.⁸ Furthermore, obstacles like language barriers, lack of culturally competent care, and lack of healthcare negatively affect the community's mental health.⁷ Considering the impact of mental health on crime, recognizing and overcoming these obstacles and stigma is imperative. Fourth, "active solicitation of input from neighborhood residents and civic organizations"⁶ could largely increase trust and transparency between the two parties, again promoting communication and accountability on both ends. Consequently, detailed data should be collected following the establishment of new regulations or methods in order to evaluate their true impact on the community and crime.

Further research will entail a deeper dive into each facet of this four-fold proposal and elucidation of connections between Suffolk County-specific issues and the past, current, and future work of the SCPD. Effective policing of any community must be done with the community in mind, and Suffolk County is no exception.

¹ "United States Agrees to Comprehensive Settlement with Suffolk County Police Department to Resolve Investigation of Discriminatory Policing Against Latinos." *The United States Department of Justice*, 16 Sept 2014. Web. 05 Aug 2020.

² "Report shows Suffolk PD has made progress with Latinos since Lucero case." *News12 Long Island*, 18 Oct 2018. Web. 05 Aug 2020.

³ Lane, Charles. "Suffolk Struggles To Reform Discriminatory Policing Against Latinos." *WSHU Public Radio*, 29 Feb 2016. Web. 05 Aug 2020.

⁴ Dasio, Stephanie. "Suffolk Police Commissioner Geraldine Hart hires Hispanic liaison officer." *Newsday*, 27 Oct 2018. Web. 05 Aug 2020.

⁵ Goldberg, Jodi. "Suffolk County police using social media to improve relations with Latino community." *Fox5NY*, 2 Jan 2020. Web. 06 Aug 2020.

⁶ Reisig, Michael D. "Community and Problem-Oriented Policing." *Crime and Justice*, vol. 39, no. 1, 2010, pp. 1–53. *JSTOR*, doi: 10.1086/652384. Web. 6 Aug 2020.

⁷ Peddie, Sandra. "Despite progress after hate crime, SCPD and Hispanics struggle with trust." *amNY*, 2 Nov 2018. Web. 04 Aug 2020.

⁸ "Latinx/Hispanic." *National Alliance on Mental Illness*, n.d. Web. 04 Aug 2020.

Ethical Analysis of New York State Ventilator Allocation to Those With Disabilities in the Age of COVID-19

Jessica Guo¹, Brooke Ellison²

¹Ward Melville High School, East Setauket, NY 11733, ²Department of Behavioral and Community Health, Stony Brook University, Stony Brook, NY 11790

The coronavirus has exhausted the public health system, and in doing so, it has magnified the systemic discrimination those with disabilities face. Over 61 million Americans- roughly 1 in 4- [1] suffer from a disability that limits major life activities, yet despite the growing population, those with disabilities experience significant inequities in healthcare [2]. Amidst the coronavirus, the demand for resources such as ventilators may exceed the supply, leading to the implementation of triage policies, and leaving the question of where those with disabilities fall. Section 1557 of the Patient Protection and Affordable Care Act (ACA), Section 504 of the Rehabilitation Act of 1973, and Americans with Disabilities Act of 1990 (ADA) all prohibit disability based discrimination in health care [2], and this study analyzes whether (and to what extent) the New York State Department of Health Ventilator Allocation Guidelines adhere to these three federal laws.

Section 1557 of the ACA and Section 504 of the Rehabilitation Act prohibit discrimination against entities who receive financial assistance/funding for healthcare on the basis of a disability [2]. The Americans with Disabilities Act also attempts to provide equal opportunities and rights to the disabled, including healthcare through Title II (Nondiscrimination on the Basis of Disability in State and Local Government Services) and Title III (Nondiscrimination on the Basis of Disability by Public Accommodations and in Commercial Facilities) [4]. This prohibits discrimination towards the disabled in state and healthcare services offered by public hospitals (Title II) and healthcare offered at private physician's offices and private hospitals (Title III). Overall, these laws require healthcare workers to decide a disabled patient's treatment course based on an individual, evidence-based assessment, rather than inherent assumptions, stereotypes, or bias.

In 2015, the New York Task Force on Life and the Law created Ventilator Allocation Guidelines in anticipation of an unpredictable and severe influenza pandemic [3]. Because of the magnitude of the coronavirus, some hospitals in the New York epicenter may begin following these guidelines. These guidelines implement emergency procedures in an attempt to resolve long established, biased quality of life speculations that curtail the rights of the disabled; however, the Task Force does balance the needs of the disabled and the needs of all other patients as equally as possible. Additionally, individuals are only subject to the allocation protocols if they enter a care facility for treatment. Resources are allocated based on a patient's likelihood of survival, which is determined by a two-step process. Patients are first screened for exclusion criteria that would deem them unfit for ventilator therapy and better suited for alternative treatment. Next, patients are given a mortality risk assessment using SOFA (Sequential Organ Failure Assessment), which clinically evaluated the function of six crucial organs/conditions- lungs, liver, brain, kidneys, blood clotting, and blood pressure. From these tests, a patient's likelihood of survival is determined and ventilators are administered. Patients who receive ventilators then undergo SOFA testing 48 and 120 hours after the onset of treatment [3]. Based on their performance, ventilator therapy is continued if improvement is seen; if not, alternate forms of medical intervention or palliative care are enacted. These guidelines are in accordance with all three aforementioned laws, as they theoretically provide equal access to healthcare, treatment, and resources for the disabled and do not have any clear prejudicial motives.

These guidelines are only to be implemented in times of dire emergency, such as the coronavirus pandemic, and can mitigate egregious partiality. However, it should be noted that these guidelines can be flawed, because although SOFA is impartial and follows ethically sound principles, humans conduct the test, and humans are subject to innate and inadvertent assumptions of the quality of life of the disabled. Thus, while these protocols moderately protect the lives of the disabled, they certainly can be optimized.

1. CDC: 1 in 4 US adults live with a disability. Centers for Disease Control and Prevention (CDC). <https://www.cdc.gov/media/releases/2018/p0816-disability.html#:~:text=One%20in%204%20U.S.%20adults,affects%201%20in%207%20adults>.
2. Pendo, E. COVID-19 and Disability-Based Discrimination in Health Care. <https://www.americanbar.org/groups/diversity/disabilityrights/resources/covid19-disability-discrimination/>
3. Ventilator Allocation Guidelines. New York State Department of Health. https://www.health.ny.gov/regulations/task_force/reports_publications/docs/ventilator_guidelines.pdf
4. What is the Americans with Disabilities Act (ADA)? ADA National Network. <https://adata.org/learn-about-ada>

Hospital Triage Policy in Texas during COVID-19

Lingzi (Susan) Zhang¹, Dr. Brooke Ellison²

¹The Hockaday School, Dallas, TX 11600;

²School of Health, Technology, and Management, Stony Brook University, Stony Brook, NY 11794

In the time of a pandemic such as COVID-19, a triage policy is often adopted to determine how and to whom scarce medical resources are allocated so that hospitals can prioritize patients and maximize the number of people that receive effective care.¹ Various factors, such as the patient's age, medical history, and signs and symptoms, are factored into the triage level assignment process to help medical workers determine the order and priority of treatment.²

By July 24, there had been 361,125 cases of COVID-19 and 4,521 deaths reported in Texas.³ Although Texas stopped releasing information regarding the amount of medical resources available, evidence shows that the situation is not optimistic: Texas Children's Hospital is currently admitting adult patients for treatment.⁴ Medical professionals in Texas reported that shortages of staff have been greatly limiting their ability to offer care.¹

Starr County Memorial Hospital, the only hospital serving the county, is overwhelmed by the number of COVID-19 patients and the insufficiency of medical resources.³ Therefore, the hospital set up an ethics and triage committee to review each case.³ The hospital president, Jose Vasque, stated that patients with significant underlying medical conditions, who have lower recovery chances, will be sent home and resources will be spared to patients with more survival potential.³ The intent behind this triage policy likely was to save the greatest number of patients with limited resources. However, this policy can marginalize people who suffer from chronic diseases, who are born with disabilities and conditions such as down syndrome that make them immunocompromised, and who are elderly, because they are more at risk and the hospital will be more likely to refuse to offer treatment.

Ultimately, the inequality in resource distribution exacerbates this situation because it can make certain groups of people more vulnerable when a pandemic such as COVID-19 erupts.³ Julia Lynch, a University of Pennsylvania professor researching health policy, believes that medical resources are constantly being rationed based on one's ability to pay in the US.¹ Therefore, a community that has been suffering from poverty likely does not have access to appropriate healthcare and resources; as a result, people from that community may have a higher chance of being affected by pre-existing medical conditions which put them more at risk for COVID-19. Under a triage policy, those people are even more vulnerable, for their limited ability to pay and their previous experience with inadequate healthcare and resources may result in the hospital removing care for them before for other patients. Therefore, it is important that hospitals treat their patients fairly regardless of economic status and have multiple opinions from the triage committees before making the decision of "who gets care."

¹ Parshley, Lois. "Who Gets to Live? How Doctors Make Impossible Decisions as COVID-19 Surges." *National Geographic*, 24 July 2020, www.nationalgeographic.com/science/2020/07/how-doctors-make-impossible-decisions-as-coronavirus-surges-cvd/.

² "Who's Next In Line? The Emergency Center Triage System." *Texas Children's Hospital*, www.texaschildrens.org/blog/2013/07/whos-next-line-emergency-center-triage-system.

³ Robinson-Jacobs, Karen. "Ethics' Panel In Covid Cases Will Help Pick Who Gets Aggressive Care, Texas Hospital Says." *Forbes*, Forbes Magazine, 24 July 2020, www.forbes.com/sites/karenrobinsonjacobs/2020/07/24/small-texas-hospital-says-ethics-panel-will-help-pick-who-gets-aggressive-covid-care/#1312fd02405b.

⁴ Alexander, Author: Chloe. "Texas Children's Hospital Admitting Adult Patients to Free up Hospital Beds in Houston." *KHOU*, 23 June 2020, www.khou.com/article/news/health/coronavirus/texas-childrens-hospital-admitting-adult-patients-as-covid-19-cases-continue-to-rise/285-5aa0a132-a318-4a41-81b3-6659086c2ef7.

Japan's Stance on Stem Cell Research Policies

Amisha Agrawal¹, Anya Chabria², Clarise Han³, Mori Ono⁴, Haris Rana⁵, Tyler Shern³, Lillian Sun⁶, Stephanie Tarrab⁷, Daniel Wang⁸, Serena Yang⁹

¹University High School, Johnson City, TN 37614, ²The Wheatley School, Old Westbury, NY 11568, ³Mission San Jose High School, Fremont, CA 94539, ⁴Community High School, Ann Arbor, MI 48104, ⁵Southside High School, Fort Smith, AR 72903, ⁶Thomas Jefferson High School for Science and Technology, Alexandria, VA 22312, ⁷Yeshivah of Flatbush Joel Braverman High School, Brooklyn, NY 11230, ⁸Huron High School, Ann Arbor, MI 48105, ⁹Dougherty Valley High School, San Ramon, CA 94582

Although Japanese culture and religion is conventionally viewed as placing little value on the embryo, different studies indicate wide-ranging perspectives.¹ The bioethics committee of the Council for Science and Technology Policy (CSTP) considers the embryo to be a “germ of life,” which implies that embryo destruction may be equated to killing a potential human but allows embryos unused for IVF for therapeutic use. Additionally, researchers were instructed to “respect the embryo,” but the CSTP did not clarify how this phrase was to be applied. There is little public debate on the topic of human embryonic stem cell research, despite attempts by the Japanese government to encourage conversation. Further debate could potentially encourage the general population to donate embryos and support human embryonic stem cell (hESC) research.² This study will examine the development of these stem cell research policies as well as public opinion in Japan.

Currently, the Ministry of Education, Culture, Sport, Science and Technology (MEXT) is working with the Ministry of Health, Labour and Welfare (MHLW) to set guidelines for research into stem cells; biomedical research is divided into basic and clinical research, which are regulated by the MEXT and MHLW respectively.⁵ Japan enacted several laws between 2000 and 2009, including regulations on cloning technology for humans, ethical guidelines on human adult stem cells, and revisions to these aforementioned policies. Although the expert panel on bioethics in the Japanese Cabinet influences the ethical guidelines passed by MEXT, there has been no coherent development of an ethical direction or more concrete standards in the field, as MHLW has not sought the advice of the expert panel so far.⁶

Many problems are present in Japanese stem cell research due to the gaps in policies. Stem cell companies are bypassing rigorous testing of their therapies in order to get them on the market as soon as possible, which reduces the effectiveness of their treatments. Scientists suspect that the efficacy of stem cell treatments used in many commercial therapies are fabricated as a marketing tactic. 10 stem-cell or spinal-cord scientists not involved with STR01 (Stemirac) stated that evidence for the treatment's efficacy is insufficient.¹

Another problem is the difference between public and scientific perceptions and expectations of stem cell research. This is made clear in a survey conducted by Japanese universities that included 2160 public responses and 1115 responses from members of the Japanese Society for Regenerative Medicine (JSRM).² The main areas that the public was interested in that differed from JSRM members were effectiveness of regulation (50.5%), probabilities of potential risks and accidents (33.5%), and clarification of responsibility and liability (32.2%). The main areas JSRM members were interested in were scientific validation (55%) and necessity of research (36.3%). Gaps in the expectations and usage of regenerative medicine were also shown through this survey. The general public expected regenerative medicine to be ready for use earlier than JSRM members.²

In the future, the different branches of the Japanese government involved in bioethics and stem cell regulation should cooperate in directing a more clear set of guidelines for stem cell usage in research and advanced clinical trials. Furthermore, there is still lots of room for improvement for Japan's rules and regulations on stem cell research.

[1] Cyranoski, David. “The Potent Effects of Japan's Stem-Cell Policies.” *Nature News*, Nature Publishing Group, 25 Sept. 2019, www.nature.com/articles/d41586-019-02847-3.

[2] Shineha, Ryuma et al. “A Comparative Analysis of Attitudes on Communication Toward Stem Cell Research and Regenerative Medicine Between the Public and the Scientific Community.” *Stem cells translational medicine* vol. 7.2 (2018): 251-257. doi:10.1002/sctm.17-0184

[3] Sleeboom-Faulkner, Margaret. “Contested Embryonic Culture in Japan—Public Discussion, and Human Embryonic Stem Cell Research in an Aging Welfare Society.” *Medical Anthropology*, vol. 29, no. 1, 2010, pp. 44–70., doi:10.1080/01459740903304256.

[4] Sleeboom-Faulkner, Margaret. “Debates on Human Embryonic Stem Cell Research in Japan: Minority Voices and Their Political Amplifiers.” *Taylor & Francis*, 8 Mar. 2008, www.tandfonline.com/doi/abs/10.1080/09505430801915455.

[5] “Act on Regulation of Human Cloning Techniques.” 2000. PDF file.

[6] Ministry of Education, Culture, Sports, Science and Technology, Japan, *Guidelines for Handling of a Specified Embryo* (2001)

[7] Dhar, Deepali, and John Hsi-En Ho. “Stem Cell Research Policies around the World.” *The Yale Journal of Biology and Medicine*, YJBM, Sept. 2009, www.ncbi.nlm.nih.gov/pmc/articles/PMC2744936/.

Medical Legal Partnerships in the Greater New York Area: Effective Implementation

Jolene Huey¹, Hugo Onghai², and Jeannie She³

¹Arcadia High School, CA 91006, ²Earl L. Vandermeulen High School, NY 11777, ³Walt Whitman High School, MD 20817

The impact of social determinants of health (SDOH) on an individual is often overlooked when prescribing immediate medical treatment. After an urgent medical issue is addressed, household conditions, employment status, and economic stability can continue to plague an individual's health. Thus, the root of many medical issues are impossible to resolve through this type of non-comprehensive healthcare. Medical Legal Partnerships (MLPs) address this shortcoming by providing patients access to lawyers who fight for them and educate them on hospital services they are unaware of. MLPs curtail the perpetuation of certain health conditions in three ways: direct, on-site medical, and legal care; active training for professionals to recognize and address legal issues; and outspoken advocacy for policies which address SDOH and the health of their community in turn.

In Nassau County, the Hofstra Law School/Northwell Hospital MLP directly serves the under-resourced community. The positive impact of this MLP cannot go unnoticed; hospital patients, medical staff, and law students have all benefited since its formation 2 years ago. Specifically, Hofstra law students have had the opportunity to enroll in the "Law and Medicine Together" course which supplies them with an introduction to SDOH and an understanding of the positive, meaningful impact of legal interventions on the outcomes of SDOH.¹ More generally though, survey data from cancer patients who obtained care from an MLP reflects that 75% of them felt that legal assistance reduced stress.²

Obstacles are frequently encountered in current MLPs, namely when organizing medical and legal records of a patient and when sourcing for necessary funding. Due to HIPAA restrictions, it is cumbersome to align patients' health and legal data.¹ This limits the partnership's ability to accurately evaluate the impact of legal assistance on the health of a patient. Additionally, funding can be insecure year-to-year for MLPs. While most funding comes from the government-affiliated Legal Services Corporation or health care and legal partners, another significant portion is attributed to a varying, unstable stream of philanthropic donations.³ Therefore, it is necessary to generate relevant empirical data⁴ to troubleshoot any shortcomings as well as vouch for federal policies which address SDOH to fuel the up-scaling of MLP establishments in other vulnerable populations and secure reliable funding.

Further research will entail pursuing the implementation of an MLP at Stony Brook Hospital in addition to literary research on the policy advocacy done by MLPs.

¹ Flowers, Kerlann. Personal interview. 4 Aug 2020.

² Paul, Edward et al. "Medical-legal partnerships: addressing competency needs through lawyers." *Journal of graduate medical education*, Vol. 1, p. 2, 2009: 304-9. doi: 10.4300/JGME-D-09-00016.1

³ Trott, Jennifer et al. Financing Medical-Legal Partnerships: View from the Field. *Medical-Legal Partnership Fundamentals*, 2019, medical-legalpartnership.org/mlp-resources/financing/.

⁴ Tobin Tyler, Liz. "Aligning Public Health, Health Care, Law and Policy: Medical-Legal Partnership as a Multilevel Response to the Social Determinants of Health." *Journal of Health and Biomedical Law*, Vol. 8, p. 211, 2012, *Roger Williams Univ. Legal Studies Paper No. 120*, ssrn.com/abstract=2078446.

Optimizing Remote Learning for Low-Income Students

Jeffrey Zhang¹, Emily Zhou², Brooke Ellison³

¹Centerville High School, Centerville, OH 45459; ²The Harker School, San Jose, CA 95129; ³Renaissance School of Medicine, Stony Brook University, NY 11794

Remote learning has quickly established itself as a valid educational medium. In 2018, more than 6.9 million students were enrolled in distance education courses at degree-granting postsecondary institutions¹. However, the imbalance in resources between low-income and middle-class households is a prominent issue that greatly affects the quality of remote education. As a result, students who are unable to access the Internet or even a computer are disadvantaged in the shift toward online learning. Recent surveys suggest that out of 1,500 families, low-income parents are 10 times more likely to report the ineffectiveness or even absence of remote learning support for their children. Furthermore, 36% of households that earn less than \$25,000 annually claim that online education is “going poorly,” a complaint that is only seen in 18% of families who make more than \$100,000 per year². Therefore, we analyzed open-source data associated with remote learning to quantify the disparity in education quality experienced by low-income students. Furthermore, we also propose various recommendations to optimize remote learning for low-income students.

Using data from the 2020 Week 1 Household Pulse Survey collected by the US Census Bureau from April 23 to May 5, we compared the percentage of devices available for educational purposes across household income ranges. According to *Figure 1*, 96% of households with an income range at or above \$150,000 had devices readily available for education purposes, while only 81% of households earning less than \$50,000 had devices readily available for educational purposes. However, *Figure 1* also depicts similar access to technology between low-income families and families earning between \$100,000 and \$149,999. Next, we analyzed the distribution of time spent on virtual education activities between different ranges of household income. Based on *Figure 2*, there is a positive correlation between time spent on virtual education activities and household income range. For instance, students whose household income was less than \$50,000 averaged around 16 hours of virtual educational activities. On the other hand, students whose household incomes were between \$100,000 and \$149,999 averaged 18.2 hours³.

In the future, we hope to draw more definite conclusions about remote learning for low-income students by gathering more data and calculating additional quantitative measurements. Nevertheless, we recommend the following actions to counteract issues low-income students may face with remote learning: 1) Employment of public resources: To lessen technological inequality between families and facilitate equal education opportunities for all. 2) Individualized instruction: With more control over their learning, students are predicted to have greater improvements in academic achievement than a mostly instructor-lead class⁴. 3) Additional channels of communication: Live video sessions for collaborative work, chats, and breakout rooms promote needed social interactions.

As the COVID-19 pandemic continues to keep students at home, the need to support those who are less fortunate and reduce inequality in education has become more of a necessity.

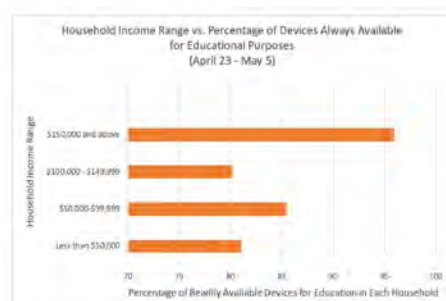


Figure 1: Comparison of Available Devices For Different Household Income Ranges

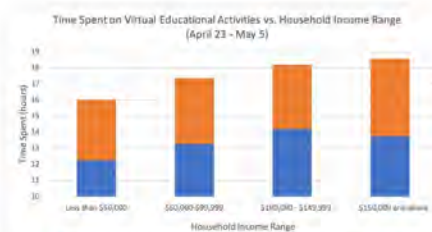


Figure 2: Comparison of Average Time Spent on Education for Different Household Income Ranges

¹ “The NCES Fast Facts Tool Provides Quick Answers to Many Education Questions (National Center for Education Statistics).” National Center for Education Statistics (NCES) Home Page, a Part of the U.S. Department of Education, nces.ed.gov/fastfacts/display.asp?id=80.

²Rosa, Shawna De La. “Survey: Lower-Income Students Struggling with Remote Learning.” Education Dive, 29 May 2020, www.educationdive.com/news/survey-lower-income-students-struggling-with-remote-learning/578828/.

³ Bureau, US Census. “Week 1 Household Pulse Survey: April 23 - May 5.” Census.gov, 20 May 2020, www.census.gov/data/tables/2020/demo/hhp/hhp1.html.

⁴ Zhang, D. 2005. Interactive multimedia-based e-learning: A study of effectiveness. *American Journal of Distance Education* 19 (3):149–62.

Role of U.S. Government in Accessibility of Assistive Technology for People with Disabilities

Amisha Agrawal¹, Varun Nimmagadda², Mori Ono³, Daniel Wang⁴, Serena Yang⁵

¹University High School, Johnson City, TN 37614, ²Novi High School, Novi, MI 48375, ³Community High School, Ann Arbor, MI 48104 ⁴Huron High School, Ann Arbor, MI 48105, ⁵Dougherty Valley High School, San Ramon, CA 94582

With recent technological advances, such as the development of new materials and composites with improved durability, strength, flexibility, and other characteristics, it has become more possible to assist those with disabilities.¹ Furthermore, as the U.S. population ages, the government is becoming increasingly focused on improving the quality of life for those who have accumulated disabilities.¹ Accessibility to these technologies is essential to serving those in need and is directly impacted by the decisions of the government.

A major obstacle to accessing assistive technology is that it must often be paid for out-of-pocket, which can result in financial burden.² Many federally mandated methods of accessing the technology are constrained by budgets and require a medical professional to justify a medical need for it. This limits the choices for people with disabilities, whose quality of life could be improved with assistive technology, even if it is not medically necessary. Other options such as Veterans Administration are available, though they may be directed for specific purposes and may have various requirements that must be met.

Another issue is the failure to implement and enforce accessibility guidelines, which is often a responsibility at the local level. For example, federal laws such as the Rehabilitation Act of 1973 and the Americans with Disabilities Act require that all school districts provide assistive devices to all disabled students, but there is no consistent standard for enforcement.^{3,4} While faculty at the University of California at Berkeley could have used university resources to ensure their massive open online courses (MOOCs) met accessibility standards, none of the MOOCs reviewed by the Department of Justice were found to be fully accessible.⁵

An additional aspect to accessibility is the availability of services that connect Americans to assistive technology. Several state governments increase accessibility by offering support programs and resources for assistive technology on e-government sites; as for accessibility, studies conclude that it is somewhat difficult to find specific information on certain support services for both intellectual and developmental disabilities as well as to receive a response from state representatives when inquiring for further resource information.⁶ Therefore, the ease and convenience of these resources can be made moot if the state's ability to relay information through their e-government web pages is inadequate.

For the future, state and local policies should align with federal laws in setting the standard for making technology accessible to people with disabilities. Federal and state policies for providing assistive technology should be fully funded and accommodate not just medical needs for the technology but also to help people with disabilities to have a high quality of life. As for state webpages and the resources displayed for attaining assistive technology, there should be a call for increased readability, quicker response times from the representatives of these organizations, and a more concise presentation of available services to increase accessibility for those in need. In addition, students with disabilities should be represented in committees so their needs can be heard.

[1] Feiman, Marc P. "Public Funding and Support of Assistive Technologies for Persons with Disabilities." 2006. PDF file.

[2]Wallace, Joseph. "Assistive Technology Funding in the United States." *NeuroRehabilitation*, vol. 28, no. 3, 2011, pp. 295–302., doi:10.3233/nre-2011-0657.

[3] Cooper, R. "Technology for disabilities. Interview by Ron Davis." *BMJ (Clinical research ed.)* vol. 319,7220 (1999): 1290. doi:10.1136/bmj.319.7220.1290

[4]"Protecting Students With Disabilities." Home, 10 Jan. 2020, www2.ed.gov/about/offices/list/ocr/504faq.html.

[5]Southern Regional Education Board. *Expanding Accessibility to Digital Spaces Through Improved Policy and Practice*. Mar. 2017, www.sreb.org/sites/main/files/file-attachments/2017_edtech_polbrief_final_5-3.pdf?1493823503.

[6] Fisher, Kathleen M, et al. "Identifying State Resources and Support Programs on E-Government Websites for Persons with Intellectual and Developmental Disabilities." *Nurs Res Pract*, vol. 2015, 2015, pp. 127638–6., doi:10.1155/2015/127638.

Special Education in Remote Learning: Shortcomings and Solutions

Junsang Yoon¹, David Zhang², Brooke Ellison³

¹Cupertino High School, CA, 95051; ²Fremont High School, CA, 94087; ⁴Center for Medical Humanities, Compassionate Care, and Bioethics, Stony Brook University, NY, 11794

Special education is a critical aspect of the education system that addresses the individual needs of students. With the current transition to remote learning in many schools as a result of the COVID-19 pandemic, it becomes very important to assess the potential impacts of remote learning on special education. A previous meta-analysis by the Department of Education in 2010 suggests that remote learning, if done correctly, can enhance student performance and engagement in a normal environment¹. However, there is currently little to no literature analyzing effects on student performance for special education. Thus, our research aims to characterize the ongoing challenges faced by students in special education, and propose certain solutions for educational administrations to consider.

Previously, students in special education would be exposed to a “two-level” experience. The teacher would act as an “educational parent” for 6-7 hours at school (first level), and the parent would become a resource for the students at home based on the coursework (second level)². With the transition to remote learning, however, this arrangement is no longer feasible.

Institutions must adapt from these existing approaches to prevent students in special education from falling behind³. Socialization also is a challenge for students in special education during remote learning. One of the five key structures of an inclusive educational environment for children in special services is a social-psychological and subjective group that incorporates interaction of students, teachers and parents⁴. Recent nationwide polling demonstrates that nearly 40% of parents whose children should be receiving individual accommodations do not believe they are receiving necessary support⁵ to ensure such inclusive environments.

From our research, we believe that effective strategies² for ensuring that the needs of children in special education involve proper training for parents; effective communication between staff, parents, and children; and ample emphasis on their socialization. Examples include instructing parents on behavioral and emotional vocabulary for effective communication about the home situation to special services, requesting daily reports or informal assessments from parents to better understand the current difficulties with their children, and encouraging peer-to-peer interactions in remote learning environments.

As a new year of school begins to start for the 2020-2021 school year, it becomes important for our schools to appropriately consider the challenges of remote learning and create solutions that do not marginalize the ones that need the most help.

¹U.S. Department of Education, Office of Planning, Evaluation, and Policy Development, *Evaluation of Evidence-Based Practices in Online Learning: A Meta-Analysis and Review of Online Learning Studies*, Washington, D.C., 2010.

²NA “NASET.org Home Page.” *NASET News Alert RSS*, 21 May 2020, www.naset.org/index.php?id=5473.

³Dennehy, Michael. “Remote learning isn't working for special education students: As the majority of students make the transition to remote learning, the children who arguably need the most help are being left behind.” *New Hampshire Business Review*, vol. 42, no. 9, 8 May 2020, p. 17. *Gale General OneFile*, <https://link-gale-com.proxy.library.stonybrook.edu/apps/doc/A629352598/ITOF?u=sunysb&sid=ITOF&xid=a41efccd>. Accessed 2 Aug. 2020.

⁴Transbaikial State University, *Socialization of Students With Disabilities in an Inclusive Educational Environment*, Chita, Russia, 2016.

⁵Foundation, ParentsTogether. “ParentsTogether Survey Reveals Remote Learning Is Failing Our Most Vulnerable Students.” *ParentsTogether*, 27 May 2020, parents-together.org/parentstogether-survey-reveals-remote-learning-is-failing-our-most-vulnerable-students/.

Stem Cell Policy in India

Lingzi (Susan) Zhang¹, Dr. Brooke Ellison²

¹The Hockaday School, Dallas, TX, 11600

²School of Health, Technology, and Management, Stony Brook University, Stony Brook, NY 11749

Stem cells are precursor cells that can develop into specialized cells such as neurons.¹ There are several types of human stem cells used in research, including embryonic stem cells, embryonic germ cells, and adult stem cells.¹ Stem cell research has become more popular in India for its potential in regenerative medicine and applications in bioengineering.² In addition, the global politicization of stem cell research has propelled India to introduce stem cell related policy to improve their global status.¹

Although there were guidelines for biomedical research with human objects in the early 2000s in India, most researchers did not abide by them because the guidelines were non-binding and controversial.¹ Therefore, due to a lack of enforcement of the guidelines, in the mid-2000s, a significant number of unproven stem-cell treatments emerged.³ In 2007, the *National Stem Cell Guidelines* were published to regulate stem cells related activities. The document was revised in 2013 and 2017, with the 2017 version being the current one.⁴

There are 10 sections in the 2017 *National Guidelines for Stem Cell Research*: ethical consideration, scientific consideration, level of manipulation, categorization of research, basic research, translational research including clinical trials, banking, procurement, exchange, publicity.³ The document mainly clarified that advertising, commercialization, and publicity of any kind of unproven stem cell therapies are not permitted and stated the types of stem cell research that are permitted, while establishing a two-level (national and institutional level) review, approval, and monitoring of clinical research involving stem cells.³ The document also addressed various ethical concerns, such as the protection of stem cell donors' privacy and procurement of stem cells.³

However, even after the 2017 guidelines were published, many clinics in India continued offering unproven stem cell therapies to obtain profit.⁴ Such issues are mainly caused by challenges in the enforcement of guidelines and cultural factors. First, the guidelines are not formal laws.⁴ Therefore, violations of these guidelines do not result in legal consequences, which explains why many clinicians ignore the guidelines. Second, the rules and regulations are incoherent; for instance, some of the terminologies, such as “minimally manipulated stem cells,” contain ambiguity, which can mislead patients.⁴ Third, there is a lack of enforcement of the guidelines. The regulatory bodies that made the guidelines do not have enforcement abilities nor legal power to punish violators; in addition, there are 7 regulatory bodies involved in stem cell regulations, which makes enforcement difficult and inefficient.⁴ Besides, the social and cultural factors in India, such as deference to clinicians, make patients more vulnerable, for it is not likely that they challenge the clinicians who try to advertise unproven therapies.⁴ In order to protect these patients and stop the fraudulent advertisement of stem cell therapies, legal backups of guidelines are needed to better enforce the regulations.⁴ The public should also be educated and updated on the status of stem cell research in India and around the world through different monitored media platforms to further protect patients.

¹ Mittal, Sanjay. “Stem Cell Research: The India Perspective.” *Perspectives in Clinical Research*, vol. 4, no. 1, 2013, p. 105, doi:10.4103/2229-3485.106408.

² “India Setting out Guidelines for Stem Cell Research.” *The Pharma Letter*, 25 July 2017, www.thepharmaletter.com/article/india-setting-out-guidelines-for-stem-cell-research.

³ Lahiry, Sandeep, et al. “The National Guidelines for Stem Cell Research (2017): What Academicians Need to Know?” *Perspectives in Clinical Research*, vol. 10, no. 4, 2019, pp. 148–54., doi:10.4103/picr.picr_23_18.

⁴ Tiwari, Shashank S., and Pranav N. Desai. “Unproven Stem Cell Therapies in India: Regulatory Challenges and Proposed Paths Forward.” *Cell Stem Cell*, vol. 23, no. 5, 2018, pp. 649–652., doi:10.1016/j.stem.2018.10.007.

Ethics of Telehealth in Psychology

Amisha Agrawal¹, Anya Chabria², Clarise Han³, Tyler Shern³, Lillian Sun⁴, Serena Yang⁵

¹University High School, Johnson City, TN 37614, ²The Wheatley School, Old Westbury, NY 11568, ³Mission San Jose High School, Fremont, CA 94539, ⁴Thomas Jefferson High School for Science and Technology, Alexandria, VA 22312, ⁵Dougherty Valley High School, San Ramon, CA 94582

When evaluating the use of telecommunications in psychological therapy, it is important to assess the ethical lens. The arguments for administering therapy through telecommunications include increased accessibility to economic advantages, while those against telepsychotherapy argue that technological issues such as breaches in confidentiality make it unreliable for treatment¹. The two positions present compelling benefits and consequences that must be weighed before telehealth can be fully implemented for psychological treatments.

The main ethical arguments in favor of telepsychotherapy include increased access and flexibility, economic advantages, and anonymity. Digital psychotherapy enhances availability to health care services, especially for those living in rural or remote areas. Perceived as convenient by both therapists and patients, the flexible format of telepsychotherapy satisfies the needs of both parties.¹ The integration of a wider range of care in the form of online materials allows for a revisitation of data and documentation of therapeutic techniques for patients.² In addition, viable alternatives to in-person treatment have been implemented to allow for further flexibility in treatment.³

Another great advantage is that, since telehealth is more cost-efficient than in-person visits,⁴ more low and middle-income individuals will be able to afford digital psychotherapy. Therapists have more flexibility online, and can reach out to underserved populations. This is especially true in developing countries, such as India.⁵ Furthermore, receiving digital therapy can increase a patient's sense of privacy and anonymity. If therapy is sought anonymously, the patient can potentially discuss personal and emotional issues more freely, leading to a better recovery.⁶

A significant issue with digital psychotherapy is the risk to privacy and security. Therapists administering psychotherapy may not be able to avoid data breaches and hacking within their communication software.¹ Additionally, the use of digital psychotherapy lends to the potential impediment of effective communication between therapists and their patients. If the mode of communication chosen is messaging, for instance, the therapist may not be able to use nonverbal cues to evaluate and treat patients.⁷ This issue is exacerbated if therapists are not trained for online counseling,¹ or if there are extreme situations (for instance, if the patient is having suicidal thoughts) that require risk assessment.⁷

Since telepsychotherapy has recently been popularized, there has been an insufficient amount of concrete research studies conducted, and many believe that the effectiveness and efficacy of digital psychotherapy may be significantly less than that of in-person treatments.⁴ According to the American Psychological Association's associate executive director of practice research and policy, Dr. Bufka, the companies that are developing telepsychotherapy may not be fully equipped with the healthcare knowledge to develop effective platforms.⁷ Additionally, the lack of regulatory guidelines and standards in the field leaves many ethical considerations unaddressed, especially in terms of cross-border practice, cultural differences, licensing, and quality of care.

In sum, the lack of privacy, effective communication, regulatory and emergency guidelines, and clear efficacy of treatment must be taken into account when considering the viability of telemedicine in the field of psychotherapy. New innovations that arise in telepsychotherapy must overcome these ethical issues to be fully considered as legitimate and prospective tools for treatment.

[1] Stoll, Julia, et al. "Ethical Issues in Online Psychotherapy: A Narrative Review." *Frontiers in Psychiatry*, vol. 10, 2020, doi:10.3389/fpsy.2019.00993.

[2] Johnson, G. R. "Toward uniform competency standards in telepsychology: A proposed framework for Canadian psychologists." *Canadian Psychology/Psychologie canadienne*, 55(4), 291–302, 2014, doi:10.1037/a0038802

[3] Brenes, Gretchen A et al. "Benefits and Challenges of Conducting Psychotherapy by Telephone." *Professional psychology, research and practice* vol. 42,6 (2011): 543-549. doi:10.1037/a0026135

[4] Barnett JE, Scheetz K. Technological advances and telehealth: Ethics, law, and the practice of psychotherapy. *Psychother: Theory Res Pract Training* (2003) 40(1/2):86–93. 10.1037/0033-3204.40.1-2.86

[5] Malhotra S, Chakrabarti S, Shah R. Telepsychiatry: Promise, potential, and challenges. *Indian J Psychiatry* (2013) 55(1):3–11. 10.4103/0019-5545.105499

[6] Chester A, Glass CA. Online counselling: A descriptive analysis of therapy services on the Internet. *Br J Guid Couns* (2006) 34(2):145–60. 10.1080/03069880600583170

[7] Novotney, Amy. "A Growing Wave of Online Therapy." *Monitor on Psychology*, American Psychological Association, Feb. 2017, www.apa.org/monitor/2017/02/online-therapy.

The Effect of Neonatal Telehealth on Early Release and Remote Monitoring: A Comprehensive Study

Jolene Huey¹, Joshua Kang²

¹Arcadia High School, CA 91006, ²Westwood High School, TX 78750

Preterm birth is the leading cause of death for children under five years of age, and about 15 million babies are born preterm each year. The Neonatal Intensive Care Unit (NICU) serves to combat complications and risks that often result from early births. However, the NICU admits a significantly larger percentage of babies born preterm, with a gestational age less than 37 weeks, than those born full term, with a gestational age between 37 and 41 weeks (Fig. 1).¹ The

locationally restrictive nature of NICUs gives parents, especially those in suburban and rural locations, significant psychological distress and places them under financial strain. Meanwhile, underserved populations are significantly affected by the scarcity of NICUs. Babies born in these areas are more likely to require transfer to hospitals that can accommodate advanced treatment, which increases their chance of fatality. The implementation of telehealth helps alleviate these problems for parents and newborns, especially for suburban, rural, and underserved populations.

Existing studies on the impact of newborn telehealth on suburban and rural locations highlight the benefits of effective telecommunication to be more effective than face-to-face interventions depending on case. These advantages can be translated to guardians who are distanced from their newborns in care: they contribute to cost savings, promote parental roles, and encourage transparent communication.

In emergency situations where certain hospitals are not equipped to give dedicated treatments, newborns are limited to consulting with specialized doctors through telephone calls or waiting for a neonatal transport team, which is risky. Telehealth strengthens doctors' abilities to give sound medical advice remotely without having to further risk the newborn's unstable condition by attempting transfer. Neonatologists can be brought virtually to the bedside and give synchronous treatment, such as video-assisted resuscitation.

Despite the strengths that telehealth brings to neonatology, obstacles in existing newborn telehealth programs prevent the up-scaling of telehealth programs in the previously described populations. For instance, lack of reimbursement for healthcare providers and hospitals is discouraging, warranting the need for policy changes. Considering that newborn monitoring via telehealth was only established in the early 2010s, more data collection is necessary to effectively address these issues. Further research on this subject aims to mitigate one of the largest problems regarding the NICU — family formation — through early discharge and remote monitoring.²

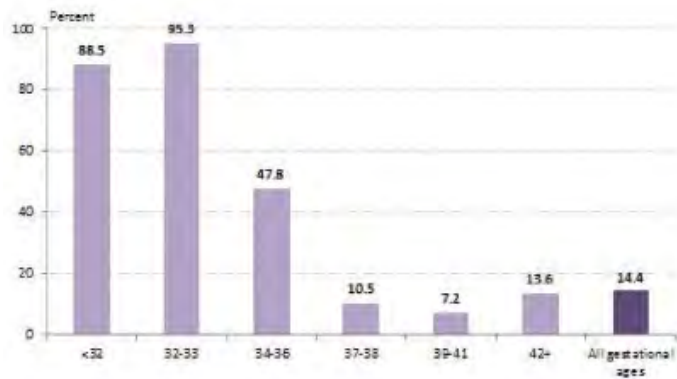
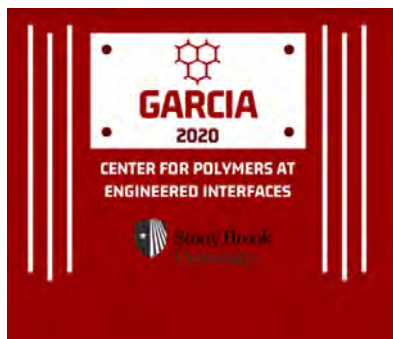


Figure 1. Specialty care nursery admissions by gestational age¹

¹ March of Dimes Perinatal Data Center. Special Care Nursery Admissions.

https://www.marchofdimes.org/peristats/pdfdocs/nicu_summary_final.pdf. Published 2011.

² Garne, Kristina et al. "Telemedicine in Neonatal Home Care: Identifying Parental Needs Through Participatory Design." *JMIR research protocols* vol. 5,3 e100. 8 Jul. 2016, doi:10.2196/resprot.5467



Luisa Pan



Jing (Samantha)
Wang



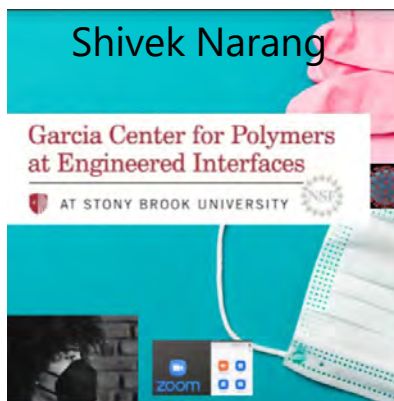
**GARCIA
SYMPOSIUM**

Online Edition: 2020

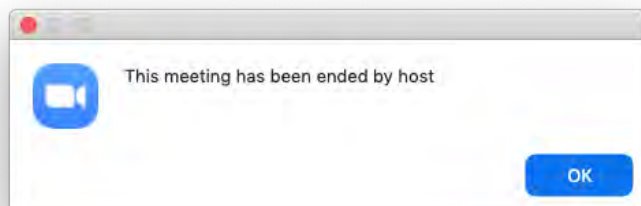
Hugo Onghai



Annie Wang



Shivek Narang



*We gratefully acknowledge
support from the
Louis Morin Charitable Trust*